Functional dissection of the meiotic drive of female-inherited accessory chromosomes in *Zymoseptoria tritici*

Dissertation

Zur Erlangung des Doktorgrades der Mathematisch-Naturwissenschaftlichen Fakultät der Christian-Albrechts-Universität zu Kiel

vorgelegt von

Jovan Komluski

Kiel, 2023

Erste Gutachterin: Prof. Dr. Eva Holtgrewe Stukenbrock

Zweite Gutachterin: Prof. Dr. Tal Dagan

Tag der mündlichen Prüfung: 04.05.2023

Approved for publication

"What we observe is not nature, but nature exposed to our method of questioning."

Werner Heisenberg, German physicist (1901-1976)

Contents

Author's contributions

This thesis consists of three chapters. Each chapter is represented by a manuscript. Jovan Komluski developed ideas and wrote manuscripts with major contributions.

Chapter I

Non-Mendelian transmission of accessory chromosomes in fungi
Jovan Komluski, Eva Holtgrewe Stukenbrock and Michael Habig

JK: Conceptualization, Investigation, Visualization, Writing-original draft
EHS: Conceptualization, Investigation, Writing- review & editing, Supervision
MH: Conceptualization, Investigation, Writing- review & editing, Supervision

---

Chapter II

Repeat-induced point mutation (RIP) and gene conversion influenced by chromatin modifications shape the genome of a plant pathogenic fungus
Jovan Komluski, Michael Habig and Eva Holtgrewe Stukenbrock

JK: Conceptualization, Formal analysis, Investigation, Visualization, Writing-original draft
MH: Conceptualization, Formal analysis, Investigation, Supervision, Writing-original draft
EHS: Conceptualization, Funding acquisition, Supervision, Writing-review & editing

---

Chapter III

Elimination of disomic chromosomes during meiosis in a plant-pathogenic fungus
Jovan Komluski, Michael Habig and Eva Holtgrewe Stukenbrock

JK: Conceptualization, Investigation, Visualization, Formal analysis, Writing-original draft

MH: Conceptualization, Investigation, Writing-review & editing, Supervision

EHS: Conceptualization, Writing-review & editing, Supervision, Project Administration, Funding acquisition

Summary

Accessory chromosomes are non-essential genetic elements that occur in the genomes of many eukaryotes. These chromosomes show presence/absence polymorphisms and are often lost and unpaired during meiosis. In some fungal species, these chromosomes confer fitness advantages, often in the form of increased virulence. However, in some species, they have a negative fitness effect, for instance, in *Zymoseptoria tritici*, a fungal wheat pathogen. Accessory chromosomes are likely maintained in populations of this pathogen despite their negative fitness cost via a meiotic drive that is restricted to female-inherited and unpaired accessory chromosomes. The mechanism of this meiotic drive is unclear, but it likely involves the additional replication of female-inherited and unpaired accessory chromosomes. The main focus of this thesis was to improve our understanding of the mechanism of meiotic drive of accessory chromosomes and to gain deeper insight into genetic changes associated with meiosis in *Z. tritici*.

In **Chapter I**, I give an overview of the structural and functional features of fungal accessory chromosomes that might be affecting their segregation patterns and discuss mechanisms that could explain non-Mendelian segregation and meiotic drives of fungal accessory chromosomes. I conclude that epigenetic modifications are potential discriminators affecting the transmission of fungal accessory chromosomes during meiosis.

In **Chapter II**, I perform *in silico* tetrad analysis to investigate genetic changes associated with meiosis-recombination, gene conversion, and mutations. I calculate the rates of these changes and find high genome-wide rates of recombination and gene conversion, with both rates being higher on accessory chromosomes than on core chromosomes. In addition, higher gene conversion rates were associated with regions enriched in heterochromatin modifications, particularly trimethylation of lysine 9 on histone 3 (H3K9me3). Most importantly, meiosis was associated with approx. three orders of magnitude higher frequency of *de novo* mutations than mitosis. I detect the signatures of repeat-induced point mutation (RIP) in the duplicated genome regions and transposable elements (TEs) responsible for 78% of meiotic mutations, which is the first experimental validation of this duplication defense mechanism in *Z. tritici*.

The additional replication that potentially causes the meiotic drive of female-inherited and unpaired accessory chromosomes in *Z. tritici* can happen prior to karyogamy or in the zygote; however, the exact stage of meiosis at which these accessory chromosomes are re-replicated is still unknown. In **Chapter III**, I observe how disomic chromosomes undergo meiosis and distinguish the stage of meiosis at which re-replication of accessory chromosomes under meiotic drive occurs. I isolated,

karyotyped, and sequenced tetrad progeny from disomic crosses with *Z. tritici* strains that included two types of disomic chromosomes, i.e., disomic accessory chromosomes were either two homologues of the same genotype or two homologues of the differentiable genotype. Male-inherited disomic accessory chromosomes are eliminated in the progeny, indicating that disomy is controlled in a parent-of-origin-specific manner in *Z. tritici*. Importantly, non-Mendelian segregation patterns of disomic chromosomes suggest that re-replication causing meiotic drive of accessory chromosomes happens before karyogamy.

In conclusion, I show that genetic changes during meiosis are a significant factor in shaping the *Z. tritici* genome and provide novel insights into the mechanism of the meiotic drive of female-inherited and unpaired accessory chromosomes in this important plant pathogen.

Zusammenfassung

Akzessorische Chromosomen sind nicht-essentielle genetische Elemente, die in den Genomen vieler Eukaryoten vorkommen. Diese Chromosomen weisen einen Polymorphismus auf und gehen während der Meiose häufig verloren und werden nicht gepaart. Bei einigen Pilzarten verschaffen diese Chromosomen Fitnessvorteile, oft in Form einer erhöhten Virulenz. Bei einigen Arten wirken sie sich jedoch negativ auf die Fitness aus, wie z. B. bei *Zymoseptoria tritici*, einem Pilzerreger für Weizen. Wahrscheinlich werden akzessorische Chromosomen in Populationen dieses Erregers trotz ihrer negativen Fitnesskosten durch einen meiotischen Antrieb aufrechterhalten, der auf weiblich vererbte und ungepaarte akzessorische Chromosomen beschränkt ist. Der Mechanismus dieses meiotischen Antriebs ist unklar, aber er beinhaltet wahrscheinlich die zusätzliche Replikation von weiblich vererbten und ungepaarten akzessorischen Chromosomen. Das Hauptaugenmerk dieser Arbeit lag darauf, den Mechanismus des meiotischen Antriebs der akzessorischen Chromosomen besser zu verstehen und tiefere Einblicke in die mit der Meiose verbundenen genetischen Veränderungen bei *Z. tritici* zu gewinnen.

In **Kapitel I** gebe ich einen Überblick über die strukturellen und funktionellen Merkmale der akzessorischen Pilzchromosomen, die ihre Segregationsmuster beeinflussen könnten, und diskutiere Mechanismen, die die nicht-Mendelische Segregation und den meiotischen Antrieb der akzessorischen Pilzchromosomen erklären könnten. Ich komme zu dem Schluss, dass epigenetische Modifikationen potenzielle Unterscheidungsmerkmale sind, die die Übertragung von Pilz-Akzessorchromosomen während der Meiose beeinflussen.

In **Kapitel II** führe ich *in-silico* Tetrad-Analysen durch, um die mit der Meiose verbundenen genetischen Veränderungen - Rekombination, Genkonversion und Mutationen - zu untersuchen. Ich berechne die Raten dieser Veränderungen und stelle hohe genomweite Raten von Rekombination und Genkonversion fest, wobei beide Raten auf akzessorischen Chromosomen höher sind als auf Kernchromosomen. Darüber hinaus wurden höhere Genkonversionsraten mit Regionen in Verbindung gebracht, die mit Heterochromatin-Modifikationen angereichert waren, insbesondere mit der Trimethylierung von Lysin 9 auf Histon 3 (H3K9me3). Am wichtigsten ist, dass die Meiose mit einer um etwa drei Größenordnungen höheren Häufigkeit von *de-novo* Mutationen verbunden war als die Mitose. In den duplizierten Genomregionen und transponierbaren Elementen (TEs), die für 78 % der meiotischen Mutationen verantwortlich sind, konnte ich die Signaturen der wiederholungs-induzierten Punktmutation (RIP) nachweisen, was die erste experimentelle Validierung dieses Duplikations-Abwehrmechanismus in *Z. tritici* darstellt.

Die zusätzliche Replikation, die möglicherweise den meiotischen Antrieb der weiblichen und ungepaarten akzessorischen Chromosomen in *Z. tritici* verursacht, kann vor der Karyogamie oder in der Zygote stattfinden; das genaue Stadium der Meiose, in dem diese akzessorischen Chromosomen neu repliziert werden, ist jedoch noch unbekannt. In **Kapitel III** beobachte ich, wie disomische Chromosomen die Meiose durchlaufen, und unterscheide das Stadium der Meiose, in dem eine erneute Replikation der akzessorischen Chromosomen unter meiotischem Antrieb stattfindet. Ich isolierte, karyotypisierte und sequenzierte Tetrad-Nachkommen aus disomischen Kreuzungen mit *Z. tritici*-Stämmen, die zwei Arten von disomische Chromosomen aufwiesen, d. h. disomische akzessorische Chromosomen waren entweder zwei Homologe desselben Genotyps oder zwei Homologe des differenzierbaren Genotyps. Männlich vererbte disomische akzessorische Chromosomen werden in der Nachkommenschaft eliminiert, was darauf hindeutet, dass die Disomie bei *Z. tritici* auf eine herkunftsspezifische Weise gesteuert wird. Wichtig ist, dass die nicht-Mendelischen Segregationsmuster der disomischen Chromosomen darauf hindeuten, dass die Replikation, die den meiotischen Antrieb der akzessorischen Chromosomen verursacht, vor der Karyogamie stattfindet.

Zusammenfassend kann ich zeigen, dass genetische Veränderungen während der Meiose ein wichtiger Faktor bei der Gestaltung des *Z. tritici*-Genoms sind und neue Einblicke in den Mechanismus des meiotischen Antriebs von weiblich vererbten und ungepaarten akzessorischen Chromosomen in diesem wichtigen Pflanzenpathogen bieten.

General Introduction

Meiosis is a highly conserved cellular process that is one of the main generators of genetic novelty in sexually reproducing organisms. Meiosis involves the pairing and segregation of homologous chromosomes and consists of one round of DNA replication and two successive divisions to ensure equal distribution of genetic material from both parents to progeny (Da Ines *et al.* 2014; Zickler and Kleckner 2015). Pairing and recombining of homologous chromosomes are crucial for their accurate segregation during meiosis (Gerton and Hawley 2005; Zickler and Kleckner 2015). In the early meiotic prophase I, homologous chromosomes form connections called synapsis to allow physical associations along their lengths (Alleva and Smolikove 2017). Synapsis formation is mediated by the synaptonemal complex (SC), a meiosis-specific protein complex, and is necessary to promote recombination between homologous chromosomes (Hesse *et al.* 2019). Synapses are in most species established via the generation of double-strand breaks (DSBs) followed by strand invasion (Zickler and Kleckner 1999). DSBs after strand invasion are resolved as crossovers (COs), the reciprocal exchanges of genetic material, or gene conversions (GCs), unidirectional exchange of genetic material in which a segment of genetic material is copied from the homolog, without the alteration of donor chromosome (Li *et al.* 2019). Gene conversion in contrast to COs directly affects the allele frequency and can either be interallelic or (also called interlocus). Interallelic gene conversion will result in changes in the allele frequency while the non-allelic gene conversion is (besides unequal crossovers) involved in gene duplication, gene expansion, and homogenization of gene families and has, for instance, been observed in gene families involved in host-pathogen interaction.

Meiosis generates novel variation by introducing *de novo* mutations and is, therefore, a central mechanism in shaping the evolution of sexually propagating species. The number and distribution of *de novo* mutations can be associated with DSBs and their repair, since a higher number of mutations occurs in the vicinity of recombination events (Rattray *et al.* 2015). In addition, the number and distribution of *de novo* mutations can also be influenced by different genome mechanisms, for instance, repeat-induced point mutation (RIP) (Wang *et al.* 2020). RIP is a fungal defense mechanism against duplicated sequences and transposable elements (TEs) that is active in the haploid nuclei before karyogamy (Fig 1) (Galagan and Selker 2004). RIP induces C:T transitions into detected duplications of minimum 400 bp length in *N. crassa*, thereby causing >90% of the *de novo* mutations (Selker 2002; Gladyshev and Kleckner 2016; Gladyshev 2017). Hence, rates of *de novo* mutations can vary and are affected by mutational processes before and during meiosis.
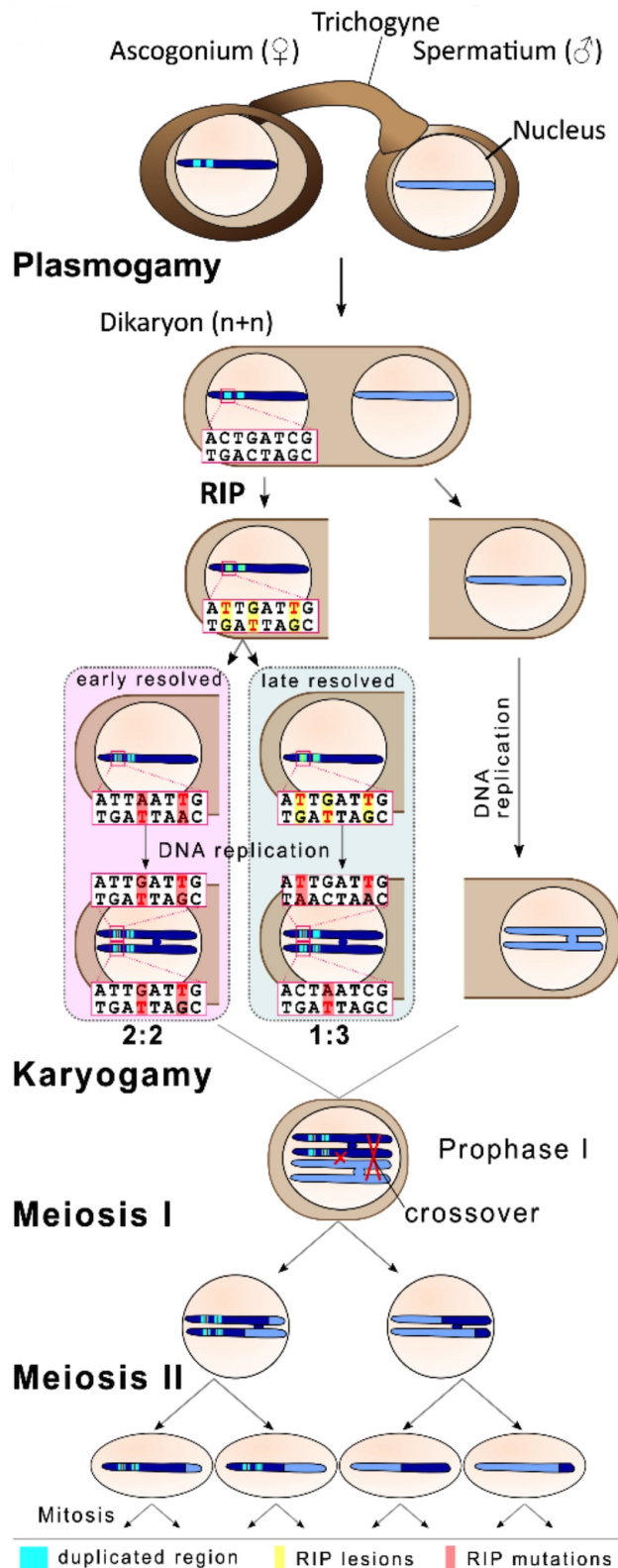
Fig 1. Repeat-induced point mutation (RIP) mechanism. In *Ascomycetes* and *Basidiomycetes*, meiosis is preceded by plasmogamy, a stage in which two gametes merge without nuclei fusion. RIP acts at the stage of haploid nuclei by introducing C:T transitions into duplicated sequences. RIP induces mutations before or after the DNA replication that precedes meiosis. If RIP mutations are induced prior to DNA replication, the mutations will have 2:2 segregation, while post-DNA replication-induced mutation will have 3:1 segregation. After plasmogamy, haploid nuclei are fused (karyogamy) and followed by two rounds of meiosis and mitosis.

Segregation of genetic elements can also be skewed during meiosis, leading to non-proportional inheritance of generic material in the progeny. The meiotic drive is, by definition, the inheritance of genetic elements on higher frequencies than expected by Mendelian segregation, and it is active in various unicellular and multicellular organisms (Kruger and Mueller 2021). Transmission advantages that occur due to meiotic drive result in the over-representation of genetic elements despite their neutral or negative fitness cost. Meiotic drives occur during symmetric (i.e., all daughter cells are identical) and asymmetric meioses (i.e., daughter cells differ from each other, and only a subset of daughter cells provides genetic material to the next generation). A prime example of meiotic drives in symmetric meiosis is spore killer alleles (*Sk2* or *Sk3*) in *N. crassa*, where ascospores without this allele die (Hammond *et al.* 2012; Svedberg *et al.* 2021). In contrast to symmetric meioses, in female animal meiosis, asymmetric cytokinesis produces the egg cell and polar bodies and only the genetic material of the egg cell is transmitted to the next generation. Therefore centromere drive biases segregation of linked chromosomes to the egg cell in asymmetric meioses, ensuring the transmission of these chromosomes to the progeny (Henikoff *et al.* 2001; Malik 2009; Akera *et al.* 2017). Hence, the meiotic drive is an important mechanism that allows the perpetuation of genetic elements independently of their effect on the fitness of an individual.

Accessory chromosomes often show meiotic drive during meiosis. Accessory chromosomes are entire chromosomes that are, by definition, present in some, but not all, members of a population. Accessory chromosomes do not recombine with essential chromosomes and deviate from Mendelian inheritance (Houben 2017). In fungal species, accessory chromosomes are also named supernumerary, (conditionally) dispensable, or lineage-specific chromosomes. In plants and animals, these chromosomes are called "B" chromosomes. The function of accessory chromosomes in these species is often unknown, and their fitness effect is assumed to be neutral or even negative since these chromosomes are not necessary for an organism's normal growth and development (Houben *et al.* 2014; Houben 2017). Fungal accessory chromosomes, in contrast to "B" chromosomes, can have beneficial fitness effects, for instance, an increase in virulence because of a virulence gene on an accessory chromosome (Ma *et al.* 2010). How accessory chromosomes originated is unclear and there are two hypotheses about their origin. The first hypothesis implies that accessory chromosomes are derived from essential ("A") chromosomes from the same or related species (Martis *et al.* 2012). This hypothesis is based on similarities between the families of repetitive elements shared between core and accessory chromosomes (Grandaubert *et al.* 2015) and after the detection of novel accessory chromosomes formed after non-allelic recombination that led to the breakage-fusion-bridge

cycle (McClintock 1941; Croll *et al.* 2013). According to the second hypothesis based on the observed differences in codon usage between core and accessory chromosomes, accessory chromosomes develop via horizontal gene transfer from different species (Goodwin *et al.* 2011). Accessory chromosomes often have a neutral or negative effect on host fitness, however they are maintained in the host genome via meiotic drive (Ågren and Clark 2018). The chromosomal drive of accessory chromosomes can be a consequence of differences in their mitotic transmission, for instance, in the rye, where non-disjunction of sister chromatids during first pollen mitosis causes non-equal mitotic transmission that affects meiotic segregation (Houben 2017). In the fungal wheat pathogen *Zymoseptoria tritici,* accessory chromosomes are subject to a meiotic drive that increases their frequency in the progeny when these chromosomes are unpaired and inherited from the female parental strain. In contrast, male-inherited and unpaired accessory chromosomes are transmitted to half of the progeny as expected according, to Mendelian segregation (Fig 2B). The exact mechanism of this drive is unknown (Habig *et al.* 2018) (Fig 2C).

Z. tritici is an excellent model for studying the maintenance of accessory chromosomes during meiosis due to its unique set of accessory chromosomes. *Z. tritici* is a haploid, filamentous fungus with a highly structured, bipartite genome with one of the largest compartments of accessory chromosomes among fungi. The reference isolate IPO323 consists of 13 core chromosomes that are essential and are present in all of the isolates, while the remaining eight chromosomes are called accessory chromosomes and show presence/absence polymorphisms among isolates (Goodwin *et al.* 2011). Accessory chromosomes in the reference isolate IPO323 differ in size from 409 kb (accessory chromosome 21) to 773 kb (accessory chromosome 14), are gene-poor, highly repetitive and are highly enriched in trimethylation of lysine 27 of the histone H3 (H3K27me3), the facultative heterochromatin mark that is absent on core chromosomes (Wittenberg *et al.* 2009; Goodwin *et al.* 2011; Grandaubert *et al.* 2015; Schotanus *et al.* 2015). In addition, population data suggests that accessory chromosomes have lower recombination rates than core chromosomes, in contrast to data from crossing isolates (Croll *et al.* 2015; Stukenbrock and Dutheil 2018). Interestingly, the presence of accessory chromosomes in the genome of this pathogen infers fitness cost. Isogenic deletion strains of *Z. tritici* lacking specific accessory chromosomes produce more asexual spores than the reference strain with a complete set of accessory chromosomes on a wheat cultivar Runal (Habig *et al.* 2017). Accessory chromosomes are maintained in the genome of *Z. tritici* via meiotic drive despite their negative fitness cost (Habig *et al.* 2018). The meiotic drive of accessory chromosomes counterbalances frequent losses of these chromosomes during meiosis and mitosis in *Z. tritici*

(Wittenberg *et al.* 2009; Möller *et al.* 2018). Interestingly, this drive is specific to unpaired accessory chromosomes that are female-inherited (Habig *et al.* 2018). *Z. tritici* is a heterothallic fungus, i.e., two individuals with different mating types [*mat1-1* and *mat1-2*] are necessary to form a diploid zygote (Kema *et al.* 1996). During sexual mating, the female partner produces a sexual structure called ascogonium that receives spermatium with the male nucleus through bridge-like structure trichogyne (Crous 1998; Kema *et al.* 2018). The female parental role is associated with the mitochondrial transmission, and individuals of both mating types can provide mitochondria and thus act as a female parent (Ni *et al.* 2011; Kema *et al.* 2018). Since individuals of both mating types can act as a female parent, it is unclear why is the meiotic drive in *Z. tritici* restricted to unpaired and female-inherited accessory chromosomes. Interestingly, the meiotic drive is reported for all accessory chromosomes except for the accessory chromosome 14, which is the largest accessory chromosome. Furthermore, shortened unpaired accessory chromosome 14 shows a segregation advantage (Croll *et al.* 2013), indicating that chromosome size is an additional factor affecting the meiotic drive of the female-inherited and unpaired accessory chromosomes. The exact mechanism of the meiotic drive of the unpaired and female-inherited accessory chromosomes in *Z. tritici* is still unknown; however, it likely involves additional replication of these chromosomes.

The main objective of this research was to determine the mechanism of the meiotic drive of the unpaired and female-inherited accessory chromosomes in *Z. tritici*. In addition, I estimate rates of genetic changes during meiosis – recombination, gene conversion, and mutation – and identify processes affecting rates of these changes.
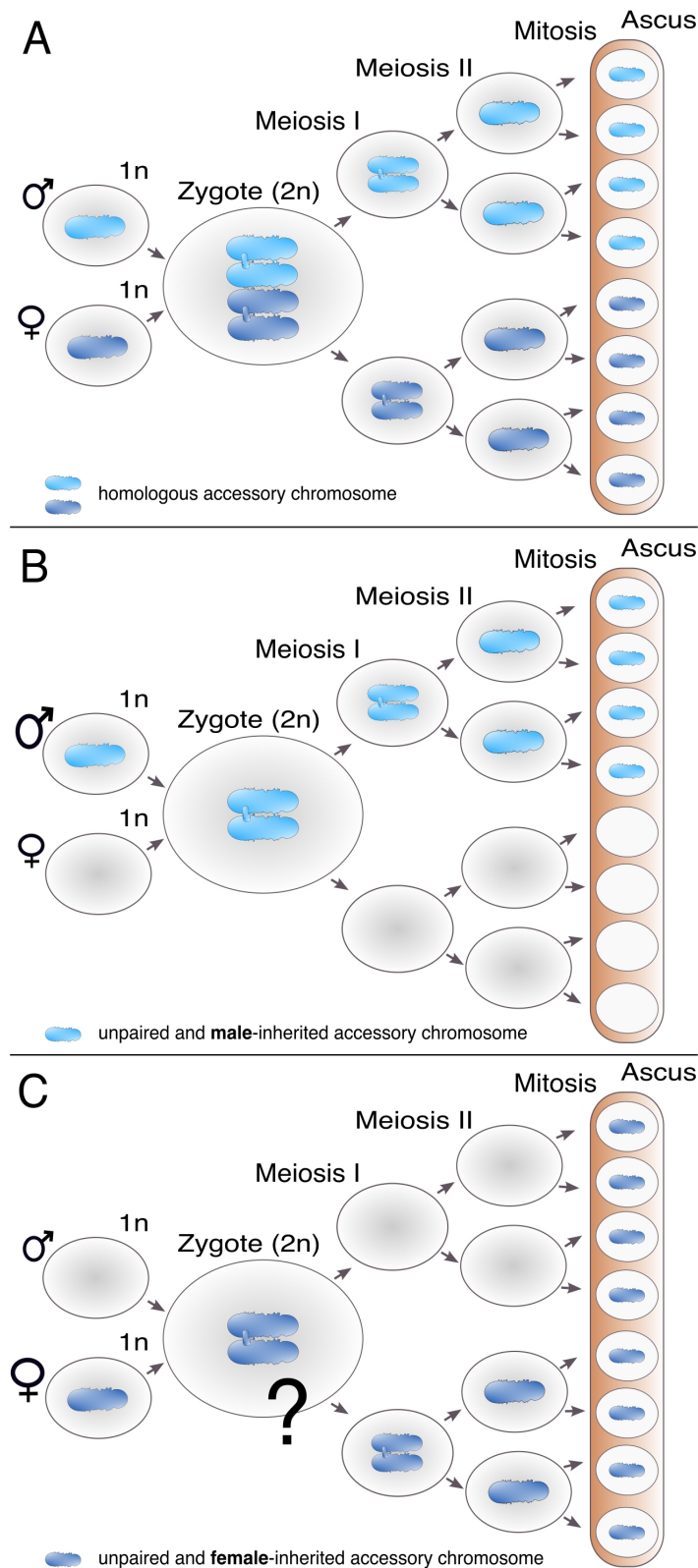
Fig 2. Dynamics of accessory chromosomes during meiosis in *Z. tritici*. **A** During meiosis, accessory chromosomes are first replicated, followed by the pairing of homologous accessory chromosomes, two rounds of meiotic division, and one round of mitosis. As a result, paired accessory chromosomes have 4:4 segregation in eight ascospores that are the product of meiosis in *Z. tritici*. **B** Accessory chromosomes that are unpaired and male-inherited during meiosis are transmitted to 50% of the progeny as expected in accord with Mendelian segregation. **C** Meiotic drive of accessory chromosomes in *Z. tritici* is restricted exclusively to accessory chromosomes that are unpaired and female-inherited. These chromosomes are inherited in higher frequencies than expected by Mendelian segregation. For simplification, recombination events are omitted from the figure.

Scope of the Thesis

Chapter I

"Non-Mendelian transmission of accessory chromosomes in fungi"

Jovan Komluski, Eva H. Stukenbrock and Michael Habig

The review is published in Chromosome Res. 2022 Sep;30(2-3):241-253.doi:10.1007/s10577-022-09691-8

Fungal accessory chromosomes (also called B chromosomes in plants and animals) often show non-Mendelian transmission during meiosis. Accessory chromosomes in fungi are similar to B chromosomes in plants and animals since they are non-essential and show presence/absence polymorphisms within a population; however, how fungal accessory chromosomes are transmitted during meiosis is poorly understood. This review discusses potential mechanisms that can cause the non-Mendelian transmission or meiotic drives of fungal accessory chromosomes.

- What are the possible mechanisms causing the non-Mendelian transmission or meiotic drives of fungal accessory chromosomes?

- What are the distinguishing structural features of fungal accessory chromosomes affecting their segregation during meiosis?

Chapter II

"Repeat-induced point mutation and gene conversion coinciding with heterochromatin shape the genome of a plant pathogenic fungus"

Jovan Komluski, Michael Habig and Eva Holtgrewe Stukenbrock

This manuscript is published as a preprint on *bioRxiv* (doi: https://doi.org/10.1101/2022.11.30.518637) and currently under revision in *mBio* journal

Meiosis is associated with genetic changes in the genome via recombination, gene conversion, and mutations. Rates of recombination in *Z. tritici* are known from population studies; however, gene conversion rates and meiotic mutation rates are unknown. Furthermore, the effect of chromatin

modifications on rates of genetic changes associated with meiosis is poorly understood for many species. In addition, meiosis generates novel mutation on which selection can act; however the mutation rates during meiosis in *Z. tritici* are unknown. In some fungi, meiotic mutation rates are influenced by repeat-induced point mutation (RIP), but if RIP is active in *Z. tritici* is unknown.

Here, I performed a bioinformatic analysis of tetrad progeny to address the following questions:

- How do gene conversion and recombination rates differ between core and accessory chromosomes?

- What is the effect of chromatin modifications on gene conversion and recombination?

- What is the mutation rate during meiosis in *Z. tritici*?

- Is repeat-induced point mutation (RIP) active in *Z. tritici*?

My results show:

- Higher recombination and gene conversion rates on accessory chromosomes.

- Elevated gene conversion rates and recombination rates in regions enriched in heterochromatin marks, particularly H3K9me3.

- The mutation rate during meiosis is approxim. three orders of magnitude higher than the mutation rate during mitosis in *Z. tritici*.

- RIP is active in *Z. tritici* and causes 77% of *de novo* mutations during meiosis.

Chapter III

"Elimination of disomic chromosomes in a plant pathogenic fungus"

Jovan Komluski, Michael Habig and Eva Holtgrewe Stukenbrock
Manuscript prepared for submission

The meiotic drive of accessory chromosomes in *Z. tritici* is restricted to accessory chromosomes that are female-inherited and unpaired during meiosis. These chromosomes are likely re-replicated during meiosis, but the exact stage of this additional replication is unknown. In addition, disomy of accessory

chromosomes is an often outcome of meiosis in *Z. tritici* however, the frequency of disomic chromosomes in natural isolates of this fungal pathogen is low.

In this study, I conducted *in planta* disomic crosses to answer the following questions:

- How are disomic accessory chromosomes maintained in *Z. tritici*?
- At which stage are accessory chromosomes that are female-inherited and unpaired during meiosis additionally replicated?

Our results demonstrate:

- Elimination of disomic accessory chromosomes in an origin-of-parent-specific manner during meiosis.
- Additional replication of unpaired and female-inherited accessory chromosomes prior to karyogamy.

Chapter I

Non-Mendelian transmission of accessory chromosomes in fungi

Jovan Komluski, Eva H. Stukenbrock and Michael Habig

Environmental Genomics, Christian-Albrechts University of Kiel, Am Botanischer Garten 1-9, 24118 Kiel, Germany

Max Planck Institute for Evolutionary Biology, August-Thienemann-Straße 2, 24306 Plön, Germany

Abstract

Non-Mendelian transmission has been reported for various genetic elements, ranging from small transposons to entire chromosomes. One prime example of such a transmission pattern are B chromosomes in plants and animals. Accessory chromosomes in fungi are similar to B chromosomes in showing presence/absence polymorphism and being non-essential. How these chromosomes are transmitted during meiosis is however poorly understood—despite their often high impact on the fitness of the host. For several fungal organisms, a non-Mendelian transmission or a mechanistically unique meiotic drive of accessory chromosomes have been reported. In this review, we provide an overview of the possible mechanisms that can cause the non-Mendelian transmission or meiotic drives of fungal accessory chromosomes. We compare processes responsible for the non-Mendelian transmission of accessory chromosomes for different fungal eukaryotes and discuss the structural traits of fungal accessory chromosomes affecting their meiotic transmission. We conclude that

research on fungal accessory chromosomes, due to their small size, ease of sequencing, and epigenetic profiling, can complement the study of B chromosomes in deciphering factors that influence and regulate the non-Mendelian transmission of entire chromosomes.

Glossary box

Accessory chromosomes: Chromosomes that show presence/absence polymorphism between individuals of a population. These chromosomes are therefore considered non-essential. In plants and animals chromosomes these chromosomes are called B chromosomes and are typically considered to have a neutral or negative fitness cost.

In fungal species these are also called supernumerary chromosomes, minichromosomes, lineage specific chromosomes or (conditionally) dispensable chromosomes. Here, these chromosomes can encode genes that confer beneficial fitness effect under certain conditions (e.g., environments or hosts).

Ascospores: Haploid gametes, that are produced by fungi of the phylum Ascomycota. Ascospores that resulted from a single meiotic event are often contained in a sac-like structure (the ascus). This facilitates the collection of all products of a single meiotic event for a tetrad analysis.

H3K27me3: Posttranslational tri-methylation of the lysine at position 27 of core histone H3. In fungi, this posttranslational histone modification is considered a mark for facultative heterochromatin and is often enriched in the subtelomeric regions. Facultative heterochromatin is considered to be changing in its effect on transcription (transcriptionally silent ↔ transcriptionally active) over time and/or conditions.

H3K9me2/3: Posttranslational di- or trimethylation of the lysine at position 9 of the core histone H3. Considered to be a mark for constitutive heterochromatin (transcriptionally silent) and enriched on transposable elements.

Karyogamy: The fusion of two haploid nuclei of a dikaryon, which itself was the result of a fusion of the cytoplasms of two different fungal cells, called plasmogamy. The resulting cell is diploid and in ascomycetes usually enters meiosis to produce haploid ascospores.

Symmetric/Asymmetric Meiosis. Either all meiotic products are indistinguishable from each other and capable of transmitting genetic information (symmetric meiosis), e.g., many male meioses in animals or the meiotic products differ from each other and only a subset is capable of transmitting

genetic information (asymmetric meiosis), e.g., female meioses in animals, that result in the oocyte capable of transmitting genetic information and the polar bodies, which usually die.

Tetrad Analysis: Collection and analysis of all products of a single meiotic event. Allows for the distinction between different modes of meiotic drive (preferential segregation, preferential survival or additional replication).

Introduction

Non-Mendelian transmission represents a deviation from Mendel's axiom of equal probabilities for a heterozygous gene or chromosome to be transmitted to the meiotic progeny. Therefore, any process that increases or decreases the probability of transmission of a genetic element during meiosis will result in such non-Mendelian transmission. Non-Mendelian transmission is widespread and can affect short sequences as well as entire chromosomes (Hurst and Werren 2001). Here, we will focus on non-Mendelian segregation affecting entire chromosomes in fungi—which is restricted to mainly two processes: (i) meiotic chromosome drives and (ii) losses and disomies of entire chromosomes during meiosis.

Meiotic drives increase the frequency of a genetic element relative to the rest of an individual's genome. Small transmission advantages due to a meiotic drive can result in a rapid invasion of the genetic elements despite a neutral or negative fitness effect. Genetic elements that increase their transmission by a meiotic drive are therefore often considered selfish genetic elements (Werren et al. 1988; Hurst et al. 1992; Lyttle 1993; Hurst et al. 1996; Hurst and Werren 2001; McLaughlin and Malik 2017; Gardner and Ubeda 2017; Ågren and Clark 2018; Courret et al. 2019). Several studies have demonstrated that the symmetry of the meiotic cell divisions can predispose a system to the invasion of a specific type of meiotic drives (Kruger and Mueller 2021). Meiotic as well as mitotic cell divisions can be categorized as being either symmetric, i.e., all daughter cells are indistinguishable from each other or asymmetric where the daughter cells differ from each other. Symmetric meiotic cell divisions, e.g., many male meiotic cell divisions in animals, appear to be more prone to the invasion of drives that cause a difference in the fitness of gametes with and without the drive element (Kruger and Mueller 2021). One well-described example is the segregation distorter (SD) in *Drosophila* affecting the male meiosis, where the sperm cells that do not carry the drive element become functionally defective (Hurst and Werren 2001; Courret et al. 2019). Similarly, in male mice, the t-haplotype

represents a poison–antidote system that results in sperm mobility impairment (Herrmann et al. 1999, Bauer et al. 2005). In fungi, with symmetric meiosis, meiotic drive systems employing similar mechanisms seem to be prevalent. For example, in several species of the genus *Neurospora*, only the meiotic progeny (called ascospores) that carry the spore killer allele (*Sk-2* or *Sk-3*) survive, while ascospores without this allele typically deteriorate and die (Hammond et al. 2012; Svedberg et al. 2021). An additional example of an symmetric meiotic drive is the *wtf* poison–antidote system in yeast, where the *wtf* driver in *Schizosaccharomyces pombe* and *S. cambucha* encodes pre-meiotically expressed poison and the post-meiotically expressed antidote (Nuckolls et al. 2017; Hu et al. 2017), thus allowing only survival of spores carrying the *wtf* drive element. Similar systems are the *Het-s* drive and the *Spok* genes in the fungus *Podospora anserina* (Vogan et al. 2019; Grognet et al. 2014), as well as the qHMS7 locus in rice, *Oryza sativa* (Yu et al. 2018).

Asymmetric meiotic cell divisions, in which only a subset of the resulting meiotic daughter cells will provide genetic material to the next generation, on the other hand, appear to be more prone to the invasion of drive mechanisms that manipulate their segregation during the cell division. For instance, during female animal meiosis, asymmetric cytokinesis results in the production of the egg cell as well as polar bodies (which in many organisms usually die). Only the genetic material of the egg cell will be transmitted to the next generation. This asymmetric cell division is exploited by genetic elements that increase their segregation to the egg cell instead of to the polar bodies (Hurst and Werren 2001). In this regard, centromeres appear pivotal to the drive mechanism by affecting the segregation of the linked chromosomes; accordingly, these drive mechanisms are termed centromere drive (Henikoff et al. 2001; Malik 2009; Akera et al. 2017). Such a centromere drive has also been reported in monkeyflower (*Mimulus guttatus*) populations (Fishman and Willis 2005; Fishman and Saunders 2008) and in mice (Chmátal et al. 2014). In summary, based on examples from different groups of organisms, it is currently considered that the symmetry of meiotic cell divisions is one of the main factors that predisposes a system to the invasion of certain meiotic drive systems with either killing or segregation manipulation.

Accessory chromosomes are non-essential genetic elements in plants, animals, and fungi, and are often transmitted in a non-Mendelian way. These chromosomes, also known as B, supernumerary or (conditionally) dispensable chromosomes, are entire chromosomes that are by definition present in some but not all members of a population. Several fungal species (so far mainly described in genomes of plant pathogenic species) contain one or more distinct accessory chromosomes, which can

encompass a sizable portion of the fungal genome (Galazka and Freitag 2014; Mehrabi et al. 2017; Bertazzoni et al. 2018; Habig and Stukenbrock 2020). Accessory chromosomes in fungi, in contrast to accessory chromosomes (called B chromosomes) in plants and animals, more often confer a fitness benefit for the host individual (Han et al. 2001) but with some examples where the accessory chromosomes confer a negative fitness effect (Balesdent et al. 2013; Habig et al. 2017; Rouxel and Balesdent 2017). Some of these fungal accessory chromosomes contain genes that are indeed essential for the successful infection of certain plant hosts (Hatta et al. 2002; Ma et al. 2010). Fungal accessory chromosomes are similar to B chromosomes in plants and animals in their deviation from Mendelian segregation during meiosis. This non-Mendelian inheritance of fungal accessory chromosomes appears to involve either chromosome losses and duplications or transmission of an accessory chromosome to more progeny than predicted by Mendelian segregation, i.e., meiotic drive (Coleman et al. 2009; Croll et al. 2013; He et al. 1998; Mehrabi et al. 2017; Orbach et al. 1996; Wittenberg et al. 2009; Xu and Leslie 1996; Fouché et al. 2018; Habig et al. 2018). Fungal accessory chromosomes are unique among accessory chromosomes due to their functional diversity and their differences in mechanisms causing non-Mendelian segregation and meiotic drive. In this review, we will focus on mechanisms that could explain non-Mendelian transmission and the meiotic drive of fungal accessory chromosomes. First, we will give an overview of the structural and functional features of accessory chromosomes, which may be affecting their deviating transmission pattern.

Structure and function of accessory chromosomes in fungi

B chromosomes in plants and animals have been known since the beginning of the twentieth century (Wilson 1907). In contrast, the small accessory chromosomes of fungi were discovered much later by electrophoretic separation of chromosomes of different fungal individuals using pulsed-field gel electrophoresis (PFGE). Hence, the first reports of fungal accessory chromosomes in the phytopathogenic fungi *Nectria haematococca*, *Cochliobolus heterostrophus*, *Magnaporthe grisea*, and *Fusarium solani* date back only to the early 1990s (Miao et al. 1991; Mills and McCluskey 1990; Orbach et al. 1996; Talbot et al. 1993). Next-generation sequencing subsequently enabled more detailed analyses of accessory chromosomes in different fungal species. The comparatively small size of fungal genomes and the correspondingly short chromosome lengths facilitate these sequencing approaches. For many fungal organisms, chromosome-scale assemblies from telomere to telomere have been available for many years, including detailed annotations of genetic and epigenetic features. Furthermore, many fungi can easily be propagated in a haploid form, which facilitate sequencing and

simplifies genomic analysis. Hence, fungi represent excellent model organisms for studying meiotic drive and chromosomes transmission mechanisms.

Fungal accessory chromosomes appear to share certain specific, albeit non-unique, sequence characteristics. Accessory chromosomes vary in size from ~0.2 to ~3.5 Mb (Habig and Stukenbrock 2020), are enriched in transposons or repetitive sequences, and show lower gene densities and differences in codon usage compared to the essential core (also called A) chromosomes (Coleman et al. 2009; Ma et al. 2010; Goodwin et al. 2011). The accessory chromosomes appear mostly heterochromatic with an enrichment of the histone modification H3K9me2/3 (see glossary box), which is associated with constitutive heterochromatin (Freitag 2017; Studt et al. 2016; Connolly et al. 2013; Schotanus et al. 2015). Interestingly, fungal accessory chromosomes appear to have a unique histone modification pattern by being also enriched with H3K27me3 throughout their entire length (Galazka and Freitag 2014; Schotanus et al. 2015; Connolly et al. 2013; Studt et al. 2016; Fokkens et al. 2018; Erlendson et al. 2017). Interestingly, H3K27me3 seems to be also involved in the unique pattern of histone modifications found on B chromosomes of rye (Carchilan et al. 2007; Gonzalez-Sanchez et al. 2014). The presence of facultative heterochromatin therefore appears to be a distinctive trait of fungal accessory chromosomes while showing some overlap with epigenetics marks of B chromosomes. Finally, it is important to note that accessory chromosomes of fungi cannot be identified exclusively based on their sequence composition and structural characteristics. In some cases, core chromosomes can also comprise segments of low gene density, distinct heterochromatin structures, and high repeat content. Therefore, identifying accessory chromosomes in fungi currently solely relies on their presence/absence polymorphism.

Several fungal accessory chromosomes appear to have a positive fitness effect—at least under certain conditions. The functional relevance of fungal accessory chromosomes has mainly been addressed in plant pathogenic species (Bertazzoni et al. 2018; Mehrabi et al. 2017; Soyer et al. 2018; Habig and Stukenbrock 2020). Some of these chromosomes contain genes required for pathogenicity or growth within specific plant hosts or conditions. As an example, in the filamentous fungus *Alternaria alternata*, the AK-toxin gene cluster controlling host-specific pathogenicity resides on a 1.05-Mb accessory chromosome and the absence of this chromosome leads to avirulent phenotypes of this plant pathogen (Hatta et al. 2002). Likewise, the accessory chromosome 14 of the plant pathogenic isolates of *Fusarium oxysporum f.* sp. *lycopersici* contains genes required to infect tomatoes (Ma et al. 2010). It is important to note, that in a few cases, fungal accessory chromosomes do confer a

fitness disadvantage. In the wheat pathogen *Zymoseptoria tritici*, the deletion of whole accessory chromosomes resulted in strains with increased fitness (Habig et al. 2017). Hence, the fitness effects of fungal accessory chromosomes appear to be—in contrast to the B chromosomes in plants and animals—only in a few cases negative but mostly neutral or positive. Based on the identification of virulence-related genes on accessory chromosomes, it has been suggested that these small chromosomes represent dynamic genomic compartments promoting the rapid evolution of new adaptive traits (Croll and McDonald 2012). Such compartments with increased rates of evolution may be favored by the co-evolutionary interaction of pathogens with their host without affecting conserved housekeeping genes encoded by core chromosomes (Chuma et al. 2011; Taylor et al. 2017). In support of such a scenario, we recently demonstrated that the mutation rate on accessory chromosomes indeed is significantly higher than on the core chromosomes (Habig et al. 2021).

The origin of fungal accessory chromosomes is still unresolved and includes two main non-exclusive hypotheses. The first speculates that accessory chromosomes originated from core chromosomes (Galazka and Freitag 2014). This is supported by the distribution of families of repetitive elements (Grandaubert et al. 2015) that are shared between core and accessory chromosomes. Furthermore, genome sequencing of meiotic progenies demonstrated a breakage-fusion-bridge cycle as a process that gave rise to a new accessory chromosome in *Z. tritici* (Croll et al. 2013). In addition, recent macrosynteny analyses in the rice blast pathogen *Magnaporthe oryzae* followed the emergence of accessory mini-chromosomes via structural rearrangements and segmental duplication of core chromosomes (Langner et al. 2021). The second hypothesis of accessory chromosome origin proposes that accessory chromosomes originate via horizontal chromosome transfer from different lineages or species (Mehrabi et al. 2011). This idea is supported by differences in codon usage between core and accessory chromosomes (Goodwin et al. 2011) as well as experimental or phylogenetic evidence of horizontal transfer of entire chromosomes between distinct lineages (Akagi et al. 2009a, b; He et al. 1998; Ma et al. 2010; Masel et al. 1996). Since accessory chromosomes might have a different inheritance pattern (see next section), it is important to note that differences in sequence composition of core and accessory chromosomes may not necessarily relate to distinct origins but rather reflect differences in mutational processes, epigenetic marks, transmission, and evolutionary histories.

Non-Mendelian segregation and meiotic drives of accessory chromosomes in fungi

Many fungi have a sexual reproductive cycle but can also reproduce asexually (see Fig 1). In addition, the distinction between somatic and germline cells cannot be defined in fungi, since individual cells are —in most cases—totipotent. Hence, the distribution of accessory chromosomes is not solely affected by their inheritance during meiosis but also by their transmission during mitotic growth. We will therefore use the term "transmission" to generally describe the behavior of accessory chromosomes during cell divisions, considering both mitotic and meiotic cell divisions, to emphasize that both types of cell divisions affect the presence/absence polymorphisms of accessory chromosomes. We will briefly introduce transmission patterns of fungal accessory chromosomes during mitotic divisions before focusing on their transmission during meiotic cell divisions. It is important to note, that the small size of fungal accessory chromosomes makes the microscopic analysis of their transmission during mitotic or meiotic cell divisions very challenging. At the same time, this small chromosome size in concert with the ease of access to haploid cells and, in the case of sexually reproducing fungi, the ease of access to entire tetrads allows a very detailed analysis of their transmission pattern via whole-genome sequencing. The availability of high-quality genome assemblies spanning chromosomes from telomere to telomere further facilitates such genome-based analyses, which are therefore the focus of this review.
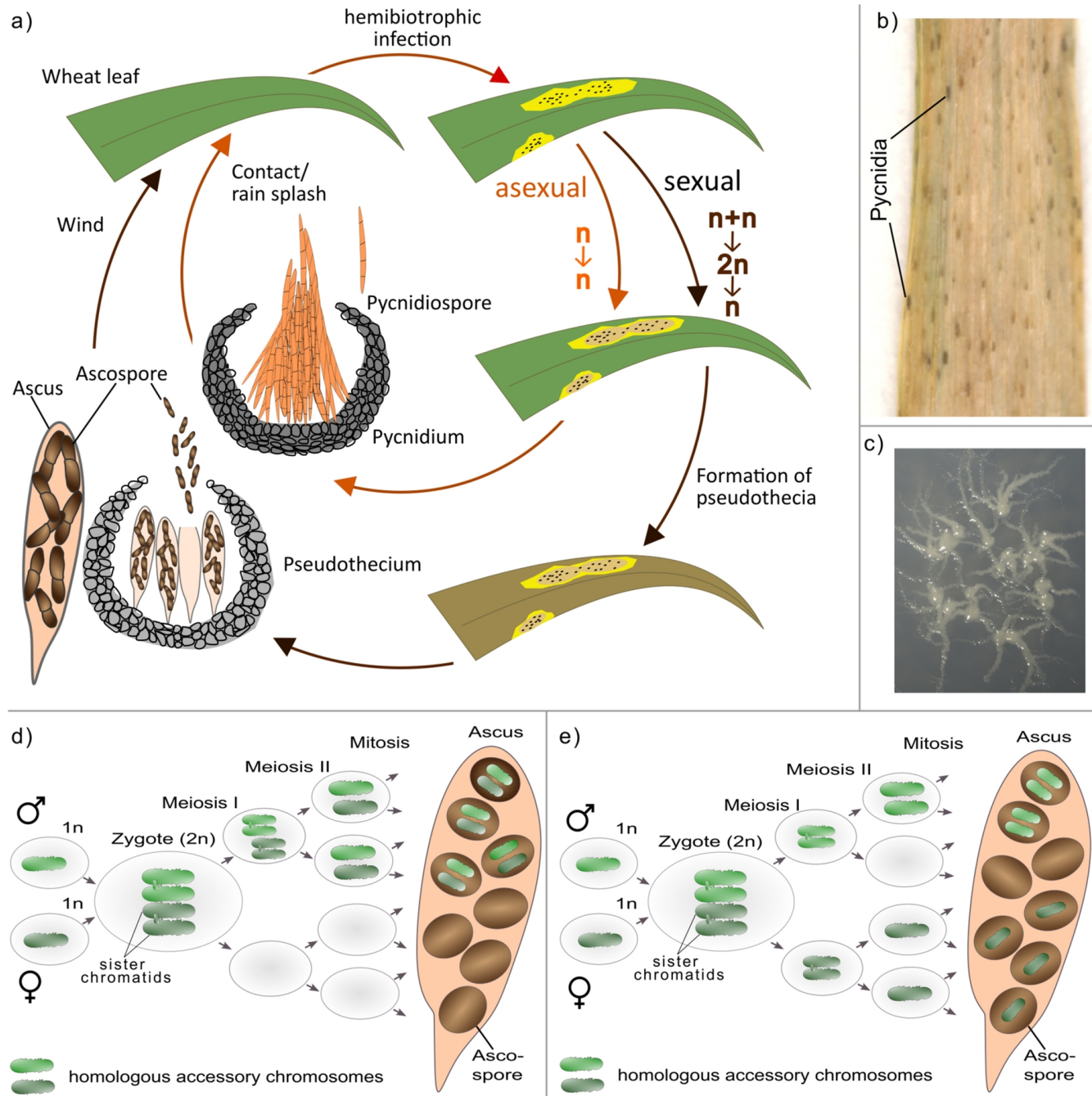
Fig 1. a Life cycle of *Z. tritici* as an example of an Ascomycete life cycle containing both asexual and sexual reproduction. Asexual reproduction results in pycnidiospores (asexual haploid spores), produced by asexual fruiting body (pycnidia) in infected wheat leaves (adapted from Ponomarenko 2011). The asexual cycle is assumed to only contain haploid cells. Sexual reproduction in *Z. tritici* results in ascospores (sexual haploid spores) produced in the sexual fruiting body (pseudothecium). Here, two specialized haploid cells fuse to form a diploid zygote which undergoes two meiotic cell divisions and one mitotic cell division to produce eight haploid ascospores contained in a sac-like structure (ascus). **b** Example pictures of asexual fruiting body (pycnidia) formed by *Z. tritici* on necrotic leaf tissue lesion carrying asexual pycnidiospores on a wheat leaf infected with *Z.*

tritici. **c** Example picture of in vitro growth of *Z. tritici* growing on xylose minimum medium. **d–e** Models for losses and disomies of fungal accessory chromosomes due to nondisjunction of **d** homologous chromosomes or **e** sister chromatids during meiotic cell divisions. **d** Homologous accessory chromosomes fail to segregate at first meiotic division which leads to their disomy in half of the progeny and the absence of respective homologous accessory chromosomes in the remaining half of ascospores. **e** Nondisjunction of sister chromatids during the second meiotic division causes loss and disomy of accessory chromosomes. In contrast to disomic progeny from **d**, disomic accessory chromosomes are identical and chromosomes are absent in 25% of the progeny. For the sake of clarity, no recombination events are depicted

Fungal accessory chromosomes are frequently lost during mitotic propagation in several fungi. In the asexual tomato pathogen, *F. oxysporum f.* sp. *lycopersici* accessory chromosomes are lost during mitotic growth at a frequency of 1 in 35,000 spores (Vlaardingerbroek et al. 2016). Much higher loss rates of accessory chromosomes have been reported for members of the genus *Zymoseptoria*. Here, *Z. tritici* and its sister species *Z. ardabiliae* showed a loss of accessory chromosomes in 1 out of 50 spores (Möller et al. 2018; Habig et al. 2021). Interestingly, temperature greatly impacts the stability of chromosomes whereby an increased temperature (28°C) dramatically increases the loss rate of accessory chromosomes in *Z. tritici* (Möller et al. 2018; Habig et al. 2021). These increased losses of accessory chromosomes during mitotic cell divisions do not appear to be a result of sister chromatid nondisjunction during mitosis but rather due to aberrant DNA replication possibly impacted by the histone modification H3K27me3 (Habig et al. 2021). Accessory chromosomes in *Z. tritici*, *F. oxysporum*, *F. asiaticum*, and *Gibberella fujikuroi* are enriched in the histone modification H3K27me3 (Galazka and Freitag 2014; Schotanus et al. 2015; Fokkens et al. 2018). This histone modification appears to destabilize accessory chromosomes and increase the mutation rate (Möller et al. 2019; Habig et al. 2021). H3K27me3 appears to be a hallmark of accessory chromosomes as H3K27me3 on core chromosomes is restricted to the subtelomeric regions and moreover associates these regions with the nuclear envelope (Erlendson et al. 2017; Harr et al. 2015, 2016). We speculate that the enrichment throughout the entire length of the fungal accessory chromosomes might associate the entire chromosome with the nuclear envelope and thereby affect DNA replication (Möller et al. 2019; Habig et al. 2021) and the transmission of accessory chromosomes during mitotic divisions. Possibly, this effect of histone modifications on DNA replication of accessory chromosomes could also be pivotal during the meiotic transmission of the accessory chromosomes and their meiotic drive.

Accessory chromosomes often show a non-Mendelian transmission during meiotic cell divisions in fungi that undergo sexual reproduction. This can involve either chromosome losses or segregation distortion and/or meiotic drives. Losses of accessory chromosomes during meiotic cell divisions

appear frequently. As an example, *L. maculans*, the stem canker agent of oilseed rape (*Brassica napus*), contains an accessory chromosome (termed conditionally dispensable chromosome (CDC) in this species) that is lost in approximately 5% of the progeny following meiosis (Balesdent et al. 2013; Leclair et al. 1996). It is however unclear whether this loss is accompanied by disomy of the same chromosome in one of the other products of the meiotic cell division—and therefore is the result of nondisjunction of chromosome homologs or sister chromatids. Nondisjunction events that lead to the loss of accessory chromosome occur during first or second meiotic divisions and are associated with a corresponding chromosome duplication or disomy (Fig 1). The accessory chromosome of the rice blast fungus *M. oryzae* (called mini-chromosomes in this species) also shows non-Mendelian transmission during crosses due to nondisjunction during meiosis I or meiosis II (Orbach et al. 1996). Loss and corresponding disomy of the accessory chromosome PDA1-CDC in *N. haematococca* MPVI (called conditionally dispensable chromosome in this species) suggest the occurrence of nondisjunction of chromosomes in meiosis I (Miao et al. 1991; Garmaroodi and Taga 2007, 2015). Accessory chromosomes in *Z. tritici* also show non-Mendelian inheritance with up to 20% of the progeny from a meiotic cross being reported to have lost one or more accessory chromosomes (Fouché et al. 2018; Wittenberg et al. 2009). Correspondingly, disomies of accessory chromosomes are a frequent result of meiosis in *Z. tritici*, which would indicate meiotic nondisjunction events (Fouché et al. 2018). Furthermore, we confirmed both nondisjunctions as well as losses of accessory chromosomes in *Z. tritici* via tetrad analysis of all meiotic products of individual meioses and showed that simultaneously nondisjunctions were absent for the core chromosomes (Habig et al. 2018). In summary, non-Mendelian inheritance due to nondisjunction appears to be a common process for fungal accessory chromosomes. One could speculate that the apparent higher frequency of nondisjunctions in fungal accessory chromosomes compared to core chromosomes could be due to either (i) a functional difference in the centromeres of the accessory chromosomes or (ii) a higher probability to observe nondisjunctions in accessory chromosomes due to their non-essential role and therefore possibly lack of lethal gene-doses effect or (iii) mechanistic differences in the meiosis of core and accessory chromosomes. In *Z. tritici*, the centromeres of core and accessory chromosomes are indistinguishable based on their sequence composition and structure (Schotanus et al. 2015). Nevertheless, disomies of certain core chromosomes occur during longtime mitotic propagation ruling out a lethal gene-doses effect of these disomies. Consequently, it is very plausible that the difference in the frequency of nondisjunctions for core and accessory chromosomes relates to differences in their meiotic behavior. Nondisjunction events will not by themselves change the relative frequency of accessory chromosomes in a population compared to core chromosomes, provided that disomies of

accessory chromosomes have no fitness effect. Therefore, other mechanisms conferring a transmission advantage or a fitness advantage are likely involved in the maintenance and the dynamics of accessory chromosomes in fungal organisms.

Several fungal accessory chromosomes increase in frequency during meiotic cell divisions (Balesdent et al. 2013; Fouché et al. 2018; Goodwin et al. 2011; Tzeng et al. 1992; Wittenberg et al. 2009). In fungi of the phylum *Ascomycota*, haploid individuals can sexually reproduce by fusion of specialized cells (plasmogamy) followed by fusion of the two separate haploid nuclei (karyogamy) eventually resulting in a diploid zygote which then undergoes meiosis to produce the haploid meiotic products. These meiotic products are contained in an eponymous sac (ascus) (see Fig 1). By detailed analyses of the ascospores contained in one ascus, the transmission of the accessory chromosomes from the haploid parental strain via the diploid zygote to the haploid ascospores can be easily tracked. The non-essential nature of accessory chromosomes allows for a more encompassing analysis of their transmission as any loss, disomy, or other large-scale chromosomal events are non-lethal and therefore visible in the ascospore progenies. Although accessory chromosomes provide excellent model systems to study molecular mechanisms associated with meiosis, we still lack detailed insights into the underlying aspects of their transmission advantages. The first report of a transmission advantage of a fungal accessory chromosome was on accessory chromosome 16 of *C. heterostrophus*, the causal pathogen of the disease southern corn leaf blight (Tzeng et al. 1992). Although only one of the two haploid parental strains contained the accessory chromosome 16, two-thirds of meiotic products inherited the chromosome (Tzeng et al. 1992). Similarly, in *Leptosphaeria maculans*, the causal pathogen of stem canker of oilseed rape, 83% of the meiotic products contained the accessory chromosome (called mini-chromosome in this species), although only one of the parental strains contained the accessory chromosome (Balesdent et al. 2013). These transmission advantages of unpaired accessory chromosomes (i.e., chromosomes inherited from only one of the parental strains) may reflect the presence of a meiotic chromosome drive. Possibly this transmission advantage could be due to increased survival of meiotic progeny containing the accessory chromosome or alternatively the unpaired accessory chromosomes could be subject to an additional replication. Thus, the mechanism affecting the transmission of fungal accessory chromosomes in these two species still remains unclear. Tetrad analyses and genome analyses of ascospore progenies should be applied to these two species to identify the underlying mechanisms of accessory chromosome dynamics.

Tetrad analysis—the collection and analysis of all products of a single meiosis—can distinguish pre- and post-meiotic effects and has been conducted for the accessory chromosomes in the wheat pathogen *Z. tritici*. Here, unpaired accessory chromosomes are transmitted to all haploid meiotic progenies (called ascospores) revealing the presence of a meiotic drive mechanism (Habig et al. 2018). Interestingly, this meiotic drive affects only those unpaired accessory chromosomes of *Z. tritici* that were inherited from the parental strain that also provided the mitochondria to the ascospore progenies (i.e., the female parent) (Habig et al. 2018) (see Fig 2). In contrast, when the same unpaired accessory chromosome from the same parental strain was inherited from the male parent (i.e., not providing the mitochondria), the accessory chromosomes followed Mendelian segregation and were transmitted to ~50% of the progeny (see Fig 2). Interestingly, accessory chromosomes that had a homolog in each of the two parental strains also showed Mendelian segregation as well as recombination, implying canonical homologous pairing and segregation (Habig et al. 2018). This meiotic drive therefore appears mechanistically different from all previously characterized meiotic chromosome drives.
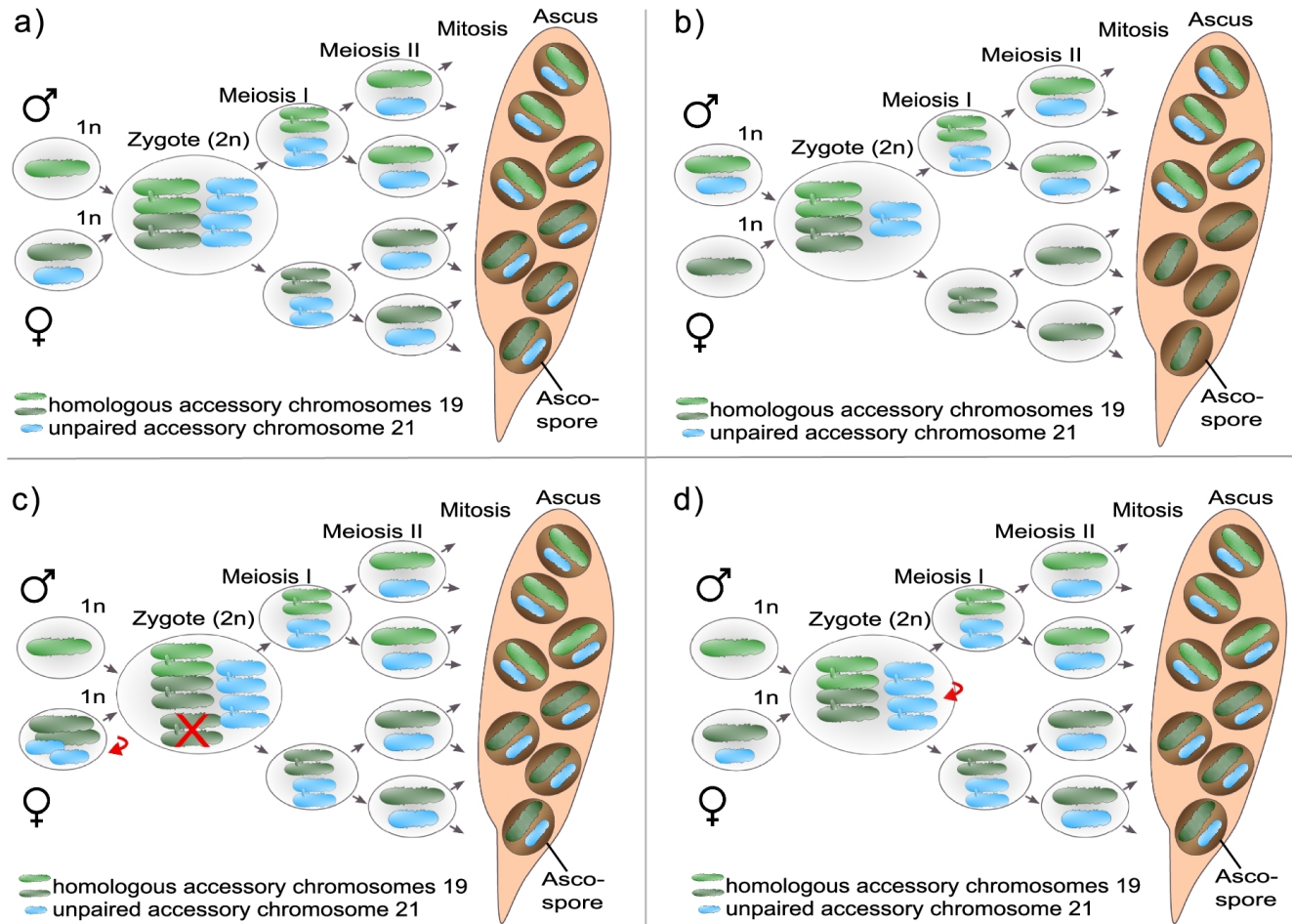
Fig 2. Meiotic drive of accessory chromosomes in *Z. tritici*. **a** Accessory chromosomes show presence/absence polymorphisms among individuals in populations and thus can be unpaired during meiosis. The chromosomal drive during meiosis in *Z. tritici* is restricted to female-inherited and unpaired accessory chromosomes (light blue) and causes an overrepresentation of female-inherited unpaired accessory chromosomes in the progeny. **b** Male-inherited unpaired accessory chromosomes (light blue) show Mendelian segregation as well as the paired accessory chromosomes (light green and dark green). The potential mechanism of the meiotic drive of accessory chromosomes likely involves additional replication that can happen either **c** prior to the fusion of two haploid gametes or **d** in the diploid zygote. If **c** is true, all chromosomes in the female haploid gamete should be amplified (red arrow), and in the zygote, the additional copies of paired accessory chromosomes must be deleted (red cross). Alternatively, **d** the unpaired female-inherited accessory chromosomes are amplified in the zygote. For simplicity, recombination events are not shown

To date, meiotic drives have been mostly categorized into two main mechanisms: (i) preferential segregation during asymmetric pre-meiotic, meiotic, or post-meiotic cell divisions or (ii) disruption of gametes that do not carry the drive element (Hurst and Werren 2001; Werren 2011). Both of these mechanistic categories do not include an additional amplification of the drive element in sensu stricto. The fact that paired accessory chromosomes of *Z. tritici* follow Mendelian segregation while the same

chromosomes show a meiotic drive when being unpaired and inherited from the female parent could be explained by either (i) an additional replication of all accessory chromosomes from the female parent followed by a selective elimination of all additional copies of paired accessory chromosomes (Fig 2) or (ii) an additional amplification of unpaired accessory chromosomes in the zygote (see Fig 2). It is important to note that complete tetrads could be isolated, and hence, no spore death is associated with the drive. Neither preferential segregation nor disruption of gametes would allow for the isolation of complete tetrads; therefore, these mechanisms cannot be responsible for the observed meiotic drive of female-inherited unpaired chromosomes (Habig et al. 2018). A recent tetrad analyses in *Z. tritici* could further pinpoint an additional replication of accessory chromosomes prior to zygote formation (unpublished data, Fig 2). Consequently, the meiotic drive in *Z. tritici* relies on a preferential elimination of additional copies of the accessory chromosomes that do have a homolog in both strains. The exact mechanism for this drive is however still unclear.

One of the main open questions is how core and accessory chromosomes are distinguished by the cell. We speculate that particular epigenetic marks could be responsible, in particular, H3K27me3, which appears to distinguish accessory chromosomes from core chromosomes (Schotanus et al. 2015), possibly via its effect on the localization of these chromosomes within the nucleus (Möller et al. 2019) and/or their replication (Habig et al. 2021). Recently, we could show that H3K27me3 affects the replication of accessory chromosomes in *Z. tritici* during mitotic propagation (Habig et al. 2021), which indicates that their replication might also be affected by H3K27me3 during meiotic transmission, possibly also playing a role in their meiotic drive. We speculate that H3K27me3 might associate the accessory chromosomes with the nuclear envelope (Möller et al. 2018; Habig et al. 2021) and that this difference in location compared to the core chromosomes can contribute to the additional replication and meiotic drive. We are currently testing this hypothesis. In summary, our crossing experiments provide evidence for the relevance of a meiotic drive of accessory chromosomes in *Z. tritici* ensuring their maintenance over evolutionary time despite their fitness cost (Habig et al. 2017). Indeed, a similar drive mechanism could exist for other fungal accessory chromosomes for which a transmission advantage is observed.

Concluding remarks

Although non-Mendelian segregation and meiotic drive appear frequent for fungal accessory chromosomes, they are mechanistically much less understood than those affecting B chromosomes in plants and animals or other genetic drive mechanisms. With fungal accessory chromosomes mainly described for pathogenic fungi, and containing genes affecting the pathogenicity, we argue that their transmission during meiosis should warrant detailed analysis. The identification of a potentially novel mechanism for a meiotic drive in *Z. tritici* serves as an example encouraging the potential discoveries in other fungal species. The general question, which unique features of accessory chromosomes affect or regulate their transmission during meiosis, is however not restricted solely to fungal accessory chromosomes but to all chromosome affected by a meiotic drive. We speculate that epigenetic modifications could be—at least for the fungal accessory chromosomes—such a distinguishing characteristic. These epigenetic modifications could play a role in the non-Mendelian transmission of accessory chromosomes in fungi but also could potentially be involved in the unique transmission pattern of B chromosomes in other eukaryotes. The small genome sizes, the general ease of access to haploid parental strains and meiotic progeny, and the non-essentiality of fungal accessory chromosomes will further facilitate studies on general meiotic processes. We consider fungal accessory chromosomes as a remarkable class of genomic components that can provide novel insights into mechanisms regulating the meiotic and mitotic transmission of chromosomes in general as well as the atypical inheritance of B chromosomes in other eukaryotes.

References

Akera T, Chmátal L, Trimm E, Yang K, Aonbangkhen C, Chenoweth DM, Janke C, Schultz RM, Lampson MA (2017) Spindle asymmetry drives non-Mendelian chromosome segregation. Science 358(6363):668–672. https://doi.org/10.1126/science.aan0092

Balesdent M, Fudal I, Ollivier B, Bally P, Grandaubert J, Eber F, Chèvre AM, Leflon M, Rouxel T (2013) The dispensable chromosome of L eptosphaeria maculans shelters an effector gene conferring avirulence towards Brassica rapa. New Phytol 198(3):887–898. https://doi.org/10.1111/nph.12178

Bauer H, Willert J, Koschorz B, Herrmann BG (2005) The t complex–encoded GTPase-activating protein Tagap1 acts as a transmission ratio distorter in mice. Nat Genet 37:969–973. https://doi.org/10.1038/ng1617

Bertazzoni S, Williams AH, Jones DA, Syme RA, Tan K-C, Hane JK (2018) Accessories make the outfit: accessory chromosomes and other dispensable DNA regions in plant-pathogenic fungi. Mol Plant-Microbe Interactions : MPMI 31(8):779–788. https://doi.org/10.1094/MPMI-06-17-0135-FI

Carchilan M, Delgado M, Ribeiro T, Costa-Nunes P, Caperta A, Morais-Cecílio L, Jones RN, Viegas W, Houben A (2007) Transcriptionally active heterochromatin in rye B chromosomes. Plant Cell 19(6):1738–1749. https://doi.org/10.1105/tpc.106.046946

Chmátal L, Gabriel SI, Mitsainas GP, Martínez-Vargas J, Ventura J, Searle JB, Schultz RM, Lampson MA (2014) Centromere strength provides the cell biological basis for meiotic drive and karyotype evolution in mice. Curr Biol 24(19):2295–2300. https://doi.org/10.1016/j.cub.2014.08.017

Croll D, McDonald BA (2012) The accessory genome as a cradle for adaptive evolution in pathogens. PLoS Pathog 8:e1002608. https://doi.org/10.1371/journal.ppat.1002608

Croll D, Zala M, McDonald BA (2013) Breakage-fusion-bridge cycles and large insertions contribute to the rapid evolution of accessory chromosomes in a fungal pathogen. PLOS Genet 9(6):e1003567. https://doi.org/10.1371/journal.pgen.1003567

Erlendson AA, Friedman S, Freitag M (2017) A matter of scale and dimensions: chromatin of chromosome landmarks in the fungi. Microbiol Spectr 5(4):4–5. https://doi.org/10.1128/microbiolspec.FUNK-0054-2017

Fishman L, Saunders A (2008) Centromere-associated female meiotic drive entails male fitness costs in monkeyflowers. Science 322(5907):1559–1562. https://doi.org/10.1126/science.1161406

Fouché S, Plissonneau C, McDonald BA, Croll D (2018) Meiosis leads to pervasive copy-number variation and distorted inheritance of accessory chromosomes of the wheat pathogen Zymoseptoria tritici. Genome Biol Evol 10(6):1416–1429. https://doi.org/10.1093/gbe/evy100

Freitag M (2017) Histone methylation by SET domain proteins in Fungi. Annu Rev Microbiol 71:413–439. https://doi.org/10.1146/annurev-micro-102215-095757

Galazka JM, Freitag M (2014) Variability of chromosome structure in pathogenic fungi—of 'ends and odds.' Curr Opin Microbiol 20:19–26. https://doi.org/10.1016/j.mib.2014.04.002

Gardner A, Úbeda F (2017) The meaning of intragenomic conflict. Nat Ecol Evol 1(12):1807–1815

Garmaroodi HS, Taga M (2007) Duplication of a conditionally dispensable chromosome carrying pea pathogenicity (PEP) gene clusters in Nectria haematococca. Mol Plant Microbe Interact 20(12):1495–1504. https://doi.org/10.1094/MPMI-20-12-1495

Garmaroodi HS, Taga M (2015) Meiotic inheritance of a fungal supernumerary chromosome and its effect on sexual fertility in Nectria haematococca. Fungal Biol 119(10):929–939. https://doi.org/10.1016/j.funbio.2015.07.004

González-Sánchez M, Heredia V, Diez M, Puertas MJ (2014) Rye B chromosomes influence the dynamics of histone H3 methylation during microgametogenesis. Cytogenet Genome Res 143(1–3):189–199. https://doi.org/10.1159/000365422

Grandaubert J, Bhattacharyya A, Stukenbrock EH (2015) RNA-seq-based gene annotation and comparative genomics of four fungal grass pathogens in the genus zymoseptoria identify novel orphan genes and species-specific invasions of transposable elements. G3 (Bethesda, Md.) 5(7):1323–1333. https://doi.org/10.1534/g3.115.017731

Grognet P, Lalucque H, Malagnac F, Silar P (2014) Genes that bias Mendelian segregation. PLoS Genet 10:e1004387. https://doi.org/10.1371/journal.pgen.1004387

Habig M, Quade J, Stukenbrock EH (2017) Forward genetics approach reveals host genotype-dependent importance of accessory chromosomes in the fungal wheat pathogen *Zymoseptoria tritici*. Mbio 8(6):e01919-e2017. https://doi.org/10.1128/mBio.01919-17

Habig M, Kema GHJ, Holtgrewe Stukenbrock E (2018) Meiotic drive of female-inherited supernumerary chromosomes in a pathogenic fungus. Elife 7:e40251. https://doi.org/10.7554/eLife.40251

Habig M, Lorrain C, Feurtey A, Komluski J, Stukenbrock EH (2021) Epigenetic modifications affect the rate of spontaneous mutations in a pathogenic fungus. Nat Commun 12(1):1–13. https://doi.org/10.1038/s41467-021-26108-y

Han Y, Liu X, Benny U, Kistler HC, VanEtten HD (2001) Genes determining pathogenicity to pea are clustered on a supernumerary chromosome in the fungal plant pathogen Nectria haematococca. Plant J 25(3):305–314. https://doi.org/10.1046/j.1365-313x.2001.00969.x

Harr JC, Luperchio TR, Wong X, Cohen E, Wheelan SJ, Reddy KL (2015) Directed targeting of chromatin to the nuclear lamina is mediated by chromatin state and A-type lamins. J Cell Biol 208(1):33–52. https://doi.org/10.1083/jcb.201405110

Hatta R, Ito K, Hosaki Y, Tanaka T, Tanaka A, Yamamoto M, Akimitsu K, Tsuge T (2002) A conditionally dispensable chromosome controls host-specific pathogenicity in the fungal plant pathogen Alternaria alternata. Genet 161(1):59–70. https://doi.org/10.1093/genetics/161.1.59

He C, Rusu AG, Poplawski AM, Irwin JA, Manners JM (1998) Transfer of a supernumerary chromosome between vegetatively incompatible biotypes of the fungus Colletotrichum gloeosporioides. Genetics 150(4):1459–1466. https://doi.org/10.1093/genetics/150.4.1459

Henikoff S, Ahmad K, Malik HS (2001) The centromere paradox: stable inheritance with rapidly evolving DNA. Science 293(5532):1098–1102. https://doi.org/10.1126/science.1062939

Herrmann BG, Koschorz B, Wertz K et al (1999) A protein kinase encoded by the t complex responder gene causes non-mendelian inheritance. Nature 402:141–146. https://doi.org/10.1038/45970

Hu W, Jiang Z-D, Suo F et al (2017) A large gene family in fission yeast encodes spore killers that subvert Mendel's law. ELife 6:e26057. https://doi.org/10.7554/eLife.26057

Hurst GDD, Werren JH (2001) The role of selfish genetic elements in eukaryotic evolution. Nat Rev Genet 2(8):597–606. https://doi.org/10.1038/35084545

Hurst GDD, Hurst LD, Johnstone RA (1992) Intranuclear conflict and its role in evolution. Trends Ecol Evol 7:373–378. https://doi.org/10.1016/0169-5347(92)90007-X

Hurst LD, Atlan A, Bengtsson BO (1996) Genetic conflicts. Q Rev Biol 71(3):317–364. https://doi.org/10.1086/419442

Kruger AN, Mueller JL (2021) Mechanisms of meiotic drive in symmetric and asymmetric meiosis. Cell Mol Life Sci 78(7):3205–3218. https://doi.org/10.1007/s00018-020-03735-0

Leclair S, Ansan-Melayah D, Rouxel T, Balesdent M (1996) Meiotic behaviour of the minichromosome in the phytopathogenic ascomycete Leptosphaeria maculans. Curr Genet 30(6):541–548. https://doi.org/10.1007/s002940050167

Lyttle TW (1993) Cheaters sometimes prosper: distortion of mendelian segregation by meiotic drive. Trends Genet 9(6):205–210. https://doi.org/10.1016/0168-9525(93)90120-7

McLaughlin RN Jr, Malik HS (2017) Genetic conflicts: the usual suspects and beyond. J Exp Biol 220(1):6–17. https://doi.org/10.1242/jeb.148148

Mehrabi R, Bahkali AH, Abd-Elsalam KA, Moslem M, Ben M'Barek S, Gohari AM, Jashni MK, Stergiopoulos I, Kema GH, de Wit PJ (2011) Horizontal gene and chromosome transfer in plant pathogenic fungi affecting host range. FEMS Microbiol Rev 35(3):542–554. https://doi.org/10.1111/j.1574-6976.2010.00263.x

Mehrabi R, Mirzadi Gohari A, Kema GHJ (2017) Karyotype variability in plant-pathogenic fungi. Annu Rev Phytopathol 55:483–503. https://doi.org/10.1146/annurev-phyto-080615-095928

Miao VP, Covert SF, VanEtten HD (1991) A fungal gene for antibiotic resistance on a dispensable ("B") chromosome. Science 254(5039):1773LP – 1776. https://doi.org/10.1126/science.1763326

Mills D, McCluskey K (1990) Electrophoretic karyotypes of fungi: the new cytology. Mol Plant-Microbe Interact 3:351–357

Möller M, Habig M, Freitag M, Stukenbrock EH (2018) Extraordinary genome instability and widespread chromosome rearrangements during vegetative growth. Genetics 210(2):517–529. https://doi.org/10.1534/genetics.118.301050

Orbach MJ, Chumley FG, Valent B (1996) Electrophoretic karyotypes of Magnaporthe grisea pathogens of diverse grasses. MPMI-Molecular Plant Microbe Interactions 9(4):261–271

Rouxel T, Balesdent M (2017) Life, death and rebirth of avirulence effectors in a fungal pathogen of B rassica crops. L eptosphaeria maculans. New Phytologist 214(2):526–532. https://doi.org/10.1111/nph.14411

Soyer JL, Balesdent M-H, Rouxel T, Dean RA (2018) To B or not to B: a tale of unorthodox chromosomes. Curr Opin Microbiol 46:50–57. https://doi.org/10.1016/j.mib.2018.01.012

Studt L, Rösler SM, Burkhardt I, Arndt B, Freitag M, Humpf HU, Dickschat JS, Tudzynski B (2016) Knock-down of the methyltransferase Kmt6 relieves H3K27me3 and results in induction of cryptic and otherwise silent secondary metabolite gene clusters in Fusarium fujikuroi. Environ Microbiol 18(11):4037–4054. https://doi.org/10.1111/1462-2920.13427

Talbot NJ, Salch YP, Ma M, Hamer JE (1993) Karyotypic variation within clonal lineages of the rice blast fungus, Magnaporthe grisea. Appl Environ Microbiol 59(2):585–593

Tzeng T-H, Lyngholm LK, Ford CF, Bronson CR (1992) A restriction fragment length polymorphism map and electrophoretic karyotype of the fungal maize pathogen Cochliobolus heterostrophus. Genetics 130(1):81–96

Vlaardingerbroek I, Beerens B, Rose L, Fokkens L, Cornelissen BJC, Rep M (2016) Exchange of core chromosomes and horizontal transfer of lineage-specific chromosomes in Fusarium oxysporum. Environ Microbiol 18(11):3702–3713. https://doi.org/10.1111/1462-2920.13281

Vogan AA, Ament-Velásquez SL, Granger-Farbos A et al (2019) Combinations of Spok genes create multiple meiotic drivers in Podospora. ELife 8:e46454. https://doi.org/10.7554/eLife.46454

Wilson EB (1907) The supernumerary chromosomes of Hemiptera. Science 26:870–871. https://doi.org/10.1126/science.26.677.870-a

Xu JR, Leslie JF (1996) A genetic map of Gibberella fujikuroi mating population A (Fusarium moniliforme). Genetics 143(1):175–189

Yu X, Zhao Z, Zheng X et al (2018) A selfish genetic element confers non-Mendelian inheritance in rice. Science 360:1130–1132. https://doi.org/10.1126/science.aar4279

Ågren JA, Clark AG (2018) Selfish genetic elements. PLoS Genet 14(11):e1007700. https://doi.org/10.1371/journal.pgen.1007700

Akagi Y, Akamatsu H, Otani H, Kodama M (2009a) Horizontal chromosome transfer, a mechanism for the evolution and differentiation of a plant-pathogenic fungus. Eukaryot Cell 8(11):1732–1738. https://doi.org/10.1128/EC.00135-09

Akagi Y, Taga M, Yamamoto M et al (2009b) Chromosome constitution of hybrid strains constructed by protoplast fusion between the tomato and strawberry pathotypes of Alternaria alternata. J Gen Plant Pathol 75:101–109

Chuma I, Isobe C, Hotta Y, Ibaragi K, Futamata N, Kusaba M, Yoshida K, Terauchi R, Fujita Y, Nakayashiki H, Valent B (2011) Multiple translocation of the AVR-Pita effector gene among chromosomes of the rice blast fungus Magnaporthe oryzae and related species. PLoS Pathog 7(7):e1002147. https://doi.org/10.1371/journal.ppat.1002147

Coleman JJ, Rounsley SD, Rodriguez-Carres M, Kuo A, Wasmann CC, Grimwood J, … Vanetten HD (2009) The genome of Nectria haematococca: contribution of supernumerary chromosomes to gene expansion. PLoS Genet 5(8):e1000618. https://doi.org/10.1371/journal.pgen.1000618

Connolly LR, Smith KM, Freitag M (2013) The Fusarium graminearum histone H3 K27 methyltransferase KMT6 regulates development and expression of secondary metabolite gene clusters. PLoS Genetics 9(10):e1003916. https://doi.org/10.1371/journal.pgen.1003916

Courret C, Chang C-H, Wei KH-C et al (2019) Meiotic drive mechanisms: lessons from Drosophila. Proc R Soc B 286:20191430. https://doi.org/10.1098/rspb.2019.1430

Fishman L, Willis JH (2005) A novel meiotic drive locus almost completely distorts segregation in Mimulus (monkeyflower) hybrids. Genetics 169(1):347–353. https://doi.org/10.1534/genetics.104.032789

Fokkens L, Shahi S, Connolly LR et al (2018) The multi-speed genome of Fusarium oxysporum reveals association of histone modifications with sequence divergence and footprints of past horizontal chromosome transfer events. 465070 https://doi.org/10.1101/465070

Goodwin SB, M'barek SB, Dhillon B, Wittenberg AHJ, Crane CF, Hane JK, … Kema GHJ (2011) Finished genome of the fungal wheat pathogen Mycosphaerella graminicola reveals dispensome structure, chromosome plasticity, and stealth pathogenesis. PLoS Genet 7(6):e1002070. https://doi.org/10.1371/journal.pgen.1002070

Habig M, Stukenbrock EH (2020) 2 Origin, function, and transmission of accessory chromosomes. Genet Biotechnol. Springer, pp 25–47. https://doi.org/10.1007/978-3-030-49924-2_2

Hammond TM, Rehard DG, Xiao H, Shiu PKT (2012) Molecular dissection of Neurospora spore killer meiotic drive elements. Proc Natl Acad Sci 109(30):12093 LP – 12098. https://doi.org/10.1073/pnas.1203267109

Harr JC, Gonzalez-Sandoval A, Gasser SM (2016) Histones and histone modifications in perinuclear chromatin anchoring: from yeast to man. EMBO Rep 17(2):139–155. https://doi.org/10.15252/embr.201541809

Langner T, Harant A, Gomez-Luciano LB, Shrestha RK, Malmgren A, Latorre SM, Burbano HA, Win J, Kamoun S (2021) Genomic rearrangements generate hypervariable mini-chromosomes in host-specific isolates of the blast fungus. PLoS Genet 17(2):e1009386. https://doi.org/10.1371/journal.pgen.1009386

Ma L-J, van der Does HC, Borkovich KA, Coleman JJ, Daboussi M-J, Di Pietro A, … Rep M (2010) Comparative genomics reveals mobile pathogenicity chromosomes in Fusarium. Nature 464(7287):367–373. https://doi.org/10.1038/nature08850

Malik HS (2009) The centromere-drive hypothesis: a simple basis for centromere complexity. In: Ugarkovic D (ed) Centromere: Structure and Evolution. Springer, Berlin, Heidelberg, pp 33–52. https://doi.org/10.1007/978-3-642-00182-6_2

Masel AM, He C, Poplawski AM et al (1996) Molecular evidence for chromosome transfer between biotypes of Colletotrichum gloeosporioides. MPMI 9:339–348. https://doi.org/10.1094/MPMI-9-0339

Möller M, Schotanus K, Soyer JL, Haueisen J, Happ K, Stralucke M, … Stukenbrock EH (2019) Destabilization of chromosome structure by histone H3 lysine 27 methylation. PLOS Genet 15(4):e1008093. Retrieved from https://doi.org/10.1371/journal.pgen.1008093

Nuckolls NL, Núñez MAB, Eickbush MT, Young JM, Lange JJ, Jonathan SY, Smith GR, Jaspersen SL, Malik HS, Zanders SE (2017) Wtf genes are prolific dual poison-antidote meiotic drivers. Elife 6:e26033. https://doi.org/10.7554/eLife.26033

Ponomarenko A (2011) SBG Septoria tritici blotch (STB) of wheat. Plant Health Instructor

Schotanus K, Soyer JL, Connolly LR, Grandaubert J, Happel P, Smith KM, … Stukenbrock EH (2015) Histone modifications rather than the novel regional centromeres of Zymoseptoria tritici distinguish core and accessory chromosomes. Epigenet Chromat 8(1):41. https://doi.org/10.1186/s13072-015-0033-5

Svedberg J, Vogan AA, Rhoades NA, Sarmarajeewa D, Jacobson DJ, Lascoux M, … Johannesson H (2021) An introgressed gene causes meiotic drive in Neurospora sitophila; Proc Natl Acad Sci 118(17):e2026605118. https://doi.org/10.1073/pnas.2026605118

Taylor JW, Branco S, Gao C, et al (2017) Sources of fungal genetic variation and associating it with phenotypic diversity. Microbiol Spectr 5:5.5.06. https://doi.org/10.1128/microbiolspec.FUNK0057-2016

Werren JH (2011) Selfish genetic elements, genetic conflict, and evolutionary innovation. Proc Natl Acad Sci USA 108 Suppl(Suppl 2):10863–10870. https://doi.org/10.1073/pnas.1102343108

Werren JH, Nur U, Wu CI (1988) Selfish genetic elements. Trends Ecol Evol 3(11):297–302. https://doi.org/10.1016/0169-5347(88)90105-X

Wittenberg AHJ, van der Lee TAJ, Ben M'Barek S, Ware SB, Goodwin SB, Kilian A, … Schouten HJ (2009) Meiosis drives extraordinary genome plasticity in the haploid fungal plant pathogen Mycosphaerella graminicola. PLOS One 4(6):e5863. Retrieved from https://doi.org/10.1371/journal.pone.0005863

Chapter II

Repeat-induced point mutation (RIP) and gene conversion influenced by chromatin modifications shape the genome of a plant pathogenic fungus

Jovan Komluski, Michael Habig and Eva H. Stukenbrock

Environmental Genomics, Christian-Albrechts University of Kiel, Am Botanischer Garten 1-9, 24118 Kiel, Germany

Max Planck Institute for Evolutionary Biology, August-Thienemann-Straße 2, 24306 Plön, Germany

Abstract

Meiosis is associated with genetic changes in the genome - via recombination, gene conversion, and mutations. The occurrence of gene conversion and mutations during meiosis may further be influenced by the chromatin conformation, similar to the effect of the chromatin conformation on the mitotic mutation rate. To date, however, the exact distribution and type of meiosis-associated changes and the role of the chromatin conformation in this context is largely unexplored. Here, we determine recombination, gene conversion, and *de novo* mutations using whole-genome sequencing of all meiotic products of 23 individual meioses in *Zymoseptoria tritici*, an important pathogen of wheat. We could confirm a high genome-wide recombination rate of 65 cM/Mb and see higher recombination rates on the accessory compared to core chromosomes. A substantial fraction of 0.16% of all polymorphic markers was affected by gene conversions, showing a weak GC-bias, and occurring at higher frequency in regions of constitutive heterochromatin, indicated by the histone modification H3K9me3. The *de novo* mutation rate associated with meiosis was approx. three orders of magnitude higher than the corresponding mitotic mutation rate. Importantly, repeat-induced point mutation (RIP), a fungal defense mechanism against duplicated sequences, is active in *Z. tritici* and responsible for the majority of these *de novo* meiotic mutations. Our results indicate that the genetic changes associated with meiosis are a major source of variability in the genome of an important plant pathogen and shape its evolutionary trajectory.

Importance

The impact of meiosis on the genome composition via gene conversion and mutations is mostly poorly understood, in particular for non-model species. Here, we sequenced all four meiotic products for 23 individual meioses and determined the genetic changes caused by meiosis for the important fungal wheat pathogen *Zymoseptoria tritici*. We found a high rate of gene conversions and an effect of the chromatin conformation on gene conversion rates. Higher conversion rates were found in regions enriched with the H3K9me3 – a mark for constitutive heterochromatin. Most importantly, meiosis was associated with a much higher frequency of *de novo* mutations than mitosis. 78% of the meiotic mutations were caused by repeat-induced point mutations – a fungal defense mechanism against duplicated sequences. In conclusion, the genetic changes associated with meiosis are therefore a major factor shaping the genome of this fungal pathogen.

Introduction

Meiosis is an important mechanism of genome evolution as it generates genetic variability for selection to act upon. Since all changes to the genome that occur prior to and during meiosis are potentially affecting the germline, meiosis is a pivotal mechanism in shaping the evolutionary trajectory of sexually propagating species. Three major classes of genetic changes are associated with meiosis; i) recombination, ii) gene conversion and iii) meiotic mutations.

Recombination is the reciprocal exchange of information between homologous chromosomes during meiosis (1). Canonical meiosis is initiated by the formation of double-strand breaks (DSBs) by the topoisomerase-like protein Spo11 at many genomic locations (2, 3). Indeed, these DSBs, which are resected to generate single-stranded DNA overhangs that can invade the homologous chromosome, are thought to guide chromosome pairing in many species (3, 4). Most DSBs are repaired and resolved as non-crossover (NCO) events which in some occasions are associated with gene conversions, while few DSBs will be resolved to crossover (CO) events and the reciprocal exchange of larger chromosome portions between homologous chromosomes (4–8). Interestingly, recombination rates, i.e. the rate of reciprocal exchanges of chromosome sections during meiosis, vary considerably between species (9, 10). The highest CO frequencies reported so far, are in fission yeast, where an average of 11-19 COs per chromosome pair by far exceed the minimum of one crossover event per chromosome considered to be required for proper chromosome pairing and segregation - with the average number of COs per chromosome in most species rarely exceeding three (11–14). Recombination rates also vary along chromosomes, with crossovers occurring in hotspots (15–18) and being mostly absent in centromeric regions (19, 20). Where crossovers are occurring seems to be affected by the synaptonemal complex, a protein structure that forms along meiotic chromosomes, as well as the chromatin structure that appears to influence the location of the DSBs (9). Accessible chromatin appears to be a hotspot for DSBs, as shown in *Saccharomyces cerevisiae* where DSBs are primarily located within regions of accessible chromatin generally found at gene promotors (21). Generally, heterochromatic marks are associated with lower recombination rates, while euchromatic marks are associated with elevated recombination rates (3, 9, 22–25). During the last decade, the use of population data for the determination of recombination rates became feasible based on the rapidly increasing availability of whole genome sequencing data (17, 18, 26, 27). However, progeny analysis and tetrad analysis are still required to analyze all the genetic processes associated with crossover events.

Gene conversion is also one of the possible outcomes of DSB formation and resolution during meiosis, but, in contrast to recombination, gene conversion directly affects the allele frequency. Gene conversion describes the non-reciprocal (i.e., unidirectional) transfer of a sequence from one locus (the donor) to a different genetic locus (the acceptor) (28). Gene conversions can either be interallelic or non-allelic (also called interlocus). The first will result in changes in the allele frequency while the latter is (next to unequal crossovers) involved in gene duplication, gene expansion, and homogenization of gene families and has for example been observed in gene families involved in host-pathogen interactions (28–31). Gene conversion is initiated by DSBs, followed by resection of the DSB end and the invasion of the single-stranded tail into homologous sequences. Sequence differences between the two homologous sequences will result in partially mismatched heteroduplex DNA (5, 28, 32). If the mismatch is repaired using the information of the invading DNA the acceptor allele will be changed to the donor allele and hence result in gene conversion as manifested by a 3:1 rather than 2:2 segregation pattern in the resulting products of a single meiosis – a tetrad. Heteroduplex DNA and repair also occur during crossover (CO) events and hence gene conversions can be categorized into those associated with CO (CO-GC) and those associated with non-crossover NCO (NCO-GC) (32). Rates of gene conversion vary considerably between species (33, 34) which appears to be mainly influenced by the tract length (i.e., the length of the sequence containing converted markers) and recombination rates (5, 34, 35). Gene conversion in some species seems to be GC-biased, probably caused by the GC-biased repair of A:C and G:T in the heteroduplex DNA (36, 37) which is assumed to have important consequences on the equilibrium GC content of genomes (34, 38). Biased gene conversion may however not be universally important as it was found not to occur in some fungi as well as in some plant and algae species (18). Although chromatin configuration and hence the histone modifications are assumed to affect the rate of gene conversions, such an association was so far not identified.

Finally, meiosis is also associated with mutations that occur before or during meiosis (39–41). Since mutations on average are considered to be deleterious, mutation rates, in general, are low but can also differ greatly between species (42). Meiosis-associated mutation rates, in turn, can differ greatly from the corresponding mitotic mutation rate in the same species indicating different mechanisms and/ or constraints. For example, the germline mutation rate in humans and mice is 1.2×10^{-8} or 5.7×10^{-9} per nucleotide per generation, respectively, two orders of magnitude lower than the corresponding mitotic mutation rate (10, 43, 44). Here, germline mutations might be linked to DSBs and their repair (45) with a higher number of mutations occurring in the vicinity of recombination events (46).

Estimates of meiosis-associated mutation rates in different fungal species also vary considerably. In *S. cerevisiae,* the meiosis-associated mutation rate is 8×10^{-8} per bp per cell generation (45), much higher than the mitotic mutation rate of 3.3×10^{-10} per bp per cell division (47). In *Neurospora crassa,* the meiosis-associated mutation rate is very high at 3.38×10^{-6} per bp per generation (48) contrasting with a much lower mitotic mutation rate of 6.7×10^{-10} per bp per cell division (49). Interestingly, this extremely high meiotic mutation rate in *N. crassa* is caused by repeat-induced point mutation (RIP), a fungal defense mechanism against duplicated sequences (Fig S1A) (41, 50). RIP is restricted to haploid parental nuclei just prior to karyogamy and meiosis and acts on duplicated sequences of a minimum length of 400 bp length in *N. crassa* (51–53). Once recognized both duplicated sequences will be mutated in a C→T manner (51–53) and RIP can sometimes leak into adjacent non-repetitive regions (54, 55). RIP signatures have been detected in the genomic sequences of many fungi, however, active RIP was experimentally confirmed only in a few fungal species (48, 56). Hence, there is a growing body of evidence that suggests that the mutational processes prior to and during meiosis differ from those during mitosis. In fungi, the meiotic mutation rate appears to be higher than the mitotic mutation rate which for some fungi is assumed to be the result of RIP.

Here, we use tetrad analysis to determine genetic changes associated with meiosis in the ascomycete fungus *Zymoseptoria tritici*, a pathogen of wheat. The haploid genome of *Z. tritici* comprises 13 core chromosomes and a set of eight smaller accessory chromosomes (57). These non-essential accessory chromosomes carry a fitness cost (58), are enriched in the facultative heterochromatin mark H3K27me3 (59), have a higher mutation rate during mitosis (60), and exhibit a meiotic drive (61). The availability of complete tetrads for *Z. tritici* allows us here to address all three major classes of genetic changes associated with sexual reproduction. In particular, the frequency and distribution of mutations associated with sexual reproduction are unknown although *Z. tritici* has an asexual and a sexual reproductive cycle with the latter being the main source of the primary inoculum during the initial stages of the infection (62). The mitotic mutation rate in *Z. tritici* has been determined experimentally by mutation accumulation experiments at 3.2×10^{-10} per bp per mitotic cell division (60), which is similar in other fungi (47, 49). Although histone modifications affect the mitotic mutation rate of *Z. tritici* (60, 63) it is unknown if the distribution of meiotic recombination events, gene conversion, and meiosis-associated mutations are also influenced by these histone modifications. Finally, although the genome of *Z. tritici* shows signatures of RIP (64), RIP has so far not been demonstrated experimentally and the efficacy of this mutational mechanism in this pathogen is not known. Given the fact that 18.6 % of the genome of *Z. tritici* is represented by TEs it is plausible that RIP is less efficient

in *Z. tritici* than in *N. crassa* or fails to recognize some duplicated regions (65). Here we study all major classes of meiosis-associated genetic changes in *Z. tritici* by analyzing whole genomes sequences of complete tetrads to i) estimate recombination and gene conversion rates for core and accessory chromosomes; ii) determine the association between recombination and gene conversions with chromatin modifications; and iii) estimate meiotic mutation rates in *Z. tritici*. The use of tetrads allowed us to detect and describe the effects of active RIP and generate a fine-scale map of recombination and gene conversion events and its association with chromatin modifications.

Results

Accessory chromosomes show higher recombination rates

To determine the distribution of recombination events during meiosis in *Z. tritici*, we used previously published tetrads and obtained whole genome sequences for the tetrad progenies (66). To this end, we included 23 tetrads comprising four ascospore isolates, totaling 92 genomes. An average of 118772 SNPs (0.3% of all analyzed genomic sites) per tetrad was used for the analysis (see Materials and Methods) with the SNP density being similar between core and accessory chromosomes (Fig S1B). The median distance between SNPs was 61 bp with few instances of distances between SNPs exceeding 5000 bp (Fig S1C). From this data, we identified individual recombination events with the CrossOver tool from the Recombine package (67) and calculated the recombination rate. A total of 1138 crossover events were observed, resulting in a genome-wide recombination rate of 65 cM/Mb consistent with previously published estimates of the recombination rate in this fungus. Intriguingly, the recombination rate was significantly higher on accessory chromosomes (92.7 cM/Mb) than on the core chromosomes (62.6 cM/Mb) (Fig 1A, Fig S1D, Table S1A-B). The recombination rate was negatively correlated with the chromosome length (Pearson's R = -0.76, *p*-value = 0.00017) (Fig 1B) but the absolute number of crossovers per chromosome was positively correlated with the chromosome length (Pearson's R = 0.96, *p*-value = 6.2 x 10^{-11}) (Fig S1E). When two or more crossovers are present in a bivalent, they tend not to occur near each other in many species - a process called crossover interference (68). We accessed the distribution of the distances between COs using the gamma distribution (69–71) and detected crossover interference ($\gamma > 1$) for both core and accessory chromosomes (see Fig 1C). When correlating the crossover frequencies with regions enriched in heterochromatin marks we found that regions enriched in heterochromatin marks (H3K27me3 or H3K9me3) were associated with higher crossover frequencies whereas the euchromatin marks H3K4me2 did not show a higher recombination rate than regions lacking all three marks (Fig 2A).

To further assess the variation in recombination rate across the genome, we estimated the recombination rates in 20 kb non-overlapping windows. We defined hotspots as those 20 kb windows that showed a significantly (*p*-value < 0.001) higher number of recombination events than expected by the Poisson distribution and identified a total of 52 recombination hotspots with more than four crossover events per 20 kb window. Recombination rates per window were highly variable, ranging from 0 to 1196 cM/Mb (Fig S2). We conclude that recombination varies considerably across the

genome, occurs in hotspots, and is higher on the accessory than on the core chromosomes. A more detailed analysis of the immediate vicinity of the crossover events allowed us to identify four motifs that were significantly overrepresented in the 1 kb sequences surrounding the crossover and to correlate recombination rates with short sequence repeats (SSRs) (Fig S3C, D). However, a more fine-scale analysis of the nine 1 kb windows with ≥4 crossovers events showed no apparent correlation between the location of TEs, SSRs, genes, and the three histone modifications H3K4me2, H3K9me3 and H3K27me3 (Fig S3A). We considered the relevance of high recombination rates with regard to gene evolution and correlated the recombination map with the coordinates of protein-coding genes. In total, we observed 376 genes in the CO hotspots. From the 376 genes observed in the CO hotspots, six encode for effector candidates and nine genes encode CAZymes (Table S1C) which are gene categories with a putative relevance in the pathogenicity of the fungus.
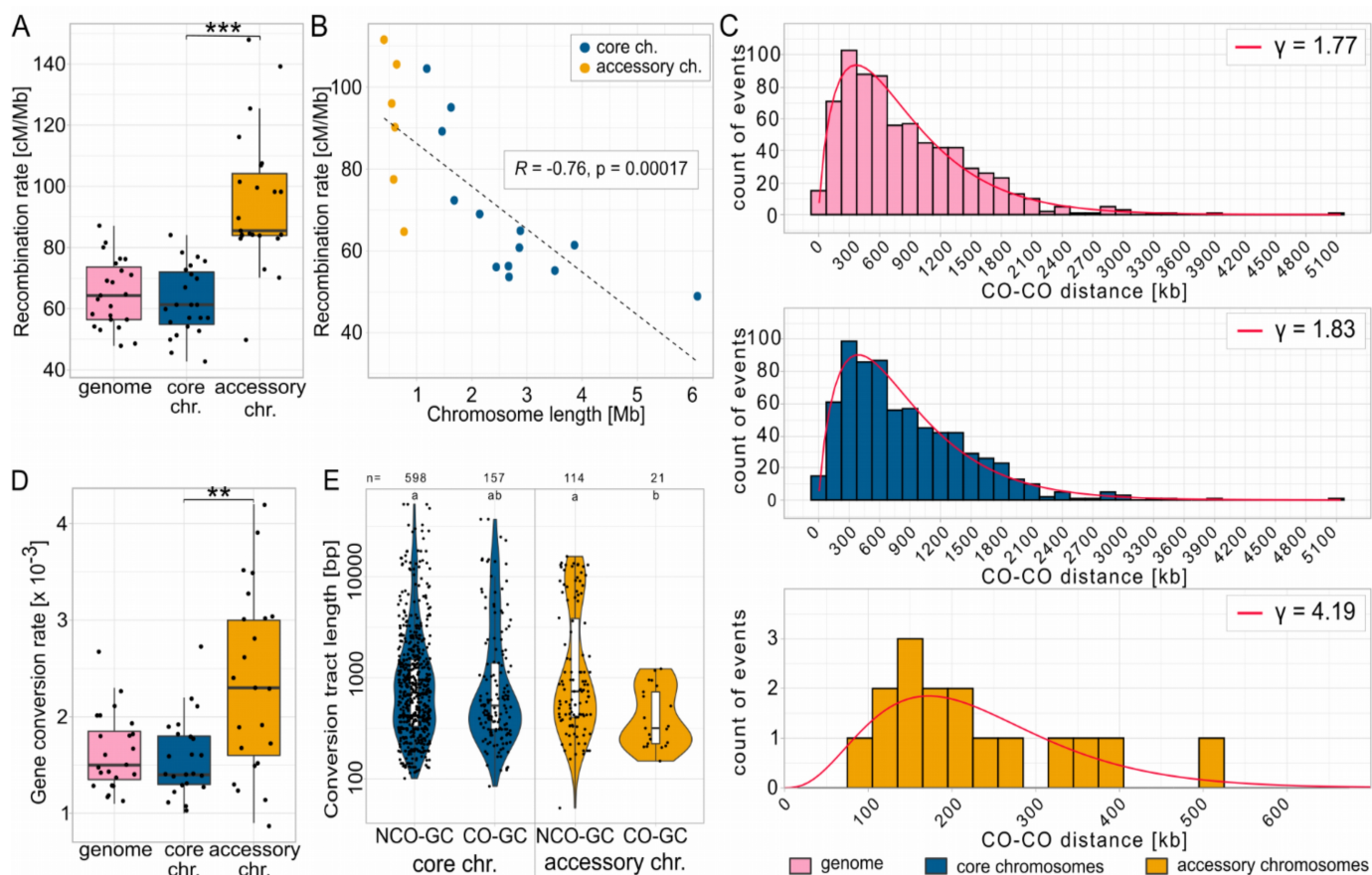

Fig 1. Comparison of recombination rates, gene conversion rates and crossover interference for various genomic compartments. **A** Recombination rates for the genome and on core and accessory chromosomes. **B** Correlation between recombination rates and chromosome length. **C** Crossover

(CO) interference. Distribution of distances between adjacent CO events (CO-CO distance) in the entire genome (pink), on core chromosomes (blue), and on accessory chromosomes (yellow). The red line represents the fitted gamma distribution for the observed CO-CO distances. γ values higher than 1 indicate positive CO interference, i.e., a lower than expected number of small CO-CO distances. **D** Gene conversion rates for the genome and core and accessory chromosomes. **E** Violin plot of non-crossover associated gene conversions (NCO-GCs) and crossover associated gene conversions (CO-GCs) tract lengths for core and accessory chromosomes. The tract lengths of the gene conversion events spanning TEs are excluded (different letters depict significantly different groups with *p*-value < 0.05 in the Wilcoxon test with Bonferroni correction). **A, D** *p*-values of paired Wilcoxon test are shown (*p < 0.05, **p < 0.005, ***p < 0.0005).

High gene conversion rates are more uniformly distributed within the genome

The genomes of ascospore progenies resulting from one meiotic event provided us with a unique opportunity to characterize the location and distribution of gene conversion events. We, therefore, identified gene conversion events along the genome and compared the gene conversion rate for different genomic compartments. We identified a total of 890 gene conversion events comprising 712 associated with non-crossover events (Non-crossover Gene Conversion NCO-GC: 80%) and 178 associated with crossover events (Crossover Gene Conversion CO-GC: 20%) (Table S2A). Each of these gene conversion events was associated with at least three converted marker (SNPs), with the total number of converted markers being 3529 and 979 for NCO-GC and CO-GC, respectively. We distinguished the gene conversion events on core and accessory chromosomes of *Z. tritici* and found that 755 gene conversion events were located on core and 135 on accessory chromosomes (Table S2B). We next explored the general patterns of converted SNPs. We observed a weak GC-bias in the gene conversions (binomial test, *p*-value = 0.0215, Fig 2C). Based on genome-wide SNPs identified among the ascospore isolates we found that the genome-wide gene conversion rate was 1.6×10^{-3} per SNP (Fig 1D, Table S2B). Hence, the gene conversion rate was significantly higher on the accessory chromosomes compared to the core chromosomes (paired Wilcoxon signed rank test, *p*-value = 1.0×10^{-3}) (Fig 1D, Fig 2D). Tract length is considered to be one of the main determinants of gene conversion rates, therefore, we estimated the median conversion tract length for both types of gene conversion events. The median tract length for non-crossovers (NCO-GC) was 539 bp, and 432 bp for gene conversions associated with crossovers (CO-GC), respectively (Fig 1E). Although the tract length on the accessory chromosomes appeared to differ from the corresponding tract length on the core chromosomes, none of these comparisons were significant (e.g. NCO-GC accessory vs. core chromosomes *p*-value = 0.927) (Fig 1E).

In the same way as we characterized the distribution of recombination hotspots along the fungal genomes, we used the map of gene conversion events to identify regions with exceptionally high gene conversion rates, here defined as gene conversion hotspots. First, to assess the distribution of gene conversion, we divided the genome into 20 kb non-overlapping windows and calculated the number of gene conversion events in each window. We identified 32 gene conversion hotspots with more than four gene conversion events per 20 kb window that were significantly different from the background with p-value < 0.001 defined by the Poisson distribution (Fig S4A-C). Of the 145 genes in the gene conversion hotspots two genes encode for effector candidates and seven genes encode for CAZymes (Table S2C). We speculate that the increased rate of gene conversion in these putative pathogenicity-related genes could be putative mechanism of rapid evolution. However, the majority of the genes associated with gene conversion hotspots (95 genes) encode proteins that have not yet been functionally annotated, preventing any meaningful enrichment analysis. Taken together, the ascospore population allowed us to precisely map and characterize gene conversion events in *Z. tritici*. We found that rates of gene conversion showed less variation across the genome than recombination rates however with both being higher on accessory chromosomes than on core chromosomes.

Gene conversion rates are higher in regions enriched in heterochromatin modifications

Previous studies in chicken B-cell lines have identified a correlation of chromatin structure with gene conversion (72) but detailed analysis of the effect of specific histone modifications is mostly missing. Thus, to investigate the potential effect of histone modifications on the rate of gene conversion in *Z. tritici*, we conducted a correlation analyses of maps of histone modifications and gene conversion rates. We focused on three histone marks which have been previously well characterized in *Z. tritici* using chromatin immunoprecipitation of antibodies targeting specific histone modifications followed by sequencing (ChIP-seq): the euchromatin mark H3K4me2, the constitutive heterochromatin mark H3K9me3 and the facultative heterochromatin mark H3K27me3 (59) (Fig 2C, Table S2D). Importantly, we excluded TEs from the full-factorial analysis of gene conversions and therefore regions enriched with H3K9me3 and H3K27me3 in this analysis are not associated with TEs.

Our analyses showed that higher gene conversion rates associate with regions enriched in heterochromatin marks, particularly in regions solely enriched with H3K9me3 as well as in regions enriched with both H3K9me3 and H3K27me3 (Fig 2B). Regions solely enriched in H3K27me3 were not associated with higher gene conversion rates which contrast with their correlation with the highest

crossover frequencies (Fig 2A). The median gene conversion rate in the regions enriched with H3K9me3 was 3×10^{-2} per converted marker per tetrad per meiosis and the median gene conversion rate in H3K9me3 and H3K27me3 regions was 1.3×10^{-2} per converted marker per tetrad per meiosis. Genome regions not enriched with either of the three histone marks H3K4me2, H3K9me3, and H3K27me3 showed the lowest gene conversion rate of 0.9×10^{-3}. In summary, the histone maps allowed us to reveal that repressive heterochromatin modifications, especially H3K9me3 but not H3K27me3 are associated with higher gene conversion rates in *Z. tritici*.
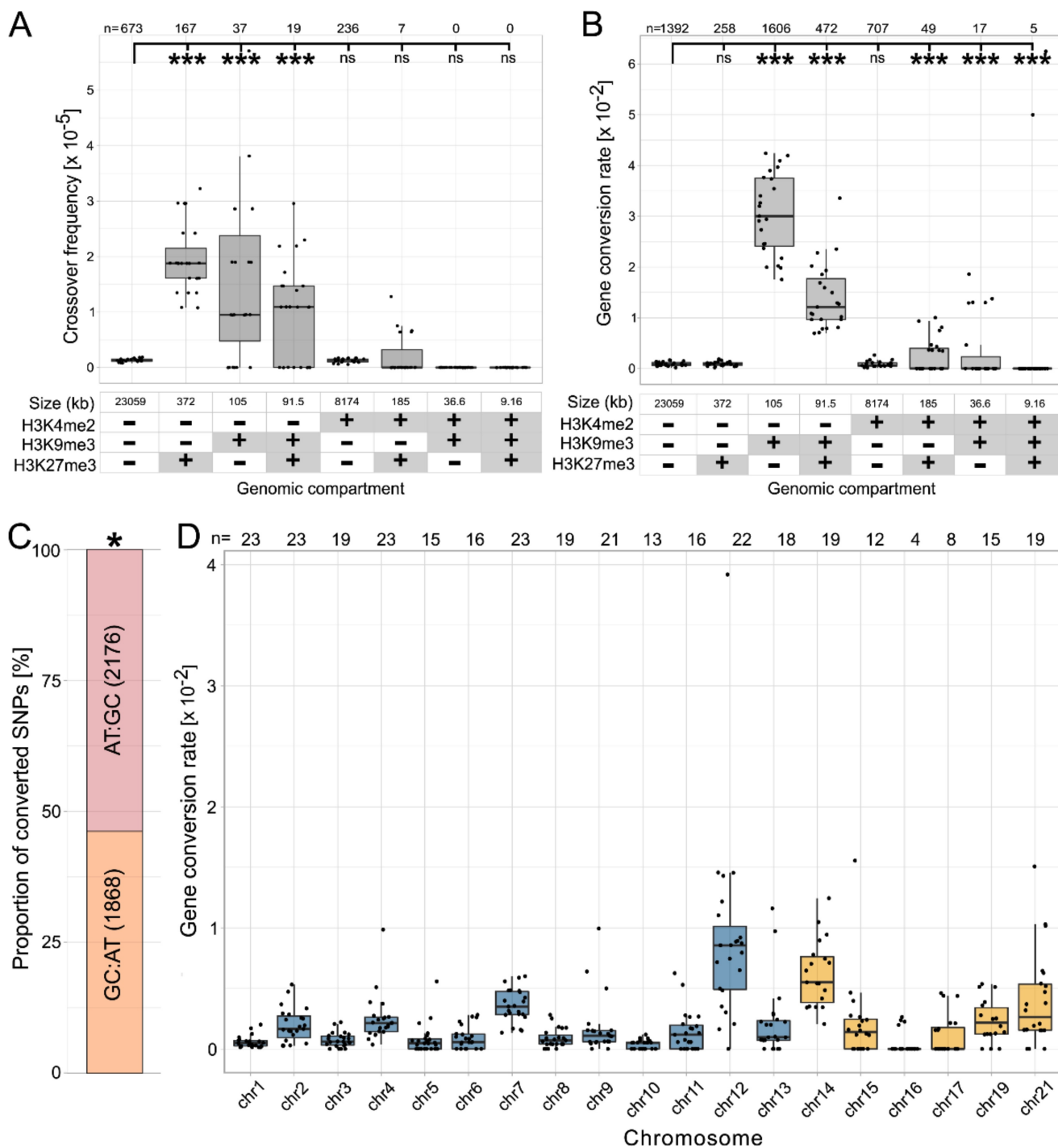
Fig 2. Correlation between crossover frequency and gene conversion rates with histone modifications, GC-biased gene conversion, and gene conversion rate per chromosome. **A, B** Correlation between **A** crossover frequencies or **B** gene conversion rates and chromatin modifications. The gene conversion rate is calculated as the number of converted markers per genomic compartment divided by the total number of markers in the genomic compartment. A genomic compartment is defined by all regions of the genome that share the presence/absence of the indicated histone modifications. The presence/absence of the specific chromatin modification (H3K4me2, H3K9me3, or H3K27me3, respectively) in the genomic compartment is depicted with +/- in the table below the x-axis. χ^2-test p-values for the comparison of the indicated genomic compartments with the genomic

compartment lacking all the indicated histone modifications are shown (*p < 0.05, **p < 0.005, ***p < 0.0005, ns: not significant). **C** GC-biased gene conversion in *Z. tritici.* The stacked barplot shows the proportion of AT to GC converted markers and the proportion of GC to AT converted markers. Binomial test *p*-values are shown (*p < 0.05, **p < 0.005, ***p < 0.0005). **D** Gene conversion rate per chromosome calculated as the proportion of converted markers from the total number of markers on the respective chromosome. The numbers above box plots show the number of tetrads with gene conversion detected on the respective chromosome. Box plots display center line, median; box limits, upper and lower quartiles; whiskers, 1.5x interquartile range; points, rate per tetrad

The majority of meiotic mutations are caused by RIP

Recombination and gene conversion as well as meiosis and meiosis-associated processes themselves are considered to be mutagenic (39–41, 46). Hence, we asked to which extent *de novo* mutations had occurred in the ascospore progenies. These mutations are distinguished by being absent in both of the parental strains, but present in the ascospores of the tetrad. Meiotic mutation rates often differ from mitotic mutation rates and are associated with recombination or pre-meiotic processes (40, 43–47). We observed a total of 526 *de novo* mutations that were absent in both of the parental strains for the ascospores of the 23 tetrads. Hence, through the sexual cycle, there were on average, 22.9 mutations per genome per generation, resulting in a mutation rate of 5.7 x 10^{-7} mutations per bp per generation (Fig 3A, Table S3A). Of these mutations that originated from the sexual cycle, 242 (42%) resided in one particular region that clearly stood out as we mapped meiotic SNPs along the genome. This high number of SNPs located in a 14001 bp region on chromosome 3 (Fig 3A-C). Every one of the 242 mutations in this region on chromosome 3 was a CG:TA transition. As we further inspected this region, we noted that the 14 kb region spanning 1668370 bp to 1682371 bp on chromosome 3 showed an increased sequencing coverage corresponding to a duplication of the region in the parent IPO94269 (Fig 3B). This means that this duplication on chromosome 3 was present in all 23 meioses and could possibly be identified by RIP, a genome defense mechanism against such duplicated regions (41). A high number of transitions in a duplicated region is the hallmark of such active RIP. Indeed, the high number of mutations in the duplicated region and the fact that all of these mutations are CG:TA transitions indicates active RIP in *Z. tritici*. Interestingly, the duplicated region on chromosome 3 showed RIP mutations in only ten of the 23 tetrads (Fig S5A). Further sequencing coverage depth revealed that, despite being present in the parental strain IPO94269, the duplicated region was lost in eleven of the tetrads. In these tetrads all four ascospores had a normalized sequencing coverage of the duplicated region of approx. 1 (Table S3B), while in twelve tetrads the duplication was still present (normalized sequencing coverage approx. 2) and therefore follow Mendelian segregation. In ten of these twelve tetrads that still had the duplication, RIP

mutations were detectable in this region, while in the remaining two tetrads no RIP mutations occurred in this region (tetrads A03-9 and S1C4_A2) (Fig. S5 A). The duplicated region contains six predicted genes, one of which has a functional annotation describing it as similar to transferase hexapeptide domain protein. Therefore, the putative function of the genes affected by the RIP of the duplication cannot yet be deduced.

We further addressed to which extent *de novo* mutations could be the result of meiosis-associated RIP. Hereby we found that 172 of the meiotic *de novo* mutations (32% of all *de novo* mutations) were detected in transposable elements (Fig 3C), and 166 of these 172 mutations (96.5%) were CG:TA transitions; the putative signature of RIP. To examine whether these mutations were also most likely caused by RIP we determined which class of transposable elements was affected. Of the 172 *de novo* mutations in TEs 152 (88.3%) were located in Class I transposons, which replicate via an RNA intermediate and are also referred to as copy-and-paste transposons (73–75). Of these 152 mutations in Class I transposons (LINE (long interspersed nuclear elements) and LTR (long terminal repeats)) 146 were CG:TA transitions with five TA:GC transitions and one G→C transversion, whilst only eleven CG:TA transitions occurred in Class II transposable elements (Fig 3D). Class II TEs are referred to as cut-and-paste transposons, which are excised and moved to new locations in the genome and hence do not create repeated sequences (74). The mutation rate in Class I (copy-and-paste) TEs is 1.3×10^{-6} per bp per generation compared to 2.8×10^{-7} per bp per generation for Class II (cut-and-paste) TEs with the vast majority of the *de novo* mutations showing RIP-like CG:TA transitions.

Investigations in a few other ascomycete fungi have provided evidence that RIP can affect the vicinity of duplicated regions by "leakage" of mutations into these non-repeated regions (54, 55). Based on these previous studies, we here also asked if RIP mutations would be present in regions adjacent to TEs. We subdivided each TE into 40 equally sized windows (average window size = 71 bp) as well as the two adjacent regions into 20 windows each (window size = 71 bp) and counted the number of *de novo* mutations in each of these windows. This approach allowed us to show that RIP mutations were not equally distributed along TE sequences. Within TEs the most distal windows showed the highest number of *de novo* mutations whereas the more central sequences were less likely to be mutated (Fig 3E). Further analysis of the effect of the different classes of transposable elements showed that the highest number of RIP mutations in the distal regions of the TEs was mainly due to LTR transposons (Fig S5B), whereas LINE and Class II transposable elements did not show such a variation of the number of mutations along the length of the transposable element (Fig S5B). In regions adjacent to

the TEs a much lower number of mutations occurred compared to the TE sequences. Overall the mutation rate in the regions adjacent to TEs was at 7.4 x 10^{-8} per bp per generation, which was lower than the genome-wide mutation rate of 1.5 x 10^{-7} per bp per generation (for regions excluding TEs and excluding the duplication). It, therefore, appears that leakage has not occurred in the vicinity of the RIP-mutated TEs. Only 21.3% (112 mutations) of all *de novo* mutations were located in the regions outside of the transposable elements and the 14 kb region on chromosome 3. These *de novo* mutations in non-TE and non-duplicated regions comprised a significantly higher proportion of TA:CG transitions and transversions (22.3%) (Fig 3C).

The segregation pattern of the *de novo* mutations varied between the different compartments with those in TEs showing a higher proportion of 1:3 segregation (Fig S5C) than those in the 14 kb duplication or the mutations outside TEs. The segregation pattern of *de novo* mutations can indicate at what stage a DNA lesion or mismatch may have occurred and at what stage this lesion or mismatch (possibly caused by RIP) was resolved. A 2:2 segregation indicates that the mismatch was resolved prior to the replication cycle of the meiosis, while a 1:3 segregation indicates that the mismatch was resolved only during replication or later. Hence the higher proportion of 1:3 segregation pattern observed in the TEs could indicate a delayed resolution of the mismatches introduced by RIP in the heterochromatic TEs compared to the resolution in other genomic compartments (Fig S1A). The 3' neighbor of the targeted cytosine has a strong influence on RIP in *N. crassa*, with a strong preference for CpA (76, 77). We therefore identified the dinucleotide context of the 242 mutations in the 14 kb duplicated regions. 240 of these were in a CpA context and the remaining two in CpT context. The rate at which a single CpA was mutated during RIP was therefore 0.54 % (Fig S5D). The mutation rate varied along the 14 kb duplication, but this did not appear to correlate with the proportion of dinucleotides in the sequence that were CpA (Fig S5E). The number of individual mutations that were induced within the duplicated region varied considerably between tetrads (Fig S5A), but also between the individual ascospores of the tetrads (Fig S5F). For the 24 ascospores containing the duplication on chromosome 3, the number of mutations within the duplication in individual ascospores varied from 0 to a maximum of 57 (median 11), with most ascospores showing 0 to 10 mutations (Fig. S5F). In summary, RIP has been proposed to be an important player in the genome evolution of *Z. tritici*. However, this is the first experimental evidence for active RIP in this fungus and we observed that the large duplication was not always mutated by the RIP mechanism and that the total number of mutations introduced by RIP was low - leaving many cytosines in the duplicated regions unaffected - which together could indicate a low efficiency of RIP in *Z. tritici*.
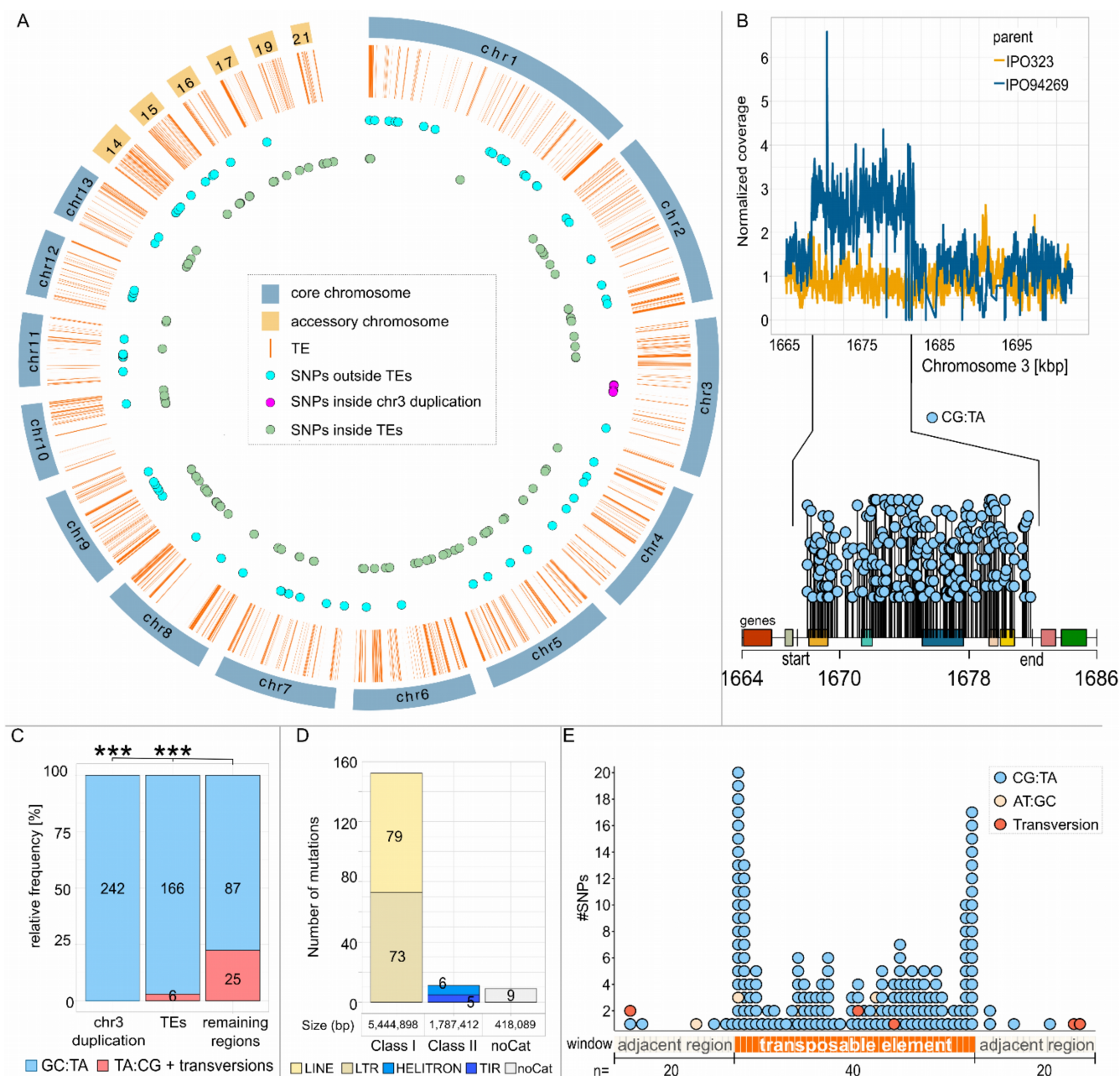
Fig 3. Genome-wide distribution of *de novo* mutations associated with meiosis in *Z. tritici.* **A** Circosplot of the meiotic SNPs distribution in the genomic features of *Z. tritici* (orange lines represent TEs; blue dots-meiotic SNPs outside the TEs; lilac dots meiotic SNPs inside the duplication on chromosome 3; green dots represent meiotic SNPs inside of the TEs). **B** RIP-like mutations in the duplicated 14 kb region on chromosome 3. The upper line graph shows the difference in normalized coverage between the IPO323 and the IPO94269 parent in the region on chromosome 3. The distributions of mutations in the duplicated chromosome 3 region and 10 kb upstream and downstream regions are shown in the lolliplot below the line graph. The start and the end on the x-axis of the lolliplot designate the start and the end of the duplicated region. Rectangles in different colors depict the genes located in this region. Each lollipop represents a single mutation. **C** Number of meiotic mutations in and out of the RIP active regions represented as their relative frequencies. CG:TA transitions are colored in lighter blue, and

TA:CG transitions and transversions are colored in red. Fisher exact test *p*-values are shown (*$p <$ 0.05, **$p <$ 0.005, ***$p <$ 0.0005). **D** Number of *de novo* mutations in different classes and families of repeats (light yellow-long interspersed nuclear element (LINE); dark yellow-long terminal repeats (LTR); marine blue-HELITRON, dark blue-tandem inverted repeats (TIR); white-noCat). **E** Distribution of meiotic SNPs along TEs. Each TE was divided into 40 equal-sized windows. Each black rectangle on the x-axis represents a window inside a TE representing 2.5% of the TE length. Beige rectangles represent windows in the regions directly adjacent to TEs. Dots above rectangles represent one mutation in each window (yellow dots-AT:GC transitions; blue dots-CG:TA transitions, red dots-transversions)

Discussion

Here we used tetrad analysis to estimate recombination rates, gene conversion rates, and *de novo* mutation rates associated with meiosis from 23 individual meioses in *Z. tritici*. The ability to dissect genetic events in individual ascospore progenies isolated from tetrads provided us with highly precise maps of meiosis-associated changes along the fungal genome. Our results show i) higher gene conversion rates and recombination rates on accessory chromosomes compared to core chromosomes, ii) a correlation of recombination rates and gene conversion rates with histone marks associated with heterochromatin, and iii) elevated *de novo* mutation rates during sexual reproduction caused by active RIP.

Our dissection of recombination events during individual meiotic events allows us to confirm the previously reported high recombination rates in *Z. tritici* - on average 65 cM/Mb. Interestingly, 35 of the 52 recombination hotspots detected in this study overlapped with previously reported recombination hotspots in *Z. tritici,* which used distinct isolates from Switzerland, indicating that recombination hot spots may be determined by certain domains or conserved marks along the genome (17). However, these are most likely not small sequence motives, as there is little similarity between those identified within our study and those from the previous study with Swiss isolates (17). In contrast to previous studies using population genomic data (18), we show that the rate of recombination is in fact higher on accessory chromosomes compared to core chromosomes (92.7 cM/Mb and 62.6 cM/Mb, respectively) and negatively correlated with chromosome size. Hence, our results are in line with the general observation that smaller chromosomes tend to have higher recombination rates (78). Earlier population-based recombination rate studies in *Z. tritici* showed, however, lower recombination rates as computed as *rho* for accessory chromosomes (*rho* = 0.001) than on core chromosomes (*rho* = 0.024) (18). *Rho* is the product of the actual recombination rate and the effective population size Ne, and we speculate that the discrepancy in recombination rate measures may reflect the lower effective population size of the accessory chromosomes compared to the core chromosomes (18). Intriguingly, we could not identify any crossovers on an accessory chromosome in nine instances, despite the presence of the respective homologous chromosomes. A minimum of one crossover per homologous chromosome pair is considered to be required for proper segregation of the homologous chromosomes (4, 79). Indeed, in four of these nine instances, we observed such segregation errors. However, in the remaining five instances the accessory chromosomes properly segregated despite the absence of crossovers. Hence, we conclude that crossovers are not essential for proper chromosome

segregation in *Z. tritici*. *spo11* deletion mutants in *S. cerevisiae* and *Sordaria macrospora* were previously used to observe the consequences of the absence of DSBs and recombination on the segregation of chromosomes during meiosis. In these fungal species the absence of DSBs and recombination caused widespread chromosome segregation errors highlighting the importance of recombination for proper segregation (80, 81). The relatively high frequency of properly segregated, non-recombined chromosomes in *Z. tritici* indicates the presence of a non-recombination-dependent segregation system which might also be involved in the meiotic drive system of the accessory chromosomes in *Z. tritici* (66).

We predict that high levels of gene conversions in *Z. tritici* can affect allele frequencies to a higher extent than recombination and thereby shape genome composition. The genome-wide gene conversion rate of 1.6×10^{-3} per SNP identified in our study is approx. twenty times lower than the genome-wide gene conversion rate in *S. cerevisiae* (3.8×10^{-2} per SNP) (33, 34) but approx. an order of magnitude higher than the genome-wide gene conversion rate in *N. crassa* ($0.7 - 2.2 \times 10^{-4}$ per SNP) (33, 34). The variation in the gene conversion rate between species might be influenced by tract length and recombination rate since gene conversion is positively correlated with both characteristics (34, 35, 37). Our data confirm this since *Z. tritici* has shorter NCO-GC and CO-GC tract lengths and lower recombination rates (539 bp, 432 bp, and 65 cM/Mb, respectively) than *S. cerevisiae* (1681 bp, 1841 bp, and 375 cM/Mb) (34). *N. crassa* in turn shows longer NCO-GC tract lengths but shorter CO-GC tract lengths and a lower recombination rate (950 bp, 284 bp, and 20 cM/Mb, respectively) than *Z. tritici* (34). Similar to recombination, accessory chromosomes have higher gene conversion rates than the core chromosomes. The smaller size of accessory chromosomes in contrast to core chromosomes could influence the gene conversion rate on accessory chromosomes since smaller chromosomes tend to have higher rates of gene conversion (34).

We found a strong association between chromatin modifications and recombination and gene conversion rates. We speculate that might be due to two non-exclusive mechanisms: The effect of histone modifications on the location of DSBs and/or their effect on DSB and heteroduplex repair. Although a direct correlation between DSB formation and H3K4me3 has been shown in *S. cerevisiae* (21), the underlying causality of this correlation and the extent to which it applies to other organisms is unclear (82, 83). Local chromatin conformation can influence how DSBs and heteroduplex DNA are repaired, thereby influencing the later stages leading to recombination and gene conversion (84–86). In contrast to *S. cerevisiae* we see an association of heterochromatin as marked by H3K9me3 and

H3K27me3 with recombination in *Z. tritici*. Similarly, and again in contrast to the scenario in yeast, we observe that gene conversion rates are highest in heterochromatin regions in *Z. tritici*. This suggests that chromatin conformation may affect gene conversion primarily through its effect on DSB and heteroduplex repair and not via its impact on accessibility. DSBs can be resolved by synthesis-dependent strand annealing (SDSA), leading to a homologous recombination-mediated pathway and hence NCO events (87, 88). Our results show increased gene conversion rates in regions enriched in H3K9me3. Several studies suggest that H3K9 di- or trimethylated (H3K9me2/3) heterochromatin promotes homologous recombination (HR) (88–92). DNA double-strand breaks promote chromatin stabilization by H3K9me3 and activate DSB signaling proteins (93). The role of H3K9me3 in promoting homologous recombination could mean that the correlation between H3K9me3 and the gene conversion rate we observed in our study is caused by the effect of H3K9me3 on recombination. However, 80% of the gene conversion events we detected are associated with non-crossover events (NCO-GC). This suggests that the correlation between H3K9me3 and gene conversions is not caused by recombination, but possibly by the effect of histone modifications on the repair of DSBs and heteroduplex DNA. In contrast to DSBs in regions enriched in H3K9me3, DSBs in regions enriched in H3K27me3 were found to be frequently repaired by microhomology-mediated end joining (MMEJ), a non-homologous repair pathway that does not promote homologous recombination and therefore does not lead to gene conversion or crossover (94, 95). We find support for a similar effect of chromatin modifications on DSB repair in our study. Indeed, increased repair of DSBs via a non-homologous pathway in the H3K27me3-enriched regions could explain the reduced gene conversion rate in the regions enriched in both H3K9me3 and H3K27me3 regions (1.3×10^{-3} per SNP) compared to regions enriched in H3K9me3 only (2.8×10^{-3} per SNP) as observed here. Similarly, the absence of an increased gene conversion rate despite the high frequency of crossovers in the regions enriched in H3K27me3 alone could be explained by MMEJ being favored by H3K27me3. However, it is unclear why H3K27me3 is associated with the highest crossover frequencies, since MMEJ should not promote homologous recombination and therefore should result in a lower crossover frequency. In wheat, high crossover rates were associated with H3K27me3, but the mechanism causing this correlation is still unclear (96). We speculate that the observed correlation between H3K27me3 and higher crossover frequencies may be driven by the enrichment of this mark on accessory chromosomes, but functional validation is still missing. In conclusion, we see indications that histone modifications could affect gene conversion rates mainly via their effect on the DSB and heteroduplex repair.

De novo mutations associated with meiosis occurred at a rate of 5.7 x 10^{-7} per bp per generation in *Z. tritici* which is approximately three orders of magnitude higher than the mitotic mutation rate (3.2 x 10^{-10} per site per cell division) which we previously determined in a mutation accumulation experiment (60). *De novo* mutations were not uniformly distributed across the *Z. tritici* genome, ranging from the highest mutation rate of 7.5 x 10^{-4} per bp per generation within the duplicated region on chromosome 3 to 1.5 x 10^{-7} per bp per generation in genomic regions excluding the duplicated region and excluding TEs. Class I and II TEs showed a mutation rate of 1.3 x 10^{-6} and 2.8 x 10^{-7} per bp per generation, respectively, which is higher than the genome mutation rate but lower than the mutation rate in the duplicated region. This is probably due to the variability of TEs within these two groups, which also contain many non-duplicated sequences. Higher meiotic than mitotic mutation rates have been reported in other fungi like *S. cerevisiae* and *N. crassa* (45, 47–49). In *N. crassa*, the difference between mutation rates during mitosis and meiosis is mostly due to RIP, a fungal defense mechanism against duplicated DNA sequences that occurs in the haploid nuclei just prior to meiosis and that induces CG:TA transitions in duplicated sequences and transposable elements (48, 51). In *Z. tritici* signatures of past RIP have been found by analyses of genome data (64, 97), and here we can confirm that RIP is an active mechanism in *Z. tritici*. This is evident as 77% of the *de novo* mutations associated with meiosis located in Class I transposable elements (copy-and-paste elements) and in the 14001 bp long region on chromosome 3 that is duplicated in the IPO94269 parent. Interestingly, RIP in *Z. tritici* is not consistently efficient in mutating duplicated sequences as we find that duplicated sequences in two of the tetrads were not mutated and the number of RIP mutations introduced even in duplicated regions is low. The duplication that was present in the parental strain IPO94269 appears to have been frequently lost during crosses. How and at what stage this loss of the duplication occurred is currently unclear. However, most likely the loss must have occurred before the RIP process, as no RIP mutations were detected in this region. Until now, RIP was experimentally demonstrated in only a few fungal species (98–103), with lower efficiency in *Leptosphaeria maculans* and *Podospora anserine* compared to the highly efficient RIP in *N. crassa* (100, 104). We consider that variation RIP efficiency may be a more common phenomenon that reflects a trade-off between the evolutionary costs of the mutations introduced by RIP and the evolutionary costs of TEs.

We find that Class I (copy-and-paste) TEs show a much higher RIP mutation rate than Class II (cut-and-paste). This observation is expected as the transposition mode of the Class I TEs results in duplicated sequences that are recognized by the RIP machinery (73). Interestingly we find that the RIP mutations are not equally distributed along the TE sequences. The most distal windows comprising

5% of the length of the TEs comprise 35% of all *de novo* meiotic mutations that occurred within the TEs. This high frequency of *de novo* mutations at the ends of TEs was mostly due to the accumulation of mutations in the distal parts of the LTR transposons. LTRs transposons contain terminal repeats of 200 bp to 500 bp in length and therefore already contain duplicated sequences in close vicinity (75). These duplicated terminal sequences in Class I transposons seem to be prominent targets for RIP. In various other fungi RIP leaks into adjacent regions from the duplicated sequences of TEs (54, 105, 106) and is thought to play a role in the rapid adaptive evolution of effector genes involved in host-pathogen interactions (54, 105, 106). However, we do not see such leakage from transposable elements in *Z. tritici* but rather lower mutation rates in the vicinity of transposable elements than in the rest of the genome, which we cannot currently explain. Taken together, we show that RIP affects transposable elements in *Z. tritici* to varying degrees, and that the mutational environment thus influences the activity of these important drivers of genome evolution.

In conclusion, we show that recombination and gene conversion are correlated with histone modifications in different ways in *Z. tritici* and that RIP is active, albeit at a lower efficiency than in *N. crassa*, in this fungus affecting duplicated sequences as well as TEs. As a result, meiotic mutation rates for *Z. tritici* are three orders of magnitude higher than the mitotic rates demonstrating the major impact that genetic changes associated with meiosis have on the genome composition of this important plant pathogen.

Materials and Methods

Fungal material. Tetrads used for the sequencing analysis were obtained from the study of Habig et al. 2018 (66) and include ascospores isolated from crosses between the Dutch isolates IPO94269 and IPO323 (available from the Westerdijk Institute (Utrecht, The Netherlands) with the accession numbers CBS115943 and CBS115941) and from the crosses between IPO94269 and whole chromosome isogenic deletion strains (Δchr14-Δchr20) of the reference strain IPO323 generated in the study of Habig et al. 2017 (58). All ascospores were cultivated for DNA extraction at 18°C at 200 rpm in YMS (4 g/L yeast extract, 4 g/L malt, 4 g/L sucrose) medium for 5-7 days inoculated directly from -80°C glycerol stocks.

Genome sequencing and data analysis. For sequencing, DNA of 84 ascospores was isolated using a phenol-chloroform extraction protocol as described previously (66). Eight ascospores were available per tetrad due to an additional mitosis that follows meiosis II in *Z. tritici*. A previous study, that sequenced all eight ascospores of two tetrads, confirmed each tetrad contained four twins as the result of the mitosis (61). Based on the molecular characterization of all ascospores of the 23 tetrads from the previous study (61), we selected four unique ascospores for each tetrad for sequencing. Library preparation and sequencing using an Illumina HiSeq3000 machine for the 84 ascopores were performed at the Max Planck-Genome-centre, Cologne, Germany. The Illumina read data is available in the Sequence Read Archive under the BioProject PRJNA904559. Please note that two tetrads (A03-4 and A08-1) that were sequenced in an earlier study were also included (66). The Illumina read data for these two tetrads is available at the Sequence Read Archive under the BioProject PRJNA438050. An overview of the included tetrads and ascospores and is given in Table S3B. We visually checked the distribution of parental haplotypes within each tetrad. Only 23 tetrads showing a 2:2 segregation of parental haplotypes and crossover events involving the homologous chromosome of two ascospores were included (see example in Fig S6). One of the original 24 tetrads was excluded from the analysis because it showed a pattern of parental haplotypes on multiple chromosomes that was inconsistent with meiotic recombination and was thought not to be the product of a single meiosis, but rather a mixture of two or more meiotic events. In addition, the parental strain IPO94269 was sequenced as described above and its Illumina reads were deposited in the BioProject PRJNA904744. The Illumina data for the IPO323 parental strains is available under the BioProject PRJNA371572.

Mapping and SNP calling. The reads of 92 ascospores of the 23 tetrads were mapped to the IPO323 reference genome with bowtie2 (version 2.3.4.1) (107). This analysis focused only on single nucleotide polymorphisms (SNPs). To obtain a high-quality SNP dataset we performed the SNP calling with two variant callers, GATK (version 4.1.6.0) (108) and Samtools (version 1.7) (109), and SNPs with QUAL≥90 that were called by both variant callers were used for the downstream processing. Variants in regions that contain transposable elements (TEs) were removed from the analysis with bedtools intersect (version 2.26.0, option -v) (110) to avoid spurious alignments. From the remaining SNPs, only variants from regions with coverage >5 in all four ascospores of a tetrad were used for the analysis to avoid false negatives due to the low coverage in one of the spores. Biallelic SNPs with minor allele frequency >0.9 and with QUAL>90 that were called by both variant callers were identified by overlapping variant call format (VCF) files from both haplotype callers with bedtools intersect and used as a core set of high-fidelity SNPs. VCF files of four spores from the same tetrad were merged with VCFtools (v0.1.15) with merge option (111) to create a variant file for each tetrad.

High-quality threshold and variant calling accepting only variants identified by two callers will potentially lead to false negative calls in some of the four spores and hence will affect the segregation ratio obtained for the SNPs. To reduce the risk of false negative calls we re-introduced high-fidelity SNP to any of the other ascospores of a tetrad if there was an indication that it was present but did not satisfy the quality requirements. This means that SNPs which were called in a tetrad but did not meet the quality threshold in some of the ascospores but met the quality threshold in at least one of the ascospores were re-introduced. SNPs on chromosomes that were deleted or absent in the parental strains were removed from the analysis of the respective progeny. Please see Table S3B for an overview of the number of high-fidelity SNPs included for each tetrad.

Identification of recombination events. To detect recombination and gene conversion events in the tetrad progeny, CrossOver.py from the Recombine package (version 2.1) for tetrad analysis in yeast (67) was modified to fit the genome characteristics of *Z. tritici* (size and number of chromosomes and the location of the centromeres (59)). Input segregation files for the CrossOver program were generated from merged tetrad VCF files for each tetrad with the custom-made bash script (see Supplementary methods). Each segregation file consisted of 7 columns: the first two columns referred to the chromosome and position of the variant, the third column served as a spacer, and the last four columns referred to the presence/absence of SNPs in four spores. 0 and 1 values in the last four columns of a segregation file designated the presence or absence of a variant at a certain position

compared to the reference genome. The program initially identifies COs as positions with 2:2 segregation where adjacent markers undergo a reciprocal genotype switch. Gene conversion tracts are then identified as regions of non-2:2 segregation. After the identification of recombination events, all double crossovers separated with a single SNP were filtered out. Gene conversions were filtered for tracts spanning ≥3 markers. The recombination rate per tetrad [cM/Mb] was calculated by the following formula:

$$\text{recombination rate} = (½ \times \text{number of CO} \times 100) / \text{genome size}$$

The gene conversion rate per tetrad was determined as the proportion of converted markers from the total number of markers identified per tetrad. Furthermore, tract lengths were determined with the midpoint method, i.e., the midpoint between two markers of a different class (e.g. converted vs. non-converted) was considered to be the position were the tract started or ended. Tracts spanning TEs were removed for the estimation of tract lengths and recombination rates. Recombination events and gene conversion events detected in this study are listed in the supplementary material (Table S1B-C and Table S2A-C, respectively). SNPs in TEs were disregarded for the determination of recombination and gene conversion events.

Estimation of meiotic mutation rates. To estimate meiotic mutation rates in *Z. tritici,* genome-wide SNPs (including SNPs in TEs) satisfying the following criteria were taken into consideration: i) read depth >5 in both parental strains and the ascospore progeny; ii) absent in both parental strains (Table S3A). Before a SNP in the progeny was considered a *de novo* mutation, both parental sequencing results were manually checked to validate that this SNP was already present but not called in the parental genomes. Only SNPs in the progeny that showed no hints in the parental genomes were included in the subsequent analysis. The per bp mutation rate was calculated as the "average number of meiotic mutations per ascus" / "the reference genome size". To verify *in silico* detected meiotic mutations, we performed Sanger sequencing of 20 randomly selected mutations from which 19 mutations were confirmed (see Supplementary Methods).

Detection of duplications. For the detection of duplications in the parental strains, Illumina reads were quality filtered as described above and mapped onto the reference genome using SpeedSeq align followed by structural variation analysis by LUMPY (112) as implemented in the SpeedSeq

package (version 0.1.2) (113). The VCF files were filtered using bcftools (version 1.6) as follows: VCF files were filtered on duplications, genotype (GT=0/1) and quality >400, and length <50000.

Correlation analysis with genomic features. The following genomic compartments were considered as these have been previously determined: Histone modifications enrichment (H3K4me2, H3K9me3, H3K27me3) as defined in (59), Gene models (65),Transposable elements (114). Simple sequence repeats (SSR) were annotated *ad initio* using GMATA (version 2.3) (115).

For motif discovery in the vicinity of crossover events 500 bp upstream and downstream genomic sequence surrounding the individual crossover events were extracted from the genome and used for motif discovery by HOMER (version 4.11) (116). The four most significant *de novo* identified motifs with a *p*-value $< 1 \times 10^{-15}$ were selected.

Data Availability

The Illumina read data is available in the Sequence Read Archive under the BioProjects PRJNA904559, PRJNA438050, PRJNA904744, and PRJNA371572. The *Z. tritici* IPO323 reference genome is available under the accession GCA_000219625.1.

References

1.   Peñalba J v., Wolf JBW. 2020. From molecules to populations: appreciating and estimating recombination rate variation. Nat Rev Genet 21:476–492.

2.   Keeney S. 2008. Spo11 and the Formation of DNA Double-Strand Breaks in Meiosis, p. 81–123. *In* Recombination and Meiosis. Springer Berlin Heidelberg, Berlin, Heidelberg.

3.   Zelkowski M, Olson MA, Wang M, Pawlowski W. 2019. Diversity and Determinants of Meiotic Recombination Landscapes. Trends in Genetics 35:359–370.

4.   Zickler D, Kleckner N. 2015. Recombination, Pairing, and Synapsis of Homologs during Meiosis. Cold Spring Harb Perspect Biol 7:a016626.

5.   Chen J-M, Cooper DN, Chuzhanova N, Férec C, Patrinos GP. 2007. Gene conversion: mechanisms, evolution and human disease. Nat Rev Genet 8:762–775.

6.   Kleckner N. 1996. Meiosis: how could it work? Proceedings of the National Academy of Sciences 93:8167–8174.

7.   Korunes KL, Noor MAF. 2017. Gene conversion and linkage: effects on genome evolution and speciation. Mol Ecol 26:351–364.

8.   Youds JL, Boulton SJ. 2011. The choice in meiosis – defining the factors that influence crossover or non-crossover formation. J Cell Sci 124:501–513.

9.   Henderson IR, Bomblies K. 2021. Evolution and Plasticity of Genome-Wide Meiotic Recombination Rates. Annu Rev Genet 55:23–43.

10.   Bergero R, Ellis P, Haerty W, Larcombe L, Macaulay I, Mehta T, Mogensen M, Murray D, Nash W, Neale MJ, O'Connor R, Ottolini C, Peel N, Ramsey L, Skinner B, Suh A, Summers M, Sun Y, Tidy A, Rahbari R, Rathje C, Immler S. 2021. Meiosis and beyond – understanding the mechanistic and evolutionary processes shaping the germline genome. Biological Reviews 96:822–841.

11.   Munz P. 1994. An analysis of interference in the fission yeast Schizosaccharomyces pombe. Genetics 137:701–707.

12.   Mercier R, Mézard C, Jenczewski E, Macaisne N, Grelon M. 2015. The Molecular Biology of Meiosis in Plants. Annu Rev Plant Biol 66:297–327.

13.   Blary A, Jenczewski E. 2019. Manipulation of crossover frequency and distribution for plant breeding. Theoretical and Applied Genetics 132:575–592.

14.   Haenel Q, Laurentino TG, Roesti M, Berner D. 2018. Meta-analysis of chromosome-scale crossover rate variation in eukaryotes and its significance to evolutionary genomics. Mol Ecol 27:2477–2497.

15.   Choi K, Henderson IR. 2015. Meiotic recombination hotspots - a comparative view. Plant J 83:52–61.

16.   Lichten M, Goldman ASH. 1995. MEIOTIC RECOMBINATION HOTSPOTS. Annu Rev Genet 29:423–444.

17.   Croll D, Lendenmann MH, Stewart E, McDonald BA. 2015. The Impact of Recombination Hotspots on Genome Evolution of a Fungal Plant Pathogen. Genetics 201:1213–1228.

18.   Stukenbrock EH, Dutheil JY. 2018. Fine-Scale Recombination Maps of Fungal Plant Pathogens Reveal Dynamic Recombination Landscapes and Intragenic Hotspots. Genetics 208:1209–1229.

19.   Haenel Q, Laurentino TG, Roesti M, Berner D. 2018. Meta-analysis of chromosome-scale crossover rate variation in eukaryotes and its significance to evolutionary genomics. Mol Ecol 27:2477–2497.

20.   Sardell JM, Cheng C, Dagilis AJ, Ishikawa A, Kitano J, Peichel CL, Kirkpatrick M. 2018. Sex Differences in Recombination in Sticklebacks. G3 (Bethesda) 8:1971–1983.

21.   Pan J, Sasaki M, Kniewel R, Murakami H, Blitzblau HG, Tischfield SE, Zhu X, Neale MJ, Jasin M, Socci ND, Hochwagen A, Keeney S. 2011. A Hierarchical Combination of Factors Shapes the Genome-wide Topography of Yeast Meiotic Recombination Initiation. Cell 144:719–731.

22.   Borde V, Robine N, Lin W, Bonfils S, Géli V, Nicolas A. 2009. Histone H3 lysine 4 trimethylation marks meiotic recombination initiation sites. EMBO J 28:99–111.

23.   Buard J, Barthès P, Grey C, de Massy B. 2009. Distinct histone modifications define initiation and repair of meiotic recombination in the mouse. EMBO J 28:2616–2624.

24.   Choi K, Zhao X, Kelly KA, Venn O, Higgins JD, Yelina NE, Hardcastle TJ, Ziolkowski PA, Copenhaver GP, Franklin CH, Mcvean G, Henderson IR. 2013. Arabidopsis meiotic crossover hot spots overlap with H2A.Z nucleosomes at gene promoters. Nature GeNetics VOLUME 45.

25.   Underwood CJ, Choi K, Lambing C, Zhao X, Serra H, Borges F, Simorowski J, Ernst E, Jacob Y, Henderson IR, Martienssen RA. 2018. Epigenetic activation of meiotic recombination near Arabidopsis thaliana centromeres via loss of H3K9me2 and non-CG DNA methylation. Genome Res 28:519–531.

26.   Fouché S, Plissonneau C, McDonald BA, Croll D. 2018. Meiosis leads to pervasive copy-number variation and distorted inheritance of accessory chromosomes of the wheat pathogen Zymoseptoria tritici. Genome Biol Evol 10:1416–1429.

27.   Chan AH, Jenkins PA, Song YS. 2012. Genome-Wide Fine-Scale Recombination Rate Variation in Drosophila melanogaster. PLoS Genet 8:e1003090.

28.   Daugherty MD, Zanders SE. 2019. Gene conversion generates evolutionary novelty that fuels genetic conflicts. Curr Opin Genet Dev. Elsevier Ltd https://doi.org/10.1016/j.gde.2019.07.011.

29.   Lazzaro BP, Clark AG. 2001. Evidence for Recurrent Paralogous Gene Conversion and Exceptional Allelic Divergence in the Attacin Genes of Drosophila melanogaster. Genetics 159:659–671.

30.   Thomas JH. Concerted Evolution of Two Novel Protein Families in Caenorhabditis Species https://doi.org/10.1534/genetics.105.052746.

31.   Buchmann K. 2014. Evolution of innate immunity: Clues from invertebrates via fish to mammals. Front Immunol 5.

32.   Lorenz A, Mpaulo SJ. 2022. Gene conversion: a non-Mendelian process integral to meiotic recombination. Heredity (Edinb) 129:56–63.

33.   Mancera E, Bourgon R, Brozzi A, Huber W, Steinmetz LM. 2008. High-resolution mapping of meiotic crossovers and non-crossovers in yeast. Nature 454:479–485.

34.   Liu H, Huang J, Sun X, Li J, Hu Y, Yu L, Liti G, Tian D, Hurst LD, Yang S. 2018. Tetrad analysis in plants and fungi finds large differences in gene conversion rates but no GC bias. Nat Ecol Evol 2:164–173.

35.   Mansai SP, Kado T, Innan H. 2011. The Rate and Tract Length of Gene Conversion between Duplicated Genes. Genes (Basel) 2:313–331.

36.   Lesecque Y, Mouchiroud D, Duret L. 2013. GC-Biased Gene Conversion in Yeast Is Specifically Associated with Crossovers: Molecular Mechanisms and Evolutionary Significance. Mol Biol Evol 30:1409–1419.

37.   Marais G. 2003. Biased gene conversion: implications for genome and sex evolution. Trends Genet 19:330–338.

38.   Pessia E, Popa A, Mousset S, Rezvoy C, Duret L, Marais GAB. 2012. Evidence for Widespread GC-biased Gene Conversion in Eukaryotes. Genome Biol Evol 4:675–682.

39.   Arbeithuber B, Betancourt AJ, Ebner T, Tiemann-Boege I. 2015. Crossovers are associated with mutation and biased gene conversion at recombination hotspots. Proceedings of the National Academy of Sciences 112:2109 LP – 2114.

40.   Arbel–Eden A, Simchen G. 2019. Elevated Mutagenicity in Meiosis and Its Mechanism. BioEssays 41:1800235.

41.   Galagan JE, Selker EU. 2004. RIP: the evolutionary cost of genome defense. TRENDS in Genetics 20:417–423.

42.   Lynch M, Ackerman MS, Gout J-F, Long H, Sung W, Thomas WK, Foster PL. 2016. Genetic drift, selection and the evolution of the mutation rate. Nat Rev Genet 17:704–714.

43.   Narasimhan VM, Rahbari R, Scally A, Wuster A, Mason D, Xue Y, Wright J, Trembath RC, Maher ER, van Heel DA, Auton A, Hurles ME, Tyler-Smith C, Durbin R. 2017. Estimating the human mutation rate from autozygous segments reveals population differences in human mutational processes. Nat Commun 8:303.

44.   Rahbari R, Wuster A, Lindsay SJ, Hardwick RJ, Alexandrov LB, al Turki S, Dominiczak A, Morris A, Porteous D, Smith B, Stratton MR, Hurles ME. 2016. Timing, rates and spectra of human germline mutation. Nat Genet 48:126–133.

45.   Rattray A, Santoyo G, Shafer B, Strathern JN. 2015. Elevated mutation rate during meiosis in Saccharomyces cerevisiae. PLoS Genet 11:e1004910.

46.   Halldorsson B v., Palsson G, Stefansson OA, Jonsson H, Hardarson MT, Eggertsson HP, Gunnarsson B, Oddsson A, Halldorsson GH, Zink F, Gudjonsson SA, Frigge ML, Thorleifsson G, Sigurdsson A, Stacey SN, Sulem P, Masson G, Helgason A, Gudbjartsson DF, Thorsteinsdottir U, Stefansson K. 2019. Human genetics: Characterizing mutagenic effects of recombination through a sequence-level genetic map. Science (1979) 363.

47.   Lynch M, Sung W, Morris K, Coffey N, Landry CR, Dopman EB, Dickinson WJ, Okamoto K, Kulkarni S, Hartl DL, Thomas WK. 2008. A genome-wide view of the spectrum of spontaneous mutations in yeast. Proceedings of the National Academy of Sciences 105:9272–9277.

48.   Wang L, Sun Y, Sun X, Yu L, Xue L, He Z, Huang J, Tian D, Hurst LD, Yang S. 2020. Repeat-induced point mutation in Neurospora crassa causes the highest known mutation rate and mutational burden of any cellular life. Genome Biol 21:142.

49.   Villalba de la Peña M, Summanen PAM, Liukkonen M, Kronholm I. 2022. Variation in spontaneous mutation rate and spectrum across the genome of Neurospora crassa. bioRxiv 2022.03.13.484164.

50.   Freitag M, Williams RL, Kothe GO, Selker EU. 2002. A cytosine methyltransferase homologue is essential for repeat-induced point mutation in Neurospora crassa. Proc Natl Acad Sci U S A 99:8802–8807.

51.   Gladyshev E. 2017. Repeat-Induced Point Mutation and Other Genome Defense Mechanisms in Fungi. Microbiol Spectr 5.

52.   Gladyshev E, Kleckner N. 2016. Recombination-Independent Recognition of DNA Homology for Repeat-Induced Point Mutation (RIP) Is Modulated by the Underlying Nucleotide Sequence. PLoS Genet 12:e1006015.

53.   SELKER E. 2002. 15 Repeat-induced gene silencing in fungi, p. 439–450. *In* Homology Effects. Elsevier.

54.   Fudal I, Ross S, Brun H, Besnard A-L, Ermel M, Kuhn M-L, Balesdent M-H, Rouxel T. 2009. Repeat-induced point mutation (RIP) as an alternative mechanism of evolution toward virulence in Leptosphaeria maculans. Molecular Plant-Microbe Interactions 22:932–941.

55.   van de Wouw AP, Cozijnsen AJ, Hane JK, Brunner PC, McDonald BA, Oliver RP, Howlett BJ. 2010. Evolution of Linked Avirulence Effectors in Leptosphaeria maculans Is Affected by Genomic Environment and Exposure to Resistance Genes in Host Plants. PLoS Pathog 6:e1001180.

56.   Hane JK, Williams AH, Taranto AP, Solomon PS, Oliver RP. 2015. Repeat-Induced Point Mutation: A Fungal-Specific, Endogenous Mutagenesis Process BT - Genetic Transformation Systems in Fungi, Volume 2, p. 55–68. *In* van den Berg, MA, Maruthachalam, K (eds.), . Springer International Publishing, Cham.

57.   Goodwin SB, M'Barek S ben, Dhillon B, Wittenberg AHJ, Crane CF, Hane JK, Foster AJ, van der Lee TAJ, Grimwood J, Aerts A, Antoniw J, Bailey A, Bluhm B, Bowler J, Bristow J, van der Burgt A,

Canto-Canché B, Churchill ACL, Conde-Ferràez L, Cools HJ, Coutinho PM, Csukai M, Dehal P, de Wit P, Donzelli B, van de Geest HC, van Ham RCHJ, Hammond-Kosack KE, Henrissat B, Kilian A, Kobayashi AK, Koopmann E, Kourmpetis Y, Kuzniar A, Lindquist E, Lombard V, Maliepaard C, Martins N, Mehrabi R, Nap JPH, Ponomarenko A, Rudd JJ, Salamov A, Schmutz J, Schouten HJ, Shapiro H, Stergiopoulos I, Torriani SFF, Tu H, de Vries RP, Waalwijk C, Ware SB, Wiebenga A, Zwiers LH, Oliver RP, Grigoriev I v., Kema GHJ. 2011. Finished genome of the fungal wheat pathogen Mycosphaerella graminicola reveals dispensome structure, chromosome plasticity, and stealth pathogenesis. PLoS Genet 7.

58.   Habig M, Quade J, Stukenbrock EH. 2017. Forward genetics approach reveals host genotype-dependent importance of accessory chromosomes in the fungal wheat pathogen Zymoseptoria tritici. mBio 8.

59.   Schotanus K, Soyer JL, Connolly LR, Grandaubert J, Happel P, Smith KM, Freitag M, Stukenbrock EH. 2015. Histone modifications rather than the novel regional centromeres of Zymoseptoria tritici distinguish core and accessory chromosomes. Epigenetics Chromatin 8:41.

60.   Habig M, Lorrain C, Feurtey A, Komluski J, Stukenbrock EH. 2021. Epigenetic modifications affect the rate of spontaneous mutations in a pathogenic fungus. Nat Commun 12:1–13.

61.   Habig M, Kema GH, Stukenbrock EH. 2018. Meiotic drive of female-inherited supernumerary chromosomes in a pathogenic fungus https://doi.org/10.7554/eLife.40251.001.

62.   Morais D, Gélisse S, Laval V, Sache I, Suffert F. 2016. Inferring the origin of primary inoculum of Zymoseptoria tritici from differential adaptation of resident and immigrant populations to wheat cultivars. Eur J Plant Pathol 145:393–404.

63.   Möller M, Schotanus K, Soyer JL, Haueisen J, Happ K, Stralucke M, Happel P, Smith KM, Connolly LR, Freitag M, Stukenbrock EH. 2019. Destabilization of chromosome structure by histone H3 lysine 27 methylation. PLoS Genet 15:e1008093.

64.   Goodwin SB, M'barek S ben, Dhillon B, Wittenberg AHJ, Crane CF, Hane JK, Foster AJ, van der Lee TAJ, Grimwood J, Aerts A, Antoniw J, Bailey A, Bluhm B, Bowler J, Bristow J, van der Burgt A, Canto-Canche B, Churchill ACL, Conde-Ferraez L, Cools HJ, Coutinho PM, Csukai M, Dehal P, de Wit P, Donzelli B, van de Geest HC, van Ham RCHJ, Hammond-Kosack KE, Henrissat B, Kilian A, Kobayashi AK, Koopmann E, Kourmpetis Y, Kuzniar A, Lindquist E, Lombard V, Maliepaard C, Martins N, Mehrabi R, Nap JPH, Ponomarenko A, Rudd JJ, Salamov A, Schmutz J, Schouten HJ, Shapiro H, Stergiopoulos I, Torriani SFF, Tu H, de Vries RP, Waalwijk C, Ware SB, Wiebenga A, Zwiers L-H, Oliver RP, Grigoriev I v, Kema GHJ. 2011. Finished genome of the fungal wheat pathogen Mycosphaerella graminicola reveals dispensome structure, chromosome plasticity, and stealth pathogenesis. PLoS Genet 7:e1002070.

65.   Grandaubert J, Bhattacharyya A, Stukenbrock EH. 2015. RNA-seq-Based Gene Annotation and Comparative Genomics of Four Fungal Grass Pathogens in the Genus Zymoseptoria Identify Novel Orphan Genes and Species-Specific Invasions of Transposable Elements. G3 (Bethesda) 5:1323–1333.

66.   Habig M, Kema GHJ, Stukenbrock EH. 2018. Meiotic drive of female-inherited supernumerary chromosomes in a pathogenic fungus. Elife 7.

67.   Anderson CM, Chen SY, Dimon MT, Oke A, DeRisi JL, Fung JC. 2011. ReCombine: a suite of programs for detection and analysis of meiotic recombination in whole-genome datasets. PLoS One2011/10/25. 6:e25509–e25509.

68.   Bishop DK, Zickler D. 2004. Early Decision: Meiotic Crossover Interference prior to Stable Strand Exchange and Synapsis. Cell 117:9–15.

69.   McPeek MS, Speed TP. 1995. Modeling interference in genetic recombination. Genetics 139:1031–1044.

70.   Zhao H, Speed T, Genetics MM-, 1995 undefined. 1995. Statistical analysis of crossover interference using the chi-square model. academic.oup.com.

71.   Chen SY, Tsubouchi T, Rockmill B, Sandler JS, Richards DR, Vader G, Hochwagen A, Roeder GS, Fung JC. 2008. Global Analysis of the Meiotic Crossover Landscape. Dev Cell 15:401–415.

72.   Cummings WJ, Yabuki M, Ordinario EC, Bednarski DW, Quay S, Maizels N. 2007. Chromatin structure regulates gene conversion. PLoS Biol 5:e246.

73.   Bourque G, Burns KH, Gehring M, Gorbunova V, Seluanov A, Hammell M, Imbeault M, Izsvák Z, Levin HL, Macfarlan TS, Mager DL, Feschotte C. 2018. Ten things you should know about transposable elements. Genome Biol 19:199.

74.   Wells JN, Feschotte C. 2020. A Field Guide to Eukaryotic Transposable Elements. Annu Rev Genet 54:539–561.

75.   Eickbush TH, Malik HS. 2007. Origins and Evolution of Retrotransposons, p. 1111–1144. *In* Mobile DNA II.

76.   Mazur AK, Gladyshev E. 2018. Partition of Repeat-Induced Point Mutations Reveals Structural Aspects of Homologous DNA-DNA Pairing. Biophys J 115:605–615.

77.   Cambareri EB, Jensen BC, Schabtach E, Selker EU. 1989. Repeat-induced G-C to A-T mutations in Neurospora. Science 244:1571–1575.

78.   Martin SH, Davey JW, Salazar C, Jiggins CD. 2019. Recombination rate variation shapes barriers to introgression across butterfly genomes. PLoS Biol 17:e2006288.

79.   Wang S, Hassold T, Hunt P, White MA, Zickler D, Kleckner N, Zhang L. 2017. Inefficient Crossover Maturation Underlies Elevated Aneuploidy in Human Female Meiosis. Cell 168:977–989.e17.

80.   Bhuiyan H, Schmekel K. 2004. Meiotic chromosome synapsis in yeast can occur without spo11-induced DNA double-strand breaks. Genetics 168:775–783.

81.   Storlazzi A, Tessé S, Gargano S, James F, Kleckner N, Zickler D. 2003. Meiotic double-strand breaks at the interface of chromosome movement, chromosome remodeling, and reductional division. Genes Dev 17:2675–2687.

82.   Tischfield SE, Keeney S. 2012. Scale matters: the spatial correlation of yeast meiotic DNA breaks with histone H3 trimethylation is driven largely by independent colocalization at promoters. Cell Cycle 11:1496–1503.

83.   Fowler KR, Sasaki M, Milman N, Keeney S, Smith GR. 2014. Evolutionarily diverse determinants of meiotic DNA break and recombination landscapes across the genome. Genome Res 24:1650–1664.

84.   Clouaire T, Legube G. 2015. DNA double strand break repair pathway choice: a chromatin based decision? Nucleus 6:107–113.

85.   Jeggo PA, Downs JA. 2014. Roles of chromatin remodellers in DNA double strand break repair. Exp Cell Res 329:69–77.

86.   Kalousi A, Soutoglou E. 2016. Nuclear compartmentalization of DNA repair. Curr Opin Genet Dev 37:148–157.

87.   Sung P, Klein H. 2006. Mechanism of homologous recombination: mediators and helicases take on regulatory functions. Nat Rev Mol Cell Biol 7:739–750.

88.   Alagoz M, Katsuki Y, Ogiwara H, Ogi T, Shibata A, Kakarougkas A, Jeggo P. 2015. SETDB1, HP1 and SUV39 promote repositioning of 53BP1 to extend resection during homologous recombination in G2 cells. Nucleic Acids Res 43:7931–7944.

89.   Baldeyron C, Soria G, Roche D, Cook AJL, Almouzni G. 2011. HP1α recruitment to DNA damage by p150CAF-1 promotes homologous recombination repair. Journal of Cell Biology 193:81–95.

90.   Lee Y-H, Kuo C-Y, Stark JM, Shih H-M, Ann DK. 2013. HP1 promotes tumor suppressor BRCA1 functions during the DNA damage response. Nucleic Acids Res 41:5784–5798.

91.   Soria G, Almouzni G. 2013. Differential contribution of HP1 proteins to DNA end resection and homology-directed repair. Cell Cycle 12:422–429.

92.   Sun Y, Jiang X, Xu Y, Ayrapetov MK, Moreau LA, Whetstine JR, Price BD. 2009. Histone H3 methylation links DNA damage detection to activation of the tumour suppressor Tip60. Nat Cell Biol 11:1376–1382.

93.   Ayrapetov MK, Gursoy-Yuzugullu O, Xu C, Xu Y, Price BD. 2014. DNA double-strand breaks promote methylation of histone H3 on lysine 9 and transient formation of repressive chromatin. Proc Natl Acad Sci U S A 111:9169–9174.

94.   Lemaître C, Grabarz A, Tsouroula K, Andronov L, Furst A, Pankotai T, Heyer V, Rogier M, Attwood KM, Kessler P, Dellaire G, Klaholz B, Reina-San-Martin B, Soutoglou E. 2014. Nuclear position dictates DNA repair pathway choice. Genes Dev 28:2450–2463.

95.   Schep R, Brinkman EK, Leemans C, Vergara X, van der Weide RH, Morris B, van Schaik T, Manzo SG, Peric-Hupkes D, van den Berg J, Beijersbergen RL, Medema RH, van Steensel B. 2021. Impact of chromatin context on Cas9-induced DNA double-strand break repair pathway balance. Mol Cell 81:2216-2230.e10.

96.   Tock AJ, Holland DM, Jiang W, Osman K, Sanchez-Moran E, Higgins JD, Edwards KJ, Uauy C, Franklin FCH, Henderson IR. 2021. Crossover-active regions of the wheat genome are distinguished by DMC1, the chromosome axis, H3K27me3, and signatures of adaptation. Genome Res 31:1614–1628.

97.   van Wyk S, Wingfield BD, de Vos L, van der Merwe NA, Steenkamp ET. 2021. Genome-Wide Analyses of Repeat-Induced Point Mutations in the Ascomycota. Front Microbiol 11.

98.   Coleman JJ, Rounsley SD, Rodriguez-Carres M, Kuo A, Wasmann CC, Grimwood J, Schmutz J, Taga M, White GJ, Zhou S, Schwartz DC, Freitag M, Ma L-J, Danchin EGJ, Henrissat B, Coutinho PM, Nelson DR, Straney D, Napoli CA, Barker BM, Gribskov M, Rep M, Kroken S, Molnar I, Rensing C, Kennell JC, Zamora J, Farman ML, Selker EU, Salamov A, Shapiro H, Pangilinan J, Lindquist E, Lamers C, Grigoriev I v, Geiser DM, Covert SF, Temporini E, Vanetten HD. 2009. The genome of Nectria haematococca: contribution of supernumerary chromosomes to gene expansion. PLoS Genet 5:e1000618.

99.   Cuomo CA, Güldener U, Xu J-R, Trail F, Turgeon BG, di Pietro A, Walton JD, Ma L-J, Baker SE, Rep M. 2007. The Fusarium graminearum genome reveals a link between localized polymorphism and pathogen specialization. Science (1979) 317:1400–1402.

100.   Graïa F, Lespinet O, Rimbault B, Dequard–Chablat M, Coppin E, Picard M. 2001. Genome quality control: RIP (repeat–induced point mutation) comes to Podospora. Mol Microbiol 40:586–595.

101.   Idnurm A, Howlett BJ. 2003. Analysis of loss of pathogenicity mutants reveals that repeat-induced point mutations can occur in the Dothideomycete Leptosphaeria maculans. Fungal Genetics and Biology 39:31–37.

102.   Ikeda K, Nakayashiki H, Kataoka T, Tamba H, Hashimoto Y, Tosa Y, Mayama S. 2002. Repeat–induced point mutation (RIP) in Magnaporthe grisea: implications for its sexual cycle in the natural field context. Mol Microbiol 45:1355–1364.

103.   Pomraning KR, Connolly LR, Whalen JP, Smith KM, Freitag M. 2013. Repeat-induced point mutation, DNA methylation and heterochromatin in Gibberella zeae (anamorph: Fusarium graminearum). Fusarium Genomics, Molecular and Cellular Biology 93–109.

104.   van de Wouw AP, Elliott CE, Popa KM, Idnurm A. 2019. Analysis of Repeat Induced Point (RIP) Mutations in *Leptosphaeria maculans* Indicates Variability in the RIP Process Between Fungal Species. Genetics 211:89–104.

105.   Rouxel T, Grandaubert J, Hane JK, Hoede C, van de Wouw AP, Couloux A, Dominguez V, Anthouard V, Bally P, Bourras S, Cozijnsen AJ, Ciuffetti LM, Degrave A, Dilmaghani A, Duret L, Fudal I, Goodwin SB, Gout L, Glaser N, Linglin J, Kema GHJ, Lapalu N, Lawrence CB, May K, Meyer M, Ollivier B, Poulain J, Schoch CL, Simon A, Spatafora JW, Stachowiak A, Turgeon BG, Tyler BM, Vincent D, Weissenbach J, Amselem J, Quesneville H, Oliver RP, Wincker P, Balesdent MH, Howlett

BJ. 2011. Effector diversification within compartments of the Leptosphaeria maculans genome affected by Repeat-Induced Point mutations. Nat Commun 2.

106.   Frantzeskakis L, di Pietro A, Rep M, Schirawski J, Wu CH, Panstruga R. 2020. Rapid evolution in plant-microbe interactions - a molecular genomics perspective. New Phytol 225:1134–1142.

107.   Langmead B, Salzberg SL. 2012. Fast gapped-read alignment with Bowtie 2. Nat Methods 9:357–359.

108.   McKenna A, Hanna M, Banks E, Sivachenko A, Cibulskis K, Kernytsky A, Garimella K, Altshuler D, Gabriel S, Daly M, DePristo MA. 2010. The Genome Analysis Toolkit: a MapReduce framework for analyzing next-generation DNA sequencing data. Genome Res 20:1297–1303.

109.   Li H, Handsaker B, Wysoker A, Fennell T, Ruan J, Homer N, Marth G, Abecasis G, Durbin R. 2009. The Sequence Alignment/Map format and SAMtools. Bioinformatics 25:2078–2079.

110.   Quinlan AR. 2014. BEDTools: The Swiss–Army Tool for Genome Feature Analysis. Curr Protoc Bioinformatics 47.

111.   Danecek P, Auton A, Abecasis G, Albers CA, Banks E, DePristo MA, Handsaker RE, Lunter G, Marth GT, Sherry ST, McVean G, Durbin R. 2011. The variant call format and VCFtools. Bioinformatics 27:2156–2158.

112.   Layer RM, Chiang C, Quinlan AR, Hall IM. 2014. LUMPY: a probabilistic framework for structural variant discovery. Genome Biol 15:R84.

113.   Chiang C, Layer RM, Faust GG, Lindberg MR, Rose DB, Garrison EP, Marth GT, Quinlan AR, Hall IM. 2015. SpeedSeq: ultra-fast personal genome analysis and interpretation. Nat Methods 12:966–968.

114.   Lorrain C, Feurtey A, Möller M, Haueisen J, Stukenbrock E. 2021. Dynamics of transposable elements in recently diverged fungal pathogens: lineage-specific transposable element content and efficiency of genome defenses. G3 (Bethesda) 11.

115.   Wang X, Wang L. 2016. GMATA: An integrated software package for genome-scale SSR mining, marker development and viewing. Front Plant Sci 7:1350.

116.   Heinz S, Benner C, Spann N, Bertolino E, Lin YC, Laslo P, Cheng JX, Murre C, Singh H, Glass CK. 2010. Simple Combinations of Lineage-Determining Transcription Factors Prime cis-Regulatory Elements Required for Macrophage and B Cell Identities. Mol Cell 38:576–589.

117.   Kema GHJ, Gohari AM, Aouini L, Gibriel HAY. 2018. Stress and sexual reproduction affect the dynamics of the wheat pathogen effector AvrStb6 and strobilurin resistance https://doi.org/10.1038/s41588-018-0052-9.

118.   Mandell GL, Douglas, R. G. Jr, Bennett JE. 1996. Introductory mycology. Introductory mycology 2169–2176.

Supplementary

All supplementary tables and texts are deposited on the supplementary USB card.

Supplementary Methods

Description of the bioinformatic procedures and tools and Sanger sequencing results.

Supplementary Tables

Table S1A: List of all crossover and associated gene conversions.

Table S1B: Summary of crossover frequencies per tetrad for the core and accessory chromosomes.

Table S1C: List of genes in crossover hotspots.

Table S2A: List of all identified gene conversions.

Table S2B: Summary of the number of SNPs and converted SNPs (total, core (=on core chromosomes), accessory (=on accessory chromosomes)).

Table S2C: List of genes in gene conversion hotspots.

Table S2D: Summary of the converted marker and non-converted marker in genomic compartments. with the indicated presence/absence of specific histone modifications.

Table S3A: List of all meiotic *de novo* mutations.

Table S3B: Overview of tetrads, spores, mapping results and the number of high-fidelity SNPs.

Supplementary Figures
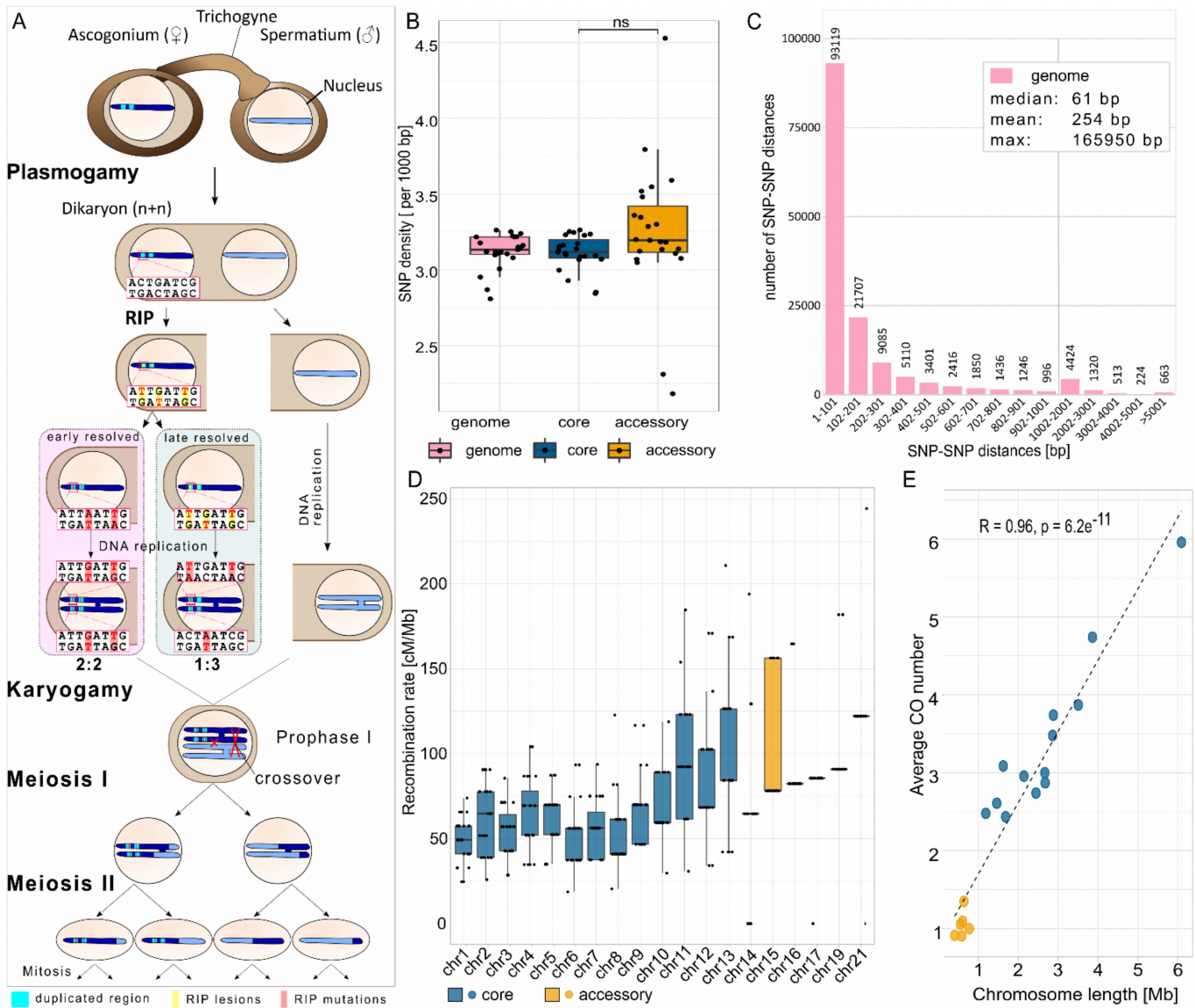
Fig S1. Distribution of SNP densities, recombination rates, and the number of crossovers (CO) per chromosome. **A** Schematic overview of the assumed sexual process in *Z. tritici* (117, 118). The spermatial nucleus is transferred via the trichogyne to the ascogonium, resulting in plasmogamy and a dikaryon with two separate nuclei. During the dikaryon stage RIP is assumed to occur, affecting replicated regions (cyan) and introducing C→T lesions that can either be resolved early, before premeiotic DNA replication, resulting in a 2:2 segregation pattern (red background), or late, with premeiotic DNA replication resolving the lesions, resulting in a 1:3 segregation pattern (green background). Meiosis I segregates homologous chromosomes, followed by chromatid separation in meiosis II. A subsequent mitosis results in the production of eight ascospores contained in an ascus

(not shown). **B** SNP density in SNPs per 1000 bp comparing the two parental strains IPO323 and IPO94269. **C** Distribution of distances between two neighboring SNPs. **D** Recombination rates per chromosome. Note that the number of crossovers on the accessory chromosomes showed little variation between tetrads (e.g., 0-3 for chromosome 14) thereby the estimated recombination rate also exhibited little variation. Box plots display center line, median; box limits, upper and lower quartiles; whiskers, 1.5x interquartile range; points, crossover frequency per genomic compartment per tetrad. **E** Average number of CO per chromosome. Points in **E** depict the average CO number for the respective chromosome length; blue points represent core chromosomes; orange points represent accessory chromosomes; the dashed line shows Pearson's correlation.
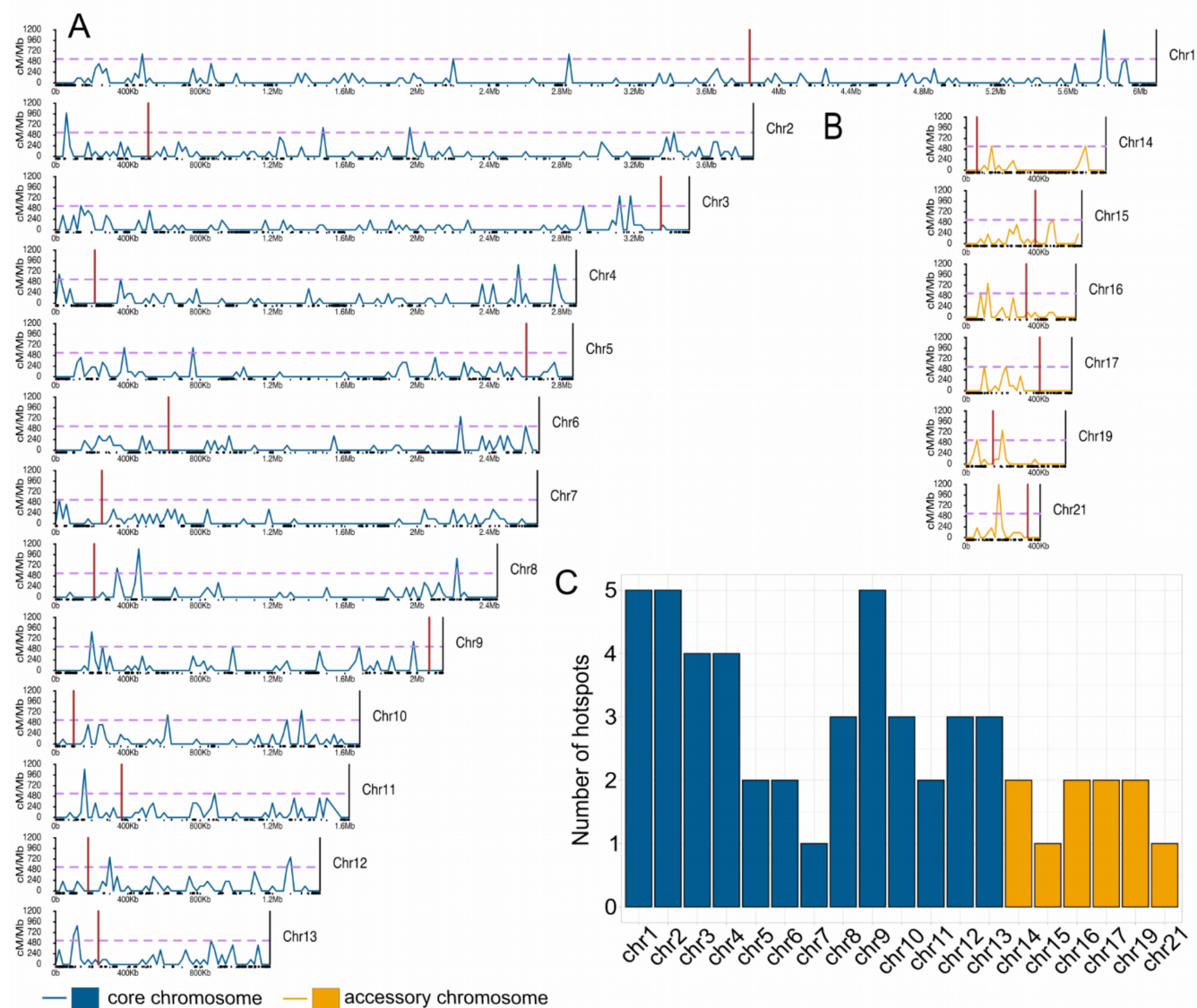
Fig S2. Distribution of recombination rates along the chromosomes in *Z. tritici*. **A** Distribution of recombination rates on core chromosomes. **B** Distribution of recombination rates on accessory chromosomes. Chromosomes are divided in 20 kb non-overlapping windows. The horizontal dashed

pink line represent threshold for hotspots with *p*-value < 0.001 defined by Poisson distribution (more than four crossover per 20 kb window). The blue lines represent crossover distribution on core chromosomes, orange lines represent crossover distribution on accessory chromosome and red horizontal lines show the centromere position. The x-axis designates the chromosome length. The black rectangles on the x-axis depict transposable elements. **C** Number of hotspots on the indicated chromosomes.
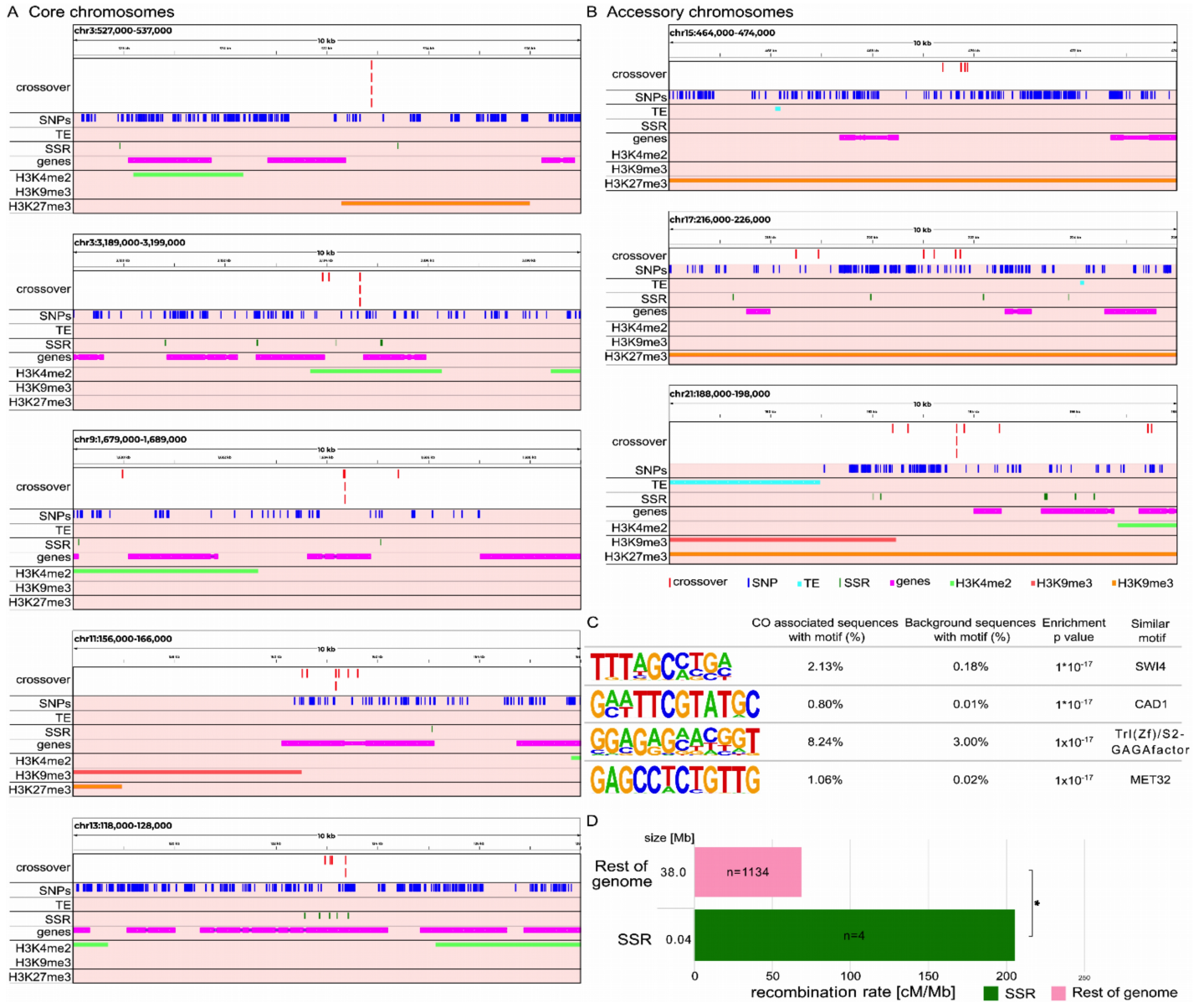

Fig S3. Details of the location of crossover events. **A, B** Display of the genomic features that are associated with the nine 1 kb windows that contained the highest number of crossover events (≥4) for **A** core chromosomes and **B** accessory chromosomes. **C** Four most significantly significantly over-represented short motifs (*p*-value < 1 x 10⁻¹⁵) in the vicinity of crossover events (500 bp upstream and downstream). **D** Recombination rate comparison between regions that are covered by simple

sequence repeats (SSR, size: 39 kb) and the rest of the genome. Statistical significance as determined by Fisher's exact test is depicted (*p-value = 0.031).
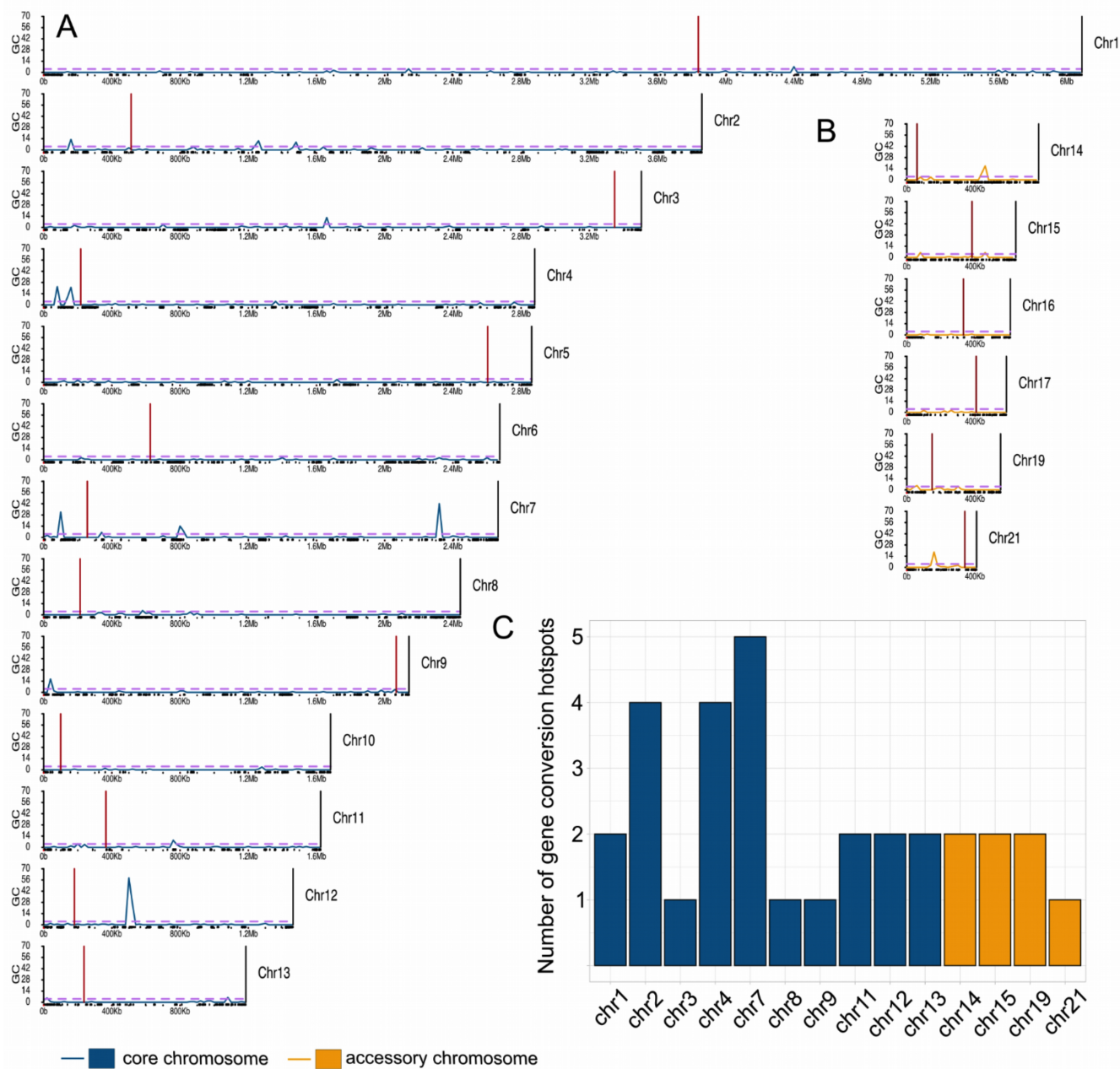

Fig S4. Distribution of gene conversions along the chromosomes in *Z. tritici*. **A** Distribution of gene conversions on core chromosomes. **B** Distribution of gene conversions on accessory chromosomes. Chromosomes are divided in 20 kb non-overlapping windows. The horizontal dashed pink line represent threshold for hotspots with *p*-value < 0.001 defined by Poisson distribution (more than 4 gene conversion events per 20 kb window). The blue lines represent crossover distribution on core chromosomes, orange lines represent crossover distribution on accessory chromosome and red

horizontal lines show the centromere position. The x-axis designates the chromosome length. Black rectangles on x-axis depict transposable elements. The y-axis shows the number of gene conversion events (NCO-GC and CO-GC). **C** Number of gene conversion hotspots on the indicated chromosomes.
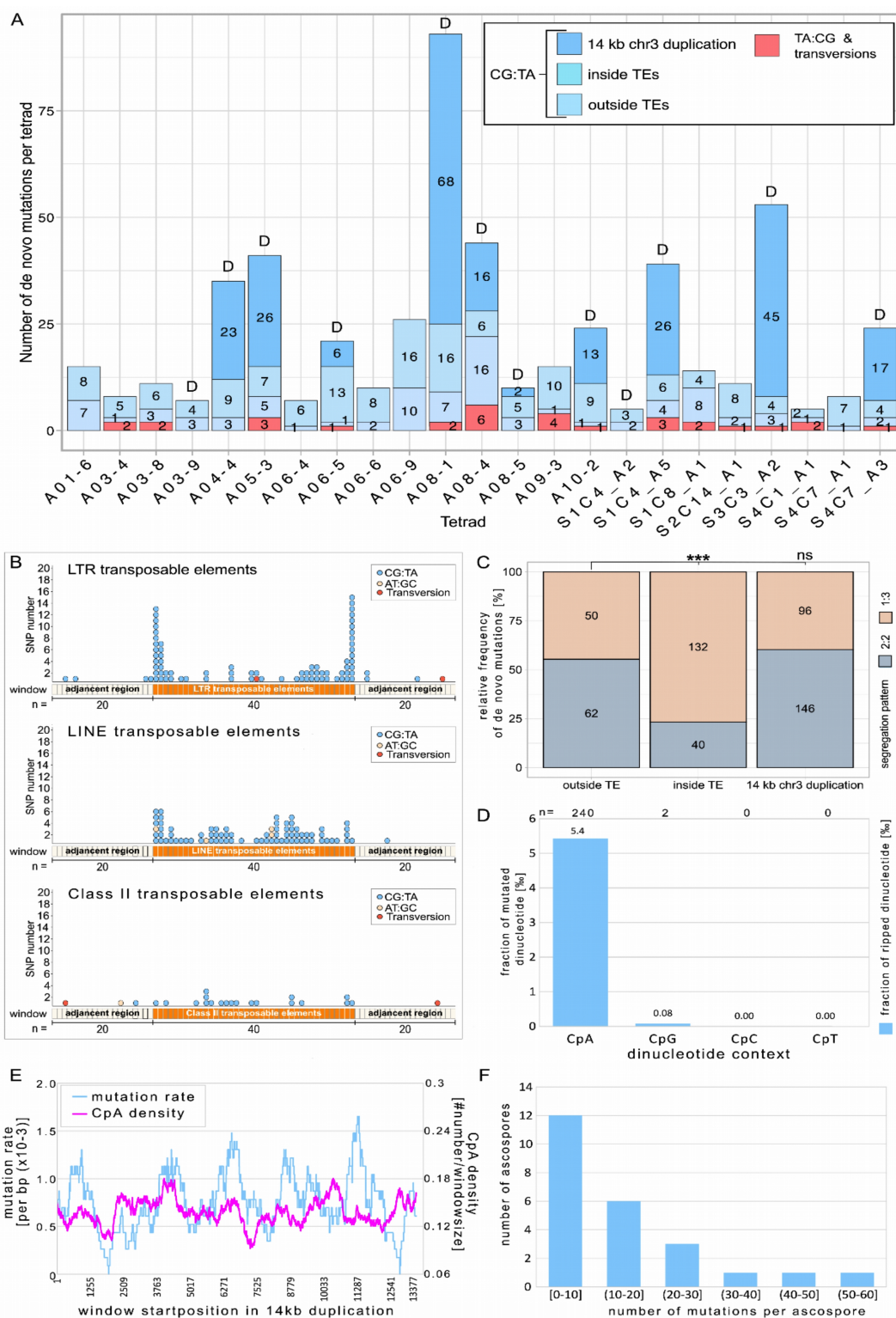
Fig S5. Distribution and segregation of *de novo* mutations. **A** Number of the *de novo* mutations per tetrad. Blue shaded bars display the number of CG:TA transitions on 14 kb duplication on chromosome 3, inside of TEs and outside of TEs per tetrad. Red bars depict the number of TA:CG

transitions and transversions. D indicates tetrads in which the 14 kb duplication is present in two of the four ascospores of the ascus. **B** Distribution of meiotic SNPs along different classes of TEs. Each TE was divided into 40 equal windows. Each black rectangle on the x-axis represents a window inside a TE representing 2.5% of the TE length. Beige rectangles represent windows in the regions directly adjacent to TEs. Dots above rectangles represent one mutation in each window (yellow dots-AT:GC transitions; blue dots-CG:TA transitions, red dots-transversions) **C** Segregation of *de novo* mutations in different genomic compartments. Light red bars show the relative frequency of *de novo* mutations with 1:3 segregation and grey bars display the relative frequency of *de novo* mutations with 2:2 segregation for the different genomic compartments. Fisher exact test *p*-values are shown (*$p < 0.05$, **$p < 0.005$, ***$p < 0.0005$). **D** Dinucleotide context of the 242 mutations within the 14 kb duplication on chromosome 3. The relative fraction (in ‰) of the dinucleotide sites that were ripped are depicted. **E** Variation of the mutation rate and the relative fraction CpA dinucleotides along the 14 kb duplication on chromosome 3 in sliding 500 bp windows. **F** Distribution of the number of RIP mutations within those ascospores that contained the duplication on chromosome 3 (marked D in Fig S5A).
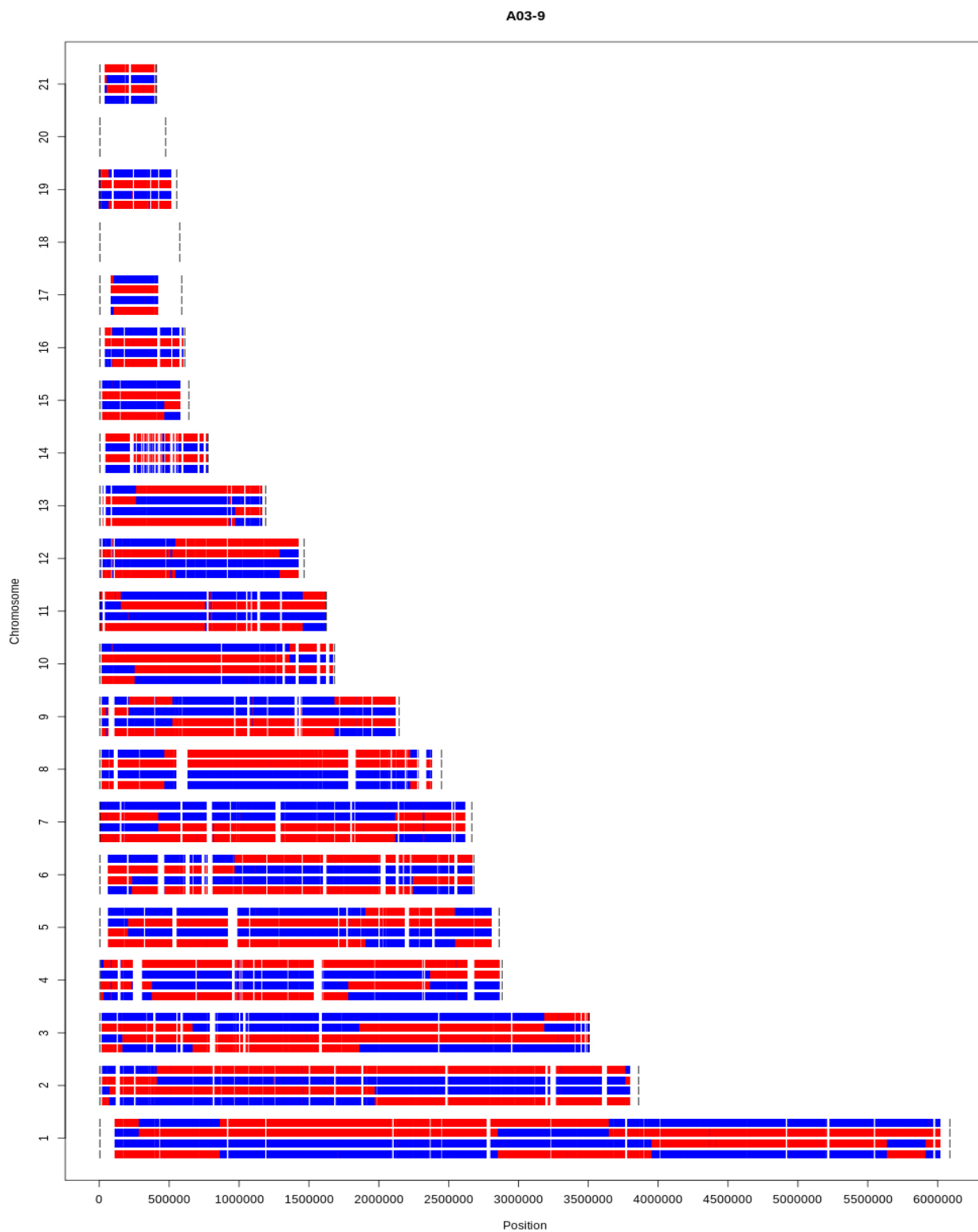
79

Fig S6. Example for the distribution of parental haplotypes within the four ascospores of the A03-9 tetrad. Blue/red represents the haplotype of the parental strain IPO323 and IPO94269 respectively.

Note that the parental haplotypes show a 2:2 segregation and crossover events involve the homologous chromosome of two ascospores. Note that chromosome 18 and chromosome 20 are not present in IPO94269 and were therefore removed from the analysis.

Chapter III

Elimination of disomic chromosomes during meiosis in a plant-pathogenic fungus

Jovan Komluski, Michael Habig and Eva H. Stukenbrock

Environmental Genomics, Christian-Albrechts University of Kiel, Am Botanischer Garten 1-9, 24118 Kiel, Germany

Max Planck Institute for Evolutionary Biology, August-Thienemann-Straße 2, 24306 Plön, Germany

Abstract (≤250 words)

Meiosis is an essential cellular process whose outcome is dependent on the proper pairing and segregation of homologous chromosomes. Errors in segregation during meiosis can lead to an uneven chromosome number, i.e., aneuploidy. Factors affecting the generation of aneuploidy are well studied; however, how aneuploid chromosomes undergo meiosis is mostly unknown. Fungal accessory chromosomes are frequently aneuploid during meiosis. One prime example are accessory chromosomes in *Zymoseptoria tritici* – a fungal wheat pathogen. Disomy is an often outcome of meiosis in this pathogen; however, frequencies of disomic accessory chromosomes in the field isolates are low. Interestingly, when unpaired during meiosis, these chromosomes are amplified by meiotic drive that increases their frequency. The mechanism of this drive is unknown; however, it seems to include an additional replication of accessory chromosomes during meiosis that can take place before karyogamy or in the fungal zygote. Here, we have isolated, karyotyped, and sequenced tetrad progeny from crosses including *Z. tritici* strains with homozygous and heterozygous disomic accessory chromosomes to i) explore the disomy maintenance and ii) determine the stage at which additional replication causing the meiotic drive of unpaired accessory chromosomes occurs. We observe the elimination of male-inherited unpaired disomic accessory chromosomes from the progeny. Next, unpaired disomic accessory chromosomes are inherited on frequencies higher than expected by Mendelian segregation, indicating that additional replication of unpaired accessory chromosomes happens prior to karyogamy. Results presented in this study provide insights into the inheritance of disomic accessory chromosomes and mechanism of their meiotic drive in *Z. tritici*.

Introduction

Meiosis is a highly conserved cellular process that involves the pairing and segregation of homologous chromosomes. During canonical meiosis, one round of genome replication is followed by the segregation of homologous chromosomes in meiosis I and the segregation of the sister chromatids in meiosis II to ensure that generated gametes carry half the genetic material of the parental cell (Lynn *et al.* 2007; Zickler and Kleckner 2015). Preparation for chromosome segregation starts during the S phase of the cell cycle when sister chromatids are linked to each other via cohesin molecules and segregation of sister chromatids is ensured by connections between sister centromere/kinetochore regions (Nasmyth and Haering 2009; Zickler and Kleckner 2015). A checkpoint pathway known as the spindle assembly checkpoint (SAC) monitors kinetochore attachment and tension and controls the proper segregation of sister chromatids by stopping the progression of the cell cycle until every sister chromatid is accurately attached to the mitotic spindle (reviewed in (Musacchio and Salmon 2007)). Chromosome segregation can, however, occur in the presence of unattached or incorrectly attached chromosomes, and therefore errors during chromosome segregation can result in aneuploid daughter cells, i.e., in daughter cells that have an unequal number of chromosomes (Siegel and Amon 2012; Covo 2020). Aberrations in kinetochore-microtubule attachment or SAC function are causes of segregation errors during meiosis (Levine and Holland 2018). These aberrations lead to unbalanced karyotypes and are well studied; however, how aneuploid chromosomes undergo meiosis needs deeper investigation.

Aneuploidy can have a detrimental or beneficial effect on the fitness of an individual. In general, aneuploidy is often associated with developmental defects and reduced fitness in eukaryotes (Sheltzer *et al.* 2011). Disomic yeast strains display transcription profiles that indicate environmental stress response (Gasch *et al.* 2000). Furthermore, prolonged replication of aneuploid cells due to the DNA replication fork rate and increased fork stalling reduce the rate of proliferation in aneuploid strains of budding and fission yeasts (Torres *et al.* 2007; Holland and Cleveland 2012; Santaguida *et al.* 2017). Increased chromosome numbers can also cause problems in chromosome pairing, recombination, and segregation during meiosis, leading to decreased fertility (Comai 2005; Bomblies *et al.* 2015, 2016). In contrast, the beneficial effects of aneuploidy are often associated with the increase in gene copy numbers on aneuploid chromosomes. Chromosomal gain is linked to drug resistance in human pathogenic fungi *Candida albicans* and *Cryptococcus neoformans* (Selmecki *et al.* 2006; Sophie *et al.* 2017). The positive fitness effect of aneuploidy is often reported for the accessory (also known as

84

supernumerary, or conditionally-dispensable (CDC)) chromosomes of plant pathogenic fungi. Disomy of PDA1-CDC in *N. haematococca* MPVI that harbors the PDA1 virulence gene causes increased virulence of this fungal pathogen in pea (Miao *et al.* 1991; Garmaroodi and Taga 2007, 2015). Once gained beneficial ploidy is fixed in the population, however, how aneuploidy is maintained over evolutionary trajectory is poorly understood.

Zymoseptoria tritici is an excellent model for studying the transmission of aneuploid chromosomes during meiosis because of its unique set of accessory chromosomes. The reference genome of IPO323 isolate consists of 13 core chromosomes and eight accessory chromosomes that often show the presence/absence polymorphisms between different isolates (Goodwin *et al.* 2011; Clémence *et al.* 2016). Disomy and losses of accessory chromosomes are a frequent product of meiosis in *Z. tritici* and often occur due to the nondisjunction of accessory chromosomes during meiosis I or meiosis II (Wittenberg *et al.* 2009; Fouché *et al.* 2018). Despite the disomy of accessory chromosomes often occurring during meiosis, frequencies of disomic isolates in wild populations of *Z. tritici* are low (Fouché *et al.* 2018), suggesting a disomy-controlling mechanism. A repeat-induced point mutation (RIP) is a fungal defense mechanism against duplications that introduces CG:TA transitions in duplicated regions and transposable elements (Selker 2002) and could potentially affect disomic chromosomes. RIP is active in *Z. tritici* (Komluski *et al.* 2022); however, if this mechanism acts on whole chromosome duplications is unknown. Besides often being lost or aneuploid during meiosis, accessory chromosomes in *Z. tritici* are subject to meiotic drive (Habig *et al.* 2018). *Z. tritici* is a heterothallic fungus with a bipolar mating system, meaning that two individuals with different mating types are necessary for successful sexual reproduction (Hassine *et al.* 2019). Both mating types can act as the female parent during reproduction; however, the meiotic drive of accessory chromosomes in *Z. tritici* is specific only to the unpaired accessory chromosomes inherited from the female parent (i.e., the parental strain that also transmits the mitochondria) (Fig 1A) (Kema *et al.* 2018; Habig *et al.* 2018). In contrast, unpaired accessory chromosomes inherited from the male parent (i.e., the parental strain that does not transmit mitochondria) are present only in half of the progeny, as expected by Mendelian segregation (Fig 1B). The exact mechanism for this drive is not known, but it potentially involves additional replication of accessory chromosomes that can happen either in the zygote or prior to karyogamy (Fig 1C; Fig 1D).
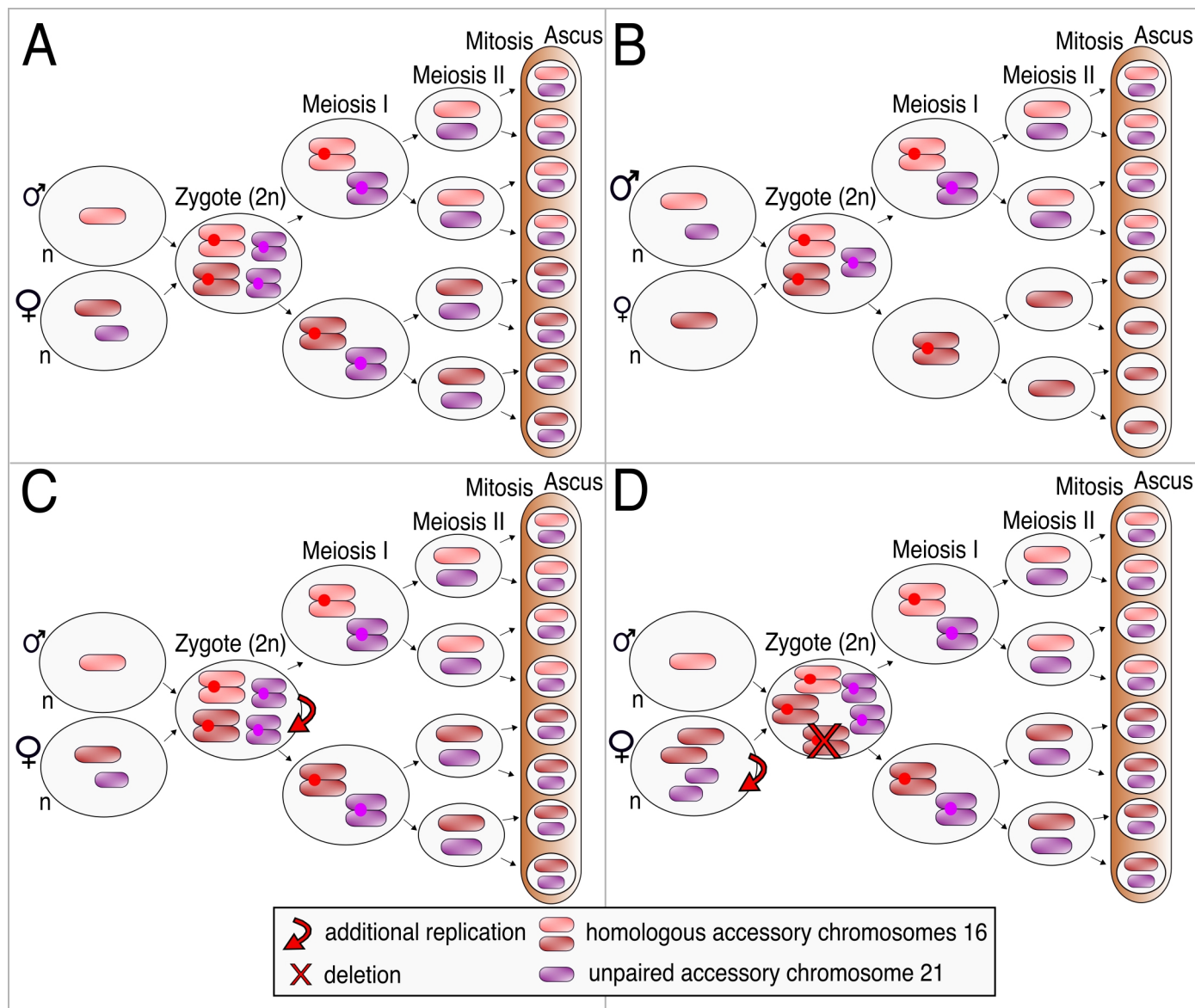
Fig 1. The meiotic drive of accessory chromosomes in *Z. tritici*. **A** Meiotic drive of accessory chromosomes is specific to unpaired accessory chromosomes inherited from the female parent (purple). As a result, female-inherited and unpaired accessory chromosomes are inherited on frequencies higher than expected by Mendelian segregation. According to Mendelian segregation, **B** unpaired accessory chromosomes inherited from the male parent (purple) are present in 50% of the progeny. **C, D** Models for the additional replication as the potential mechanism of the meiotic drive of unpaired and female-inherited accessory chromosomes in *Z. tritici*. **C** Additional replication of unpaired and female-inherited accessory chromosomes can happen in the zygote and is specific to unpaired and female-inherited accessory chromosomes. **D** Additional replication of unpaired and female-inherited accessory chromosomes can happen in the haploid nuclei prior to karyogamy and affects all accessory chromosomes from the nuclei. Therefore, additional replication before karyogamy is followed by the deletion of the extra copies of the paired accessory chromosomes.

Here, we have used *Z. tritici* as a model to monitor the segregation of unpaired disomic accessory chromosomes during meiosis to gain insights into regulation of aneuploidy in this plant pathogen. We have performed crosses with *Z. tritici* strains disomic for specific accessory chromosomes and isolated and karyotyped 19 complete tetrads, out of which we sequenced ten tetrads. Our results show the elimination of male-inherited disomic chromosomes from the progeny. Furthermore, non-Mendelian segregation of disomic chromosomes suggests that re-replication of unpaired and female-inherited accessory chromosomes that causes the meiotic drive occurs prior to karyogamy. Finally, we demonstrate that RIP does not act on disomic chromosomes. Results presented here provide insights into the maintenance of disomy and maintenance of accessory chromosomes in *Z. tritici*. Our results suggest that disomy is regulated in a parent-of-origin-specific manner in *Z. tritici* and that additional replication of accessory chromosomes before karyogamy is likely the mechanism behind the meiotic drive of accessory chromosomes in an important plant pathogen.

Results

Mitochondrial transmission is correlated to the inheritance of disomic accessory chromosomes

We here set out to assess the maintenance of disomic chromosomes in *Z. tritici*. Therefore, we performed three *in planta* crosses between T0635, T0637, and T0826 strains with homozygous disomic accessory chromosome 18 (two identical chromosome 18 derived from the IPO323 parent) and *Z. tritici* strain lacking accessory chromosome 18 and accessory chromosome 20 (IPO94269) to monitor the inheritance of disomic chromosomes during meiosis in this fungal pathogen. As a result, we isolated 509 spores from performed *in planta* crosses and verified eleven complete tetrads from two crosses (IPO94269 x T0635 and IPO94269 x T0826, respectively) via PCR karyotyping with a minimum of five segregating markers (Table 1; Table S1A).

Table 1. Summary of crosses with disomic chromosome 18 strains.

#	Parent 1	Parent 2	Disomic chromosome in Parent 2	Number of isolated ascospores	Number of isolated tetrads
4	ZT128 (IPO94269)	T0635	18 (2x IPO323)	282	10
5	ZT128 (IPO94269)	T0637	18 (2x IPO323)	90	0
6	ZT128 (IPO94269)	T0826	18 (2x IPO323)	137	1

We were interested to see if the female or male parental role affects the inheritance of disomic chromosome 18, similarly to the inheritance of monosomic accessory chromosomes. *Z. tritici* is heterothallic fungi (i.e., two individuals of both mating types are necessary for successful sexual reproduction), and both mating types can have a male or female role (Kema *et al.* 2018). The female role is associated with mitochondrial transmission. We used specific PCR markers for mitochondrial DNA to assess which of the two parental strains acted as the female parent in performed crosses. Four tetrads inherited mitochondrial DNA from the parent without accessory chromosome 18 (IPO94269), and seven tetrads inherited mitochondrial DNA from the parent with disomic accessory chromosome 18 (T0635 and T0826) (Table S1A). Segregation of accessory chromosome 18 in tetrad progenies was confirmed via PCR karyotyping with three markers distributed along the accessory chromosome 18 (Table S1A; Fig S1A; Fig S2). We observed the elimination of the disomic accessory chromosome 18 when inherited from the male parent. When the parental strain with disomic accessory chromosome 18 was male (i.e., the parent did not provide mitochondria), only one out of 16 (6.25%) ascospores inherited accessory chromosome 18 (Fig 2A, 2B) (Fisher's exact test, *p*-value = 0.001). In contrast, when the parental strain with disomic accessory chromosome 18 was female (i.e., the parent provided mitochondria), 16 out of 28 (57%) ascospores inherited accessory chromosome 18 (Fig 2A, 2C). In addition, when the parental strain with disomic accessory chromosome 18 was female, the segregation of disomic accessory chromosome 18 differed between tetrads. Four tetrads (68, 182, 185, and 186) had Mendelian segregation of accessory chromosome 18, two tetrads (136, 181) showed non-Mendelian segregation of accessory chromosome 18, and accessory chromosome 18 was lost entirely from the progeny in tetrad 177 (Fig 2C). We confirmed the ploidy status of accessory chromosome 18 in tetrad progenies with the coverage analysis of Illumina reads of five sequenced tetrads from disomic accessory chromosome 18 crosses (28, 72, 136, 181, and 182, respectively) (Fig 2D; Table S3). The ploidy status of accessory chromosome 18 differed in the tetrads when the parental strain with the disomic accessory chromosome 18 was female. All ascospores

inherited a single accessory chromosome 18 in tetrad 136; however, in tetrad 181, three ascospores inherited a disomic accessory chromosome 18, and one ascospore inherited a single accessory chromosome 18. Disomic accessory chromosome 18 was present in two ascospores in tetrad 182. The contrasting inheritance of disomic chromosome 18 from male compared to female parents indicates that the transmission of disomic chromosomes is correlated with the sexual role (i.e., the transmission of mitochondrial DNA).
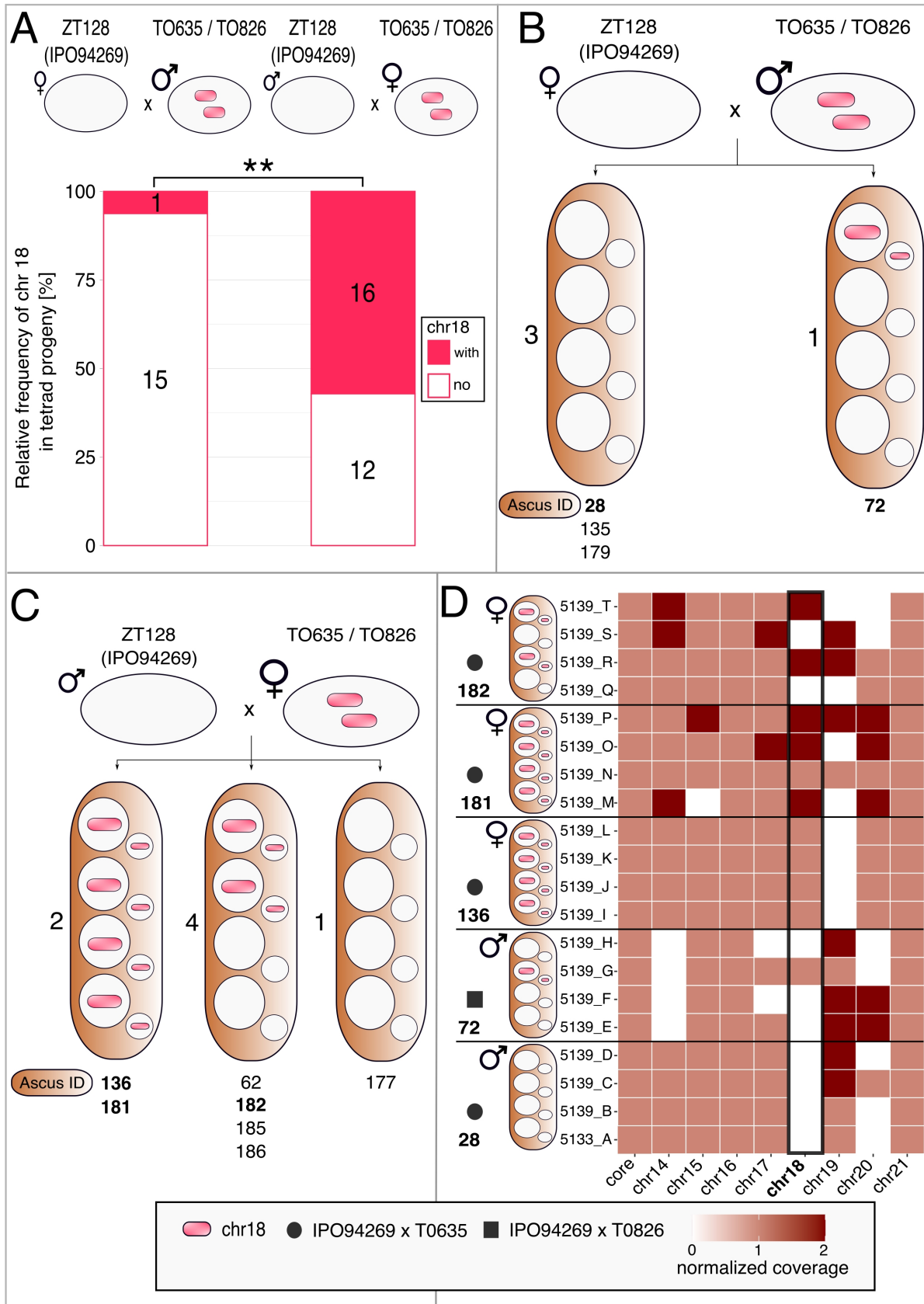
Fig 2. Segregation of chromosome 18 in the tetrad progeny. **A** Relative frequency of chromosome 18 in the tetrad progeny. The left bar shows the relative frequency of chromosome 18 in tetrads where the disomic chromosome 18 is male-inherited. The right bar displays the relative frequency of chromosome 18 in tetrads where the disomic chromosome 18 is female-inherited. Fisher's exact test p-value is shown (**$p < 0.005$). **B** Graphical representation of tetrad progeny isolated from the crosses with unpaired, male-inherited disomic accessory chromosome 18 and **C** unpaired, female-inherited disomic accessory chromosome 18. Ascus ID numbers in bold mark sequenced tetrads. **D** Heat-map of the normalized read coverage from sequenced tetrads. Asci diagrams show the segregation of chromosome 18. The black circle and black square in front of the asci represent respective cross combinations, and numbers in front of the asci mark the respective sequenced tetrad. Female/male symbols in **D** designate female/male parent with the disomic chromosome 18.

Segregation of disomic chromosome 21 suggests additional replication of unpaired and female-inherited chromosomes prior karyogamy

Additional replication is a potential mechanism of the meiotic drive of the female-inherited and unpaired accessory chromosomes in *Z. tritici*; however, the exact stage at which this additional replication happens is unknown. We have performed four different *in planta* crosses between a whole chromosome 21 IPO323 deletion strain (ZT267) and four strains that are disomic for accessory chromosome 21 (T0325, T0330, T0367, and T0372, respectively) (Table 2) to determine the stage when the additional replication causing meiotic drive occurs. Disomic accessory chromosome 21 in crossing parents is heterozygous, likely due to nondisjunction in meiosis I. Therefore, strains with disomic accessory chromosome 21 had one accessory chromosome 21 derived from IPO323 isolate and one accessory chromosome 21 derived from IPO94269 isolate and we could differentiate these chromosomes and assess their segregation during meiosis. Additional replication causing the meiotic drive of unpaired accessory chromosomes can happen in the zygote (Fig 3A) or before karyogamy (Fig 3B). Suppose additional replication of unpaired accessory chromosomes happens in the zygote. In that case, the parent with disomic chromosome 21 will contribute necessary copies of this chromosome, and no additional replication of disomic chromosome 21 will occur in our model. As a result, chromosome 21 will show Mendelian segregation. However, if additional replication of unpaired accessory chromosomes happens before karyogamy, additional replication of disomic chromosome 21 will happen and will be followed by random deletions of this chromosome. As a result, chromosome 21 will show non-Mendelian segregation in some tetrads.

We isolated 485 ascospores from *in planta* crosses and verified eight complete tetrads from crosses between the IPO323Δchr21 strain (ZT267) and three strains with disomic accessory chromosome 21

(T0325, T0367, and T0372, respectively) via PCR karyotyping with minimum five segregating markers (Table 2; Table S1B).

Table 2. Summary of crosses with disomic chromosome 21 strains.

#	Parent 1	Parent 2	Disomic chromosome in Parent 2	Number of isolated ascospores	Number of isolated tetrads
7	ZT267 (IPO323Δchr21)	T0325	21 (1x IPO323;1x IPO94269)	41	1
8	ZT267 (IPO323Δchr21)	T0330	21 (1x IPO323;1x IPO94269)	52	0
9	ZT267 (IPO323Δchr21)	T0367	21 (1x IPO323;1x IPO94269)	268	6
10	ZT267 (IPO323Δchr21)	T0372	21 (1x IPO323;1x IPO94269)	124	1

Differentiation between the female and the male parent was impossible because all isolated tetrads inherited mitochondrial DNA from the IPO94269 parental strain (Table S1B). To determine the segregation of chromosome 21 in the tetrad progeny, we performed PCR karyotyping with four segregating markers amplifying fragments of different sizes on IPO94269 chromosome 21 and IPO323 chromosome 21 (Table S1B; Table S2; Fig S1B; Fig S1C; Fig S3). Tetrads 81 and 204 showed non-Mendelian segregation of the accessory chromosome 21, with all ascospores having inherited accessory chromosome 21 from the IPO94269 parent (Fig 3C, the first asci from the left). Tetrads 90, 216, and 211 inherited the accessory chromosome 21 in half of the ascospores (Fig 3C, two asci in the middle). Two ascospores from tetrads 90 and 216 inherited chromosome 21 from the IPO94269 parent, while two ascospores in tetrad 211 inherited accessory chromosome 21 from the IPO323 parent. Accessory chromosome 21 was lost entirely in tetrads 155, 156, and 208 (Fig 3C, the first asci from the right). We selected five tetrads for Illumina sequencing to infer the ploidy status of chromosome 21 in the progeny. The coverage analysis confirmed non-Mendelian segregation of accessory chromosome 21 in tetrads 81 and 204 since accessory chromosome 21 was present in all ascospores in these tetrads (Fig 3D; Table S3). Taken together, the inheritance of accessory chromosome 21 derived from the IPO94269 parent on frequencies higher than expected by Mendelian segregation implies that additional replication of accessory chromosomes happens before karyogamy.
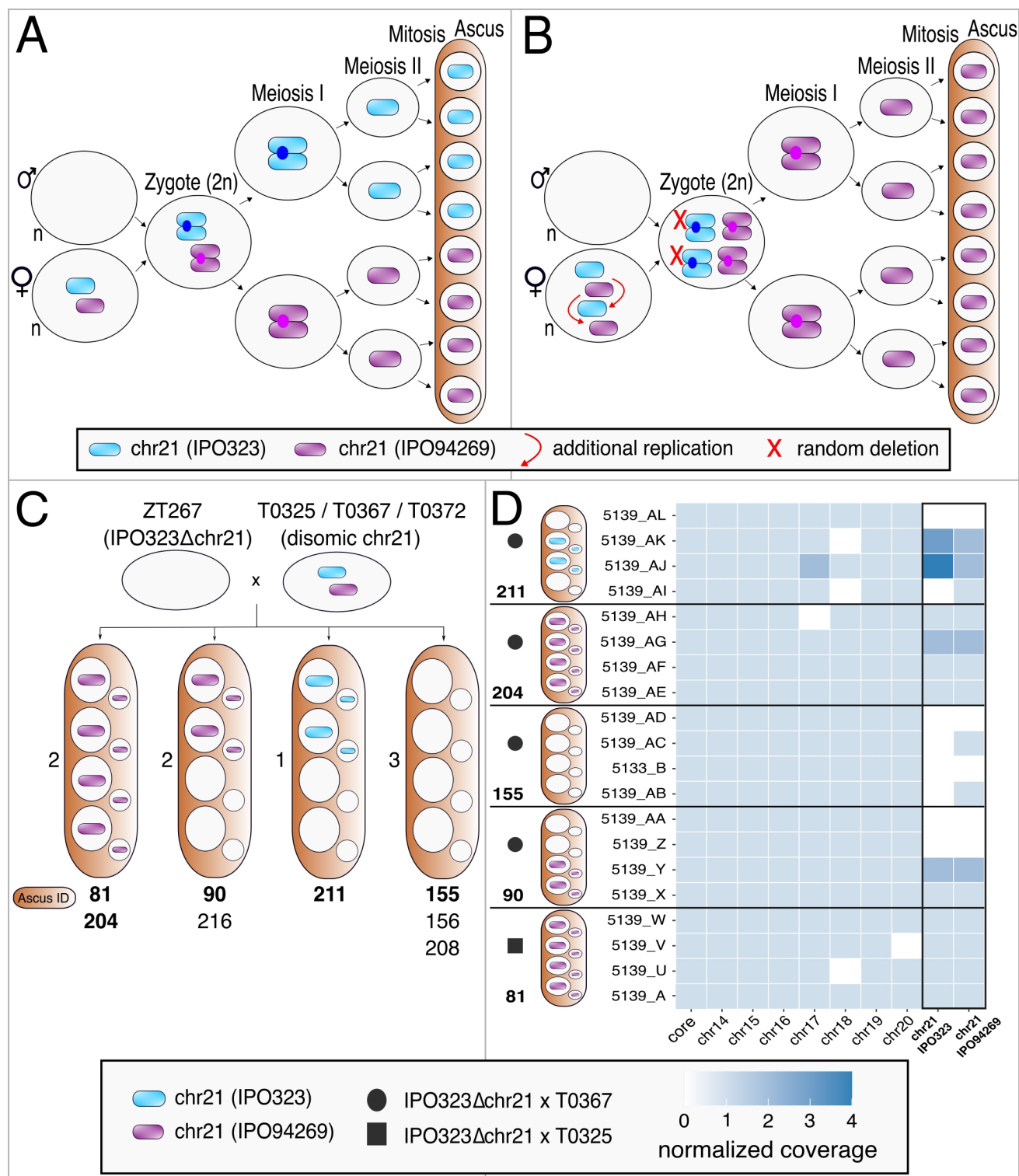
Fig 3. Segregation of chromosome 21 in tetrad progeny. **A, B** Two models for the mechanisms of meiotic drive of female-inherited and unpaired accessory chromosomes in *Z. tritici* tested in this study.

A If additional replication of the unpaired accessory chromosomes under meiotic drive happens in the zygote, disomic parent will contribute necessary copies of unpaired accessory chromosome 21. As a result, unpaired disomic accessory chromosome 21 will show Mendelian segregation. **B** Additional amplification of unpaired disomic accessory chromosome 21 happens before karyogamy and is followed by random deletions of this chromosome. As a result, chromosome 21 shows non-Mendelian segregation in the progeny. **C** Graphical representation of tetrad progeny from crosses between IPO323 strain without accessory chromosome 21 (ZT267) and strains with disomic chromosome 21 (T0325, T0367, and T0372). Parental strains with disomic chromosome 21 carry one chromosome 21 derived from the IPO323 strain and one chromosome 21 derived from the IPO94269 strain. Segregation of chromosome 21 was determined by PCR screening of the progeny with four markers specific to IPO323 chromosome 21 and four markers specific to IPO94269 chromosome 21. Asci identification numbers (Ascus ID) written under asci in bold designate sequenced tetrads. **D** Heat-map of the normalized read coverage from sequenced tetrads. Diagrams of asci show the segregation of chromosome 21 in the respective tetrad. The black circle and black square in front of the asci represent respective cross combination, and numbers in front of the asci mark the respective sequenced tetrad.

Unpaired, monosomic, female-inherited accessory chromosomes show a meiotic drive

Monosomic accessory chromosomes had contrasting behavior during meiosis in comparison with disomic accessory chromosomes in our study. Unpaired and female-inherited accessory chromosomes showed meiotic drive, as reported previously (Habig *et al.* 2018). One example of meiotic drive in our study is accessory chromosome 19 (Fig 4A). Accessory chromosome 19 was absent in two parental strains that were disomic for accessory chromosome 18 (T0635 and T0826, respectively) and therefore unpaired during meiosis. All ascospores in tetrads where the unpaired accessory chromosome 19 was female-inherited (28, 72, 135, and 179, respectively) inherited accessory the chromosome 19. In contrast, when male-inherited, accessory chromosome 19 mostly followed Mendelian segregation in tetrads (62, 181, 182, and 186, respectively) (Fig 4B). In addition, when paired, monosomic accessory chromosomes show Mendelian segregation (Fig 4C). Thus, our results show that the segregation of monosomic accessory chromosomes is differentially regulated from the segregation of disomic accessory chromosomes.
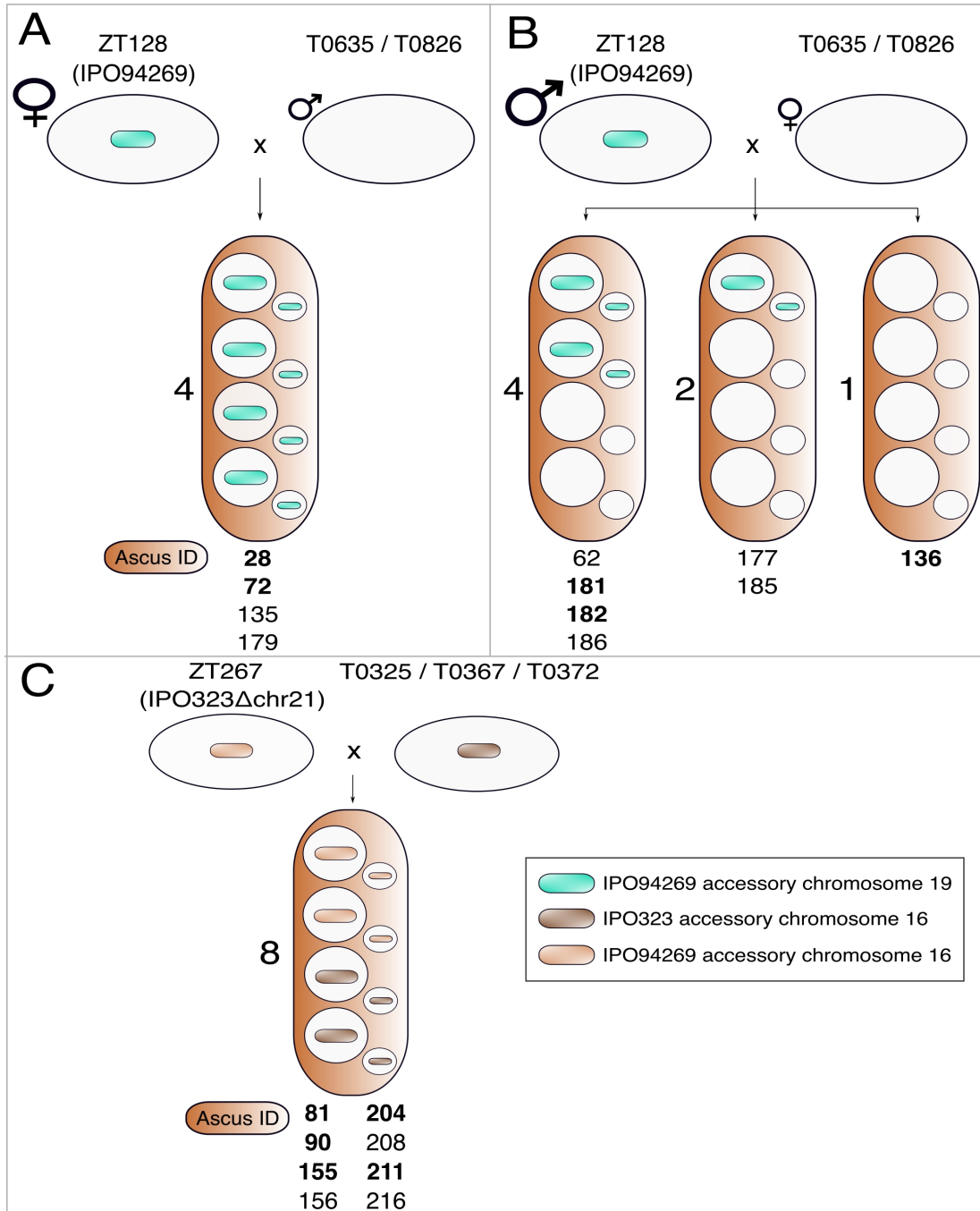
Fig 4. Segregation of unpaired and paired monosomic accessory chromosomes in tetrad progeny. Monosomic accessory chromosomes in *Z. tritici* show different segregation patterns in comparison to disomic accessory chromosomes. Segregation of the unpaired accessory chromosome 19 when **A** female-inherited and **B** male-inherited. **A** Female-inherited and unpaired accessory chromosome 19 shows meiotic drive which results in increased frequency of this chromosome in the progeny. In **B** male-inherited, unpaired accessory chromosome 19 is either Mendelian segregated or lost in progeny. 1:3 segregation of chromosome 19 in asci 177 and 185 is likely the result of the non-disjunction of sister chromatids during meiosis II. **C** Segregation of accessory chromosome 16 in tetrad progeny from crosses between ZT267 (IPO323Δchr21) and parental strains disomic for accessory

95

chromosome 21 (T0325, T0367, and T0372). Both parents carry a single accessory chromosome 16 that is Mendelian segregated in all progeny. Asci identification numbers (Ascus ID) written in bold below asci designate tetrads that are sequenced.

Repeat-induced point mutation (RIP) does not act on whole chromosome duplications

Repeat-induced point mutation (RIP) is a fungal defense mechanism against duplicated sequences and transposable elements (TEs) (Selker 2002). RIP is active in duplications and TEs in *Z. tritici* (Komluski *et al.* 2022), but whether RIP acts on the whole chromosome duplications is unknown.

To determine if RIP is acting on disomic chromosomes we identified *de novo* mutations associated with meiosis and compared the number, the spectrum and the distribution of these mutations between different disomic crosses that we conducted in our study. Crosses in this study included strains with disomic chromosomes with different types of disomies: strains with disomic accessory chromosome 18 were homozygous (i.e., these strains carried two identical accessory chromosomes 18 derived from the IPO323 parent); strains with disomic accessory chromosome 21 were heterozygous (i.e., these strains carried one accessory chromosome 21 derived from the IPO323 parent and one accessory chromosome 21 derived from the IPO94269 parent) (see Fungal and plant material in Materials and methods). *De novo* mutations occurring during meiosis were identified as mutations present in the ascospores of tetrad progenies but absent from their respective parental strains (see Identification of *de novo* mutations in Material and methods). We did not identify any *de novo* mutations on chromosome 21, and only 21 *de novo* mutations on chromosome 18 (Fig 5). The total number and per chromosome distribution of *de novo* mutations differed between crosses including strains with disomic accessory chromosome 18 and crosses including strains with disomic accessory chromosome 21. We identified in total 454 *de novo* mutations in crosses including strains with disomic accessory chromosome 18 and 261 *de novo* mutations in crosses including strains with disomic accessory chromosome 21 (Table S4). The dominant mutation type among *de novo* mutations in all crosses were CG:TA transitions which are RIP signatures. 75.8% of *de novo* mutations in crosses including strains with disomic accessory chromosome 18 were CG:TA transitions located inside 14 kb duplication on chromosome 3 in IPO94269 parent that was identified in a previous study (Komluski *et al.* 2022) (Fig 5A). In crosses including strains with the disomic accessory chromosome 21, 64.4% of *de novo* mutations were CG:TA mutations residing in transposable elements (Fig 5B). 4.9% of novel mutations were CG:TA mutations located in duplication on chromosome 11 (Fig S4).

Taken together, RIP did not act on disomic chromosomes and the genome-wide distribution of *de novo* mutations in all crosses varied depending on the size of the duplicated regions in parental strains.
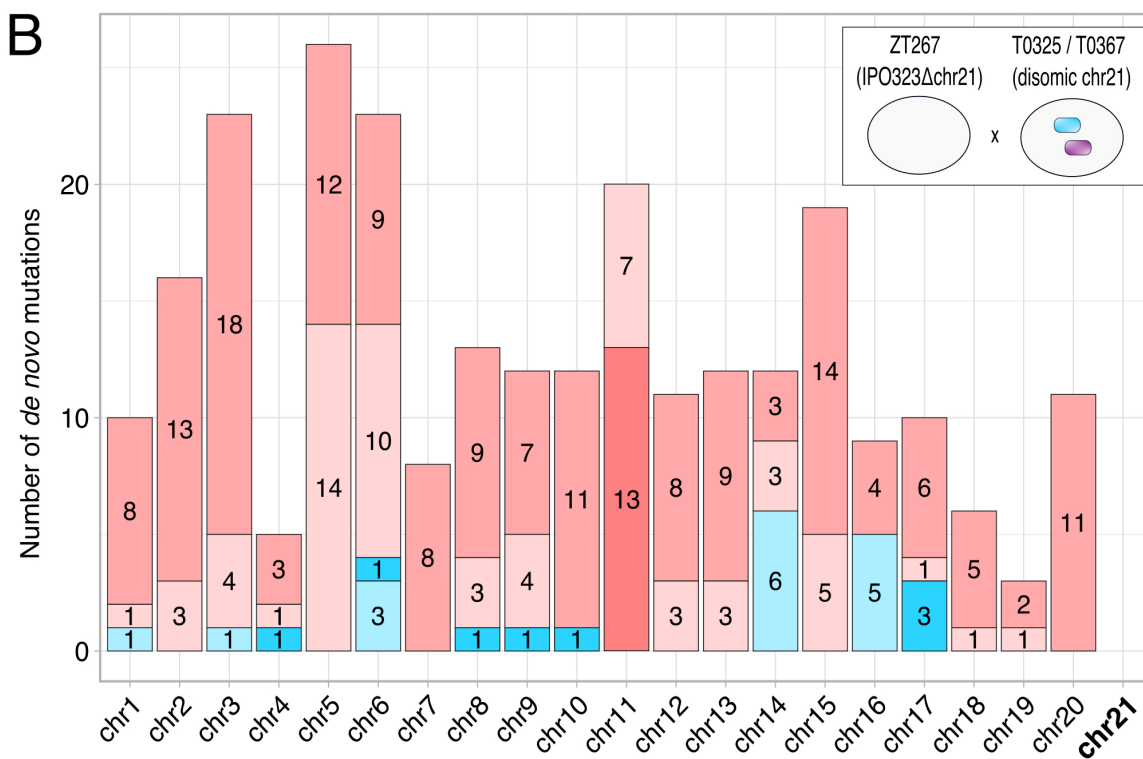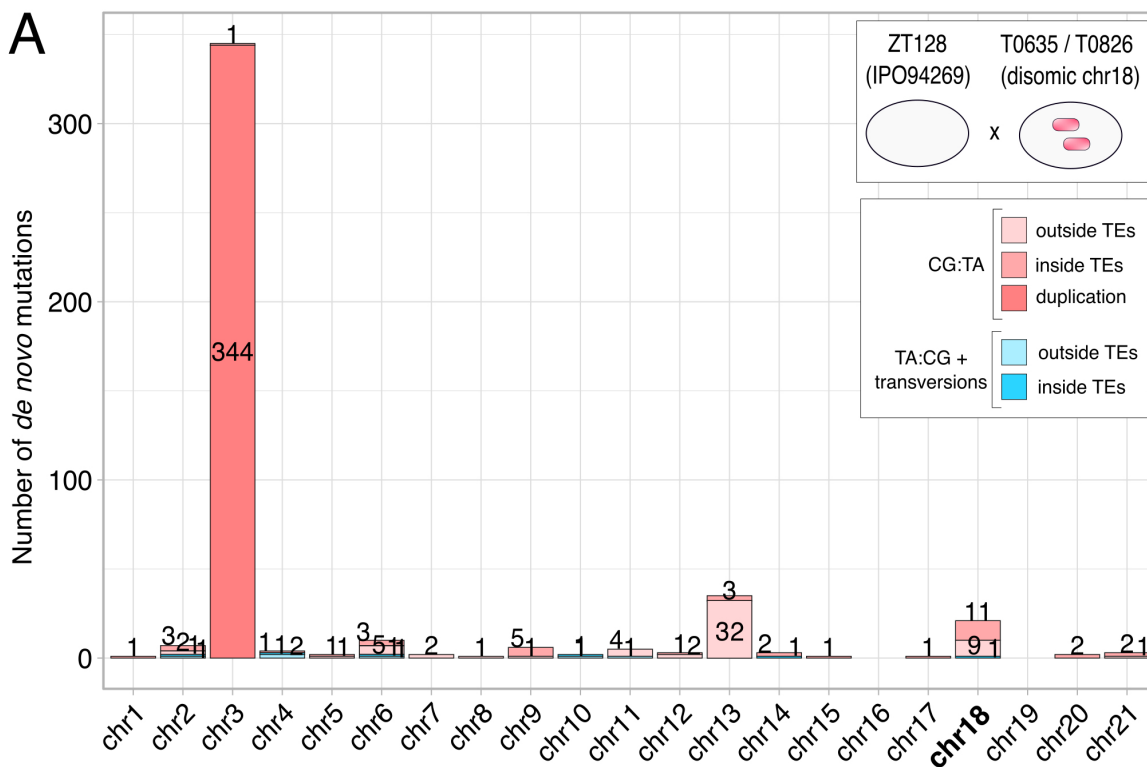
Fig 5. Spectrum and number of *de novo* mutations in disomic crosses conducted in this study. **A** Distribution of *de novo* mutations per chromosome in sequenced tetrads from crosses with disomic chromosome 18 strains. **B** Distribution of *de novo* mutations per chromosome in sequenced tetrads from crosses with disomic chromosome 21 strains. Red colored bars represent the proportion of CG:TA transitions among *de novo* mutations (light red - mutations outside transposable elements, semidark red – mutations inside transposable elements, dark red - mutations inside duplicated regions). Blue colored bars represent the proportion of TA:CG transitions and transversions among *de novo* mutations (light blue - mutations outside transposable elements, dark blue – mutations inside transposable elements).

Discussion

Here, we have isolated, karyotyped, and sequenced tetrad progeny from crosses with disomic strains of *Z. tritici*. Disomic accessory chromosomes in our crosses had different types of disomy. Disomic accessory chromosome 18 was homozygous (i.e., disomy arose from a single parental chromosome). In contrast, disomic accessory chromosome 21 was heterozygous, carrying one of each parental chromosomal copy that could be distinguished by PCR karyotyping. We used progeny from both crosses to observe how disomic chromosomes undergo meiosis in a fungal plant pathogen. Furthermore, we aimed to determine at which stage of meiosis the additional replication causing the meiotic drive of the unpaired and female-inherited accessory chromosomes in *Z. tritici* occurs. Our results show i) elimination of male-inherited disomic accessory chromosomes, ii) re-replication of unpaired accessory chromosomes prior to karyogamy, and iii) differences in the *de novo* mutation load and distribution between disomic crosses.

Segregation of disomic chromosomes differs from monosomic chromosomes and is correlated by the sexual role (i.e., the mitochondrial transmission). We observe the absence of accessory chromosome 18 from 93.7% of tetrad progeny in crosses when the parent with disomic accessory chromosome 18 is male (i.e., disomic parent does not provide mitochondria) contrasting to 57% of ascospores inheriting accessory chromosome 18 when the disomic parent was female. Importantly, unpaired monosomic accessory chromosomes in our crosses show different behavior than unpaired disomic chromosomes (Fig 4), since male-inherited unpaired monosomic accessory chromosomes are mostly Mendelian inherited or show non-Mendelian segregation that is likely a consequence of nondisjunction of sister chromatids during meiosis II. In addition, female-inherited monosomic chromosomes are transmitted to each ascospore in a tetrad in contrast to female-inherited disomic chromosomes that can be completely lost, suggesting that transmission of disomic chromosomes during meiosis is

differentially regulated than in monosomic chromosomes in *Z. tritici*. The segregation pattern of male-inherited disomic accessory chromosome 18 resembles the elimination of paternal chromosomes that occurs due to genomic imprinting. Genomic imprinting an epigenetic process that labels DNA in a sex-dependent manner thereby causing differences in chromatin conformation, histone modification, replication timing, and recombination rate (Reik and Walter 2001; Macdonald 2012). Obtaining genomic imprint requires the meiotically stable marking of males and females and maintaining that mark through DNA replication (Macdonald 2012). One example of genomic imprinting are sciarid flies, where patterns of H3K4 trimethylation differ between male and female chromosomes and are involved in programmed male chromosome elimination (Greciano and Goday 2006). Genomic imprinting can also occur in species without sex chromosomes, for instance in the mealybug, *Planococcus citri*, an insect species that exhibits paternal genome elimination through condensation of paternal chromosomes via H3K9me3-HP1 and H3K27me3-PRC2 heterochromatin pathways (Bain *et al.* 2021). The chromosome elimination we observe in our study is specific to male-inherited disomic accessory chromosomes, which implies the existence of certain differentiating cue between male- and female-inherited accessory chromosomes. Importantly, two individuals of different mating types are necessary to form a diploid zygote in *Z. tritici*, but individuals of both mating types can act as male or female partner (Waalwijk *et al.* 2002; Kema *et al.* 2018). H3K9me3 and H3K27me3 are involved in the condensation of chromosomes in *Z. tritici* (Schotanus *et al.* 2015), however, they do not necessarily play a role in the recognition of male- or female-inherited chromosomes (Bain 2019). Our data indicate the presence of a distinguishing cue between the male- and the female-inherited accessory chromosomes; however, this cue still remains to be unraveled.

Additional replication of female-inherited and unpaired accessory chromosomes is a potential mechanism of the meiotic drive in *Z. tritici*. This additional replication can happen prior to karyogamy or in the zygote (Habig *et al.* 2018). We monitored the segregation of unpaired disomic accessory chromosome 21 to identify the stage at which additional replication causing meiotic drive happens. Additional replication of unpaired disomic chromosomes before karyogamy is likely followed by random deletions and would, therefore, would lead to non-Mendelian segregation of female-inherited IPO323 chromosome 21 or female-inherited IPO94269 chromosome 21 in some of the tetrads (Fig 3B; Fig S5A; Fig S5C). The presence of two different chromosomes 21 derived from IPO323 and IPO94269 isolates in disomic parental strains enabled us to differentiate between two potential stages of additional replication that are likely causing the meiotic drive. Indeed, we observe the inheritance of IPO94269 accessory chromosome 21 on frequencies higher than expected by Mendelian segregation

in two out of eight isolated tetrads, indicating that accessory chromosomes are re-replicated before karyogamy. Unfortunately, we could not differentiate between the male and female disomic chromosome 21 parent, since all of the isolated tetrads inherited IPO94269 mitochondrial DNA (Table S1B). However, the presence of IPO94269 chromosome 21 in all ascospores of two tetrads still supports our hypothesis since accessory chromosomes are inherited at higher frequencies than expected by Mendelian segregation only when female-inherited and unpaired during meiosis. Furthermore, we observe both IPO94269 chromosome 21 and IPO323 chromosome 21 being inherited in different tetrads which confirms the true disomy of the parental strains. Interestingly, IPO94269 and IPO323 chromosome 21 are never inherited together in a single tetrad, i.e., ascospores in a single tetrad inherit either IPO323 or IPO94269 chromosome 21, suggesting that there is no fusion or recombination between these chromosomes or that the disomy *per se* is not inherited. In conclusion, the non-Mendelian segregation of IPO94269 accessory chromosome 21 that we observe in the progeny suggests that the re-replication of accessory chromosomes responsible for the meiotic drive of these chromosomes happens before karyogamy.

Accessory chromosomes show ploidy variation in tetrads from the same crosses. In tetrad 181, for instance, three ascospores were disomic for chromosome 18, in contrast to tetrad 136 from the same cross where all ascospores inherited a single chromosome 18 (Fig 2D). Furthermore, chromosome 19 is inherited at higher frequencies than expected since one of the parents in the crosses did not have chromosome 19 (Fig 2D). The number of inherited chromosomes often cannot be explained either by Mendelian segregation or by meiotic drive (e.g., IPO323 chromosome 21 is trisomic and tetrasomic in tetrad 211, but there is only one IPO323 chromosome 21 in the parental strain). We attribute these ploidy variations to stress associated with aneuploidy of parental strains. Additional chromosome copy in haploid yeast strains increases the rate of chromosome missegregation (Sheltzer *et al.* 2011). Furthermore, aneuploidy causes mitotic stress in form of lagging chromosomes or via delaying replication fork progression (Zhu *et al.* 2018). Therefore, ploidy variation of accessory chromosomes may occur as a consequence of defects during mitosis that follows meiosis or defects in cellular pathways controlling chromosome segregation, as both defect types can cause numerical whole chromosome instability (Thompson *et al.* 2010; Russo *et al.* 2015). Indeed, high frequencies of mitoses with extra centrosomes, multipolar spindles, and aberrant chromosome segregation are often the product of replication stress (Wilhelm *et al.* 2014).

RIP is a fungal defense mechanism against duplications and transposable elements (Galagan and Selker 2004) and is active in *Z. tritici* (Komluski *et al.* 2022). RIP signatures, i.e., CG:TA transitions, in duplications and TEs are the dominant *de novo* mutation type in all performed crosses in this study. Since RIP acts on duplications, it could potentially act on disomic chromosomes. Unexpectedly, disomic accessory chromosome 21 did not carry any *de novo* mutations, which is not assumed because most *de novo* mutations in *Z. tritici* are induced by RIP that acts on duplicated sequences. Strains disomic for accessory chromosome 21 that we have used for our crosses carry accessory chromosome 21 derived from the IPO323 parental strain and accessory chromosome 21 derived from the IPO94269 parental strain, which differ 58242 bp in length and have 76% identity. In *N. crassa*, RIP requires a minimum of 65% of homology between the duplicated sequences to act, but this homology requirement can vary among species (Gladyshev and Kleckner 2017). Disomic accessory chromosome 18, in comparison, carry two identical accessory chromosomes 18 derived from the IPO323 parent and 95% of *de novo* mutations detected on accessory chromosome 18 in the progeny are CG:TA transitions. However, only 20 CG:TA transitions were located on accessory chromosome 18 – much lower than expected if the RIP would act on the whole chromosome. Therefore, RIP probably cannot recognize very long duplicated sequences, and there are potential homology and size thresholds for RIP activity in *Z. tritici*. Interestingly, 75.8% of *de novo* mutations in crosses with the strains with the disomic accessory chromosome 18 reside in 14 kb chromosome 3 duplication present in the IPO94269 parent. Large duplications can pull the RIP machinery from the smaller duplicated regions (Bhat and Kasbekar 2001), which can explain the high density of RIP mutations within the chromosome 3 duplication in comparison to the rest of the genome. The absence of large duplications in parental strains from disomic accessory chromosome 21 crosses results in the higher frequency of novel RIP mutations inside of TEs (64.4%) opposite to only 9.7% of *de novo* mutations in TEs in progeny from crosses with strains disomic for accessory chromosome 18. Taken together, RIP does not act on disomic chromosomes, and duplication size dictates the genome-wide distribution and the load of novel mutations in *Z. tritici*.

In conclusion, we show that transmission of disomic chromosomes is regulated in a parent-of-origin-specific manner and that re-replication of unpaired, female-inherited accessory chromosomes before karyogamy is likely causing the meiotic drive of these chromosomes in *Z. tritici*. Results presented in this study provide insights into the inheritance of disomic accessory chromosomes and mechanisms controlling the meiotic drive of accessory chromosomes in *Z. tritici* and could explain low frequencies of disomic accessory chromosomes observed in the field isolates of this important plant pathogen.

Materials and Methods

Fungal and plant material

Fungal material used for *in planta* crosses included the following *Z. tritici* strains: IPO94269 (isolate without accessory chromosome 18 and 20), ZT267 (IPO323Δchr21), T0635 and T0826 (isolates with disomic accessory chromosome 18 (2 x IPO323chr18)) and T0325 and T0367 (isolates with disomic accessory chromosome 21 (1 x IPO323chr21; 1 x IPO94269chr21)). The Dutch isolate IPO94269 is available from the Westerdijk Institute (Utrecht, The Netherlands) with the accession number CBS115941. The accessory chromosome 21 deletion strain derived from the reference IPO323 strain (ZT267) was obtained from the study of Habig et al. 2017. Strains disomic for accessory chromosomes 18 were isolated from two crosses from the Habig et al. 2018 study: T0635 (disomic chr18) strain was isolated from a cross between IPO94269 and ZT278 (IPO323Δchr19) strain. T0826 (disomic chr18) strain was isolated from a cross between IPO94269 and ZT260 (IPO323Δchr14). Both strains disomic for accessory chromosome 21 were isolated from a cross between the reference strain IPO323 and IPO94269 from the same study (Habig *et al.* 2018). Therefore, crosses conducted in this study with strains disomic for accessory chromosome 18 were backcross with the IPO94269 parent, and crosses with strains disomic for accessory chromosome 21 were backcross with the IPO323 parent (Fig S6). Wheat cultivar Obelisk used for the *in planta* fungal mating was obtained from Wiersum Plantbreeding BV (Winschoten, The Netherlands).

Fungal growth conditions

IPO94269 was grown in liquid yeast glucose (YG) medium (30 g/L glucose and 10 g/L yeast extract) at 15°C on an orbital shaker. IPO323-derived whole chromosome deletion strains and disomic parental strains were maintained on solid YMS (4 g/L yeast extract, 4 g/L malt extract, 4 g/L sucrose, and 20 g/L agar) for seven days at 18°C to avoid formation of hyphal clumps. Cells were washed once and diluted in water including 0.05% Tween20 to cell concentration of 10^7 cells/ml for infection.

Sexual mating of *Z. tritici* strains and tetrad isolation

Sexual crosses were performed following the protocol previously described by (Kema *et al.* 1996, 2018). Two weeks old wheat plants were infected by the spraying of cell cultures until the leaf surface

was fully covered with cell suspension. The infected plants were placed in plastic bags for 48 hr. After two days, the infected plants were taken out from plastic bags and grown for 12 days at 90% humidity and 16 hr light days. All leaves except the first one were removed at 14 dpi and plants were transferred to buckets in netted sacks, fertilized, and placed outside. Infected leaves were harvested weekly for four weeks starting from 35 dpi. After harvesting, leaves were placed in tap water and kept overnight at room temperature. The shooting of ascospores was performed as follows: infected leaves were placed on the wet filter paper on the Petri dish lid, tapped dry, and covered with the bottom of the Petri dish with 2% water agar (WA). The Petri dish containing water agar was rotated for 90° every 5 min for a total of 40 min to collect ejected ascospores. The water agar plates were incubated for 18-24 hr at 18 °C. Ascospores were counted and isolated manually using a Leica dissection scope. Seven independent crosses were performed for this study (Table 1; Table 2). PCR-based karyotyping with a minimum of five segregating markers located on different core chromosomes was conducted to identify which of the isolated ascospores were members of the same ascus (Table S1A; Table S1B). After tetrad verification, segregation of chromosome 18 in the progeny from crosses with disomic chromosome 18 strains was identified via PCR karyotyping with three different segregating markers, and segregation of chromosome 21 in the progeny from crosses with disomic chromosome 21 was identified via PCR karyotyping with four different markers (Table S1A; Table S1B; Fig S2; Fig S3). Housekeeping gene GAPDH was amplified as a positive control for successful PCR reaction in all crosses. The female parent (i.e., the parent that transmitted mitochondrial DNA to the progeny) was determined by PCR amplification of regions of mitochondrial DNA specific to the IPO94269 or IPO323 parent.

Pulse field gel electrophoresis (PFGE)

We have performed pulsed-field gel electrophoresis (PFGE) on all strains that were involved in disomic accessory chromosome 21 crosses to verify true disomy of parental strains (Fig S7). Strains with disomic accessory chromosome 21 were grown in a YMS medium for 7 days. Cells were collected by centrifugation for 10 min at 3500 rpm. 5×10^8 cells were resuspended in 1 ml of water and mixed with 1 ml of 2.2% low-range ultra agarose (Bio-Rad, Munich, Germany) for plug preparation. The cell mixture was pipetted into plug-casting molds and cooled for 1 h at 4ºC. The plugs were further incubated in lysis buffer (1% SDS, 0.45 M EDTA, 1.5 mg/ml proteinase K; Roth, Karlsruhe, Germany) for 48 h at 55°C and the lysis buffer was replaced once after 24 h. Plugs were washed three times for 20 min with 1x TE buffer after incubation and stored in 5 ml of 0.5 M EDTA at 4ºC. PFGE was

performed with a CHEF-DR III PFGE system (Bio-Rad) with the following settings for the separation of small accessory chromosomes: switching time 50-150s, 5 V/cm, 120º angle, 1% pulsed-field agarose (Bio-Rad) in 0.5x TBE (Tris/borate/EDTA) buffer for 48 h. Gels were stained in 500 ml ethidium bromide staining solution (1μg/ml ethidium-bromide in H_2O) for 30 min.

Genome sequencing

Five tetrads from the crosses with the disomic chromosome 18 strain and five tetrads from crosses with the disomic chromosome 21 were selected for the whole genome sequencing to i) verify the segregation of disomic accessory chromosomes detected with PCR karyotyping, and ii) determine the ploidy of disomic chromosomes in the progeny. The DNA was isolated from 40 ascospores according to the CTAB protocol (Fagundes *et al.* 2020). Library preparation and genome sequencing were performed by the Max Planck-Genome-centre, Cologne, Germany (http://mpgc.mpipz.mpg.de/home/) using an Illumina HiSeq3000 sequencer. The Illumina read data of all disomic parental strains is available in the Sequence Read Archive under the BioProject PRJNA904559 and PRJNA438050. The Illumina reads of the IPO94269 parental strain are available under the BioProject PRJNA904744. The Illumina data for the ZT267 (IPO323Δchr21) parental strain is deposited under the BioProject PRJNA371572.

Mapping and SNP calling

Raw 150 bp paired-end reads were quality filtered with Trimmomatic (v0.36) (Bolger *et al.* 2014) and mapped to the IPO323 reference genome and the IPO94269 genome using bowtie2 (version 2.3.4.1) (Langmead and Salzberg 2012). The read coverage per chromosome was calculated from bam files with the mosdepth tool (version 0.2.6) (Pedersen and Quinlan 2018) and normalized to the mean coverage of each chromosome. In the analysis of *de novo* mutations, we have focused only on single nucleotide polymorphisms (SNPs). Variants were called by samtools (version 1.7) (Li *et al.* 2009) and further filtered with bcftools (version 1.7) (Danecek *et al.* 2021) using the following parameters: biallelic, mapping quality (QUAL≥30), and minor allele frequency >0.8.

Identification of *de novo* mutations

De novo mutations occur during meiosis, are absent from the parental genomes, and present only in the ascospore progeny. *De novo* mutations were firstly identified by removing all variants present in parental strains from the progeny in the regions with coverage >5 in all four ascospores from a single tetrad by overlapping variant call format (vcf) files of parents with vcf files of the progeny with bedtools intersect (version 2.26.0, option -v) (Quinlan and Hall 2010). After primary identification, potential *de novo* mutations were manually checked for their presence in parental genomes. If potential *de novo* mutations were not presen*t* in respective parental genomes, they were considered true *de novo* mutations.

Data availability

The Illumina read data is available in the Sequence Read Archive under the BioProjects PRJNA904559, PRJNA438050, PRJNA904744, and PRJNA371572. The *Z. tritici* IPO323 reference genome is available under the accession GCA_000219625.1.

References

Bain S. A., 2019 Epigenetic mechanisms underlying paternal genome elimination

Bain S. A., H. Marshall, A. G. de la Filia, D. R. Laetsch, F. Husnik, *et al.*, 2021 Sex-specific expression and DNA methylation in a species with extreme sexual dimorphism and paternal genome elimination. Mol. Ecol. 30: 5687–5703. https://doi.org/10.1111/mec.15842

Bhat A., and D. P. Kasbekar, 2001 Escape From Repeat-Induced Point Mutation of a Gene-Sized Duplication in Neurospora crassa Crosses That Are Heterozygous for a Larger Chromosome Segment Duplication. Genetics 157: 1581–1590. https://doi.org/10.1093/genetics/157.4.1581

Bolger A. M., M. Lohse, and B. Usadel, 2014 Trimmomatic: a flexible trimmer for Illumina sequence data. Bioinformatics 30: 2114–2120. https://doi.org/10.1093/bioinformatics/btu170

Bomblies K., J. D. Higgins, and L. Yant, 2015 Meiosis evolves: adaptation to external and internal environments. New Phytol. 208: 306–323. https://doi.org/https://doi.org/10.1111/nph.13499

Bomblies K., G. Jones, C. Franklin, D. Zickler, and N. Kleckner, 2016 The challenge of evolving stable polyploidy: could an increase in "crossover interference distance" play a central role? Chromosoma 125: 287–300. https://doi.org/10.1007/s00412-015-0571-4

Clémence P., S. Alessandra, and C. Daniel, 2016 The Evolution of Orphan Regions in Genomes of a Fungal Pathogen of Wheat. MBio 7: e01231-16. https://doi.org/10.1128/mBio.01231-16

Comai L., 2005 The advantages and disadvantages of being polyploid. Nat. Rev. Genet. 6: 836–846. https://doi.org/10.1038/nrg1711

Covo S., 2020 Genomic Instability in Fungal Plant Pathogens. Genes (Basel). 11. https://doi.org/10.3390/genes11040421

Danecek P., J. K. Bonfield, J. Liddle, J. Marshall, V. Ohan, *et al.*, 2021 Twelve years of SAMtools and BCFtools. Gigascience 10: giab008. https://doi.org/10.1093/gigascience/giab008

Fagundes W. C., J. Haueisen, and E. H. Stukenbrock, 2020 Dissecting the Biology of the Fungal Wheat Pathogen Zymoseptoria tritici: A Laboratory Workflow. Curr. Protoc. Microbiol. 59: e128. https://doi.org/https://doi.org/10.1002/cpmc.128

Fouché S., C. Plissonneau, B. A. McDonald, and D. Croll, 2018 Meiosis leads to pervasive copy-number variation and distorted inheritance of accessory chromosomes of the wheat pathogen Zymoseptoria tritici. Genome Biol. Evol. 10: 1416–1429.

Galagan J. E., and E. U. Selker, 2004 RIP: the evolutionary cost of genome defense. TRENDS Genet. 20: 417–423.

Garmaroodi H. S., and M. Taga, 2007 Duplication of a conditionally dispensable chromosome carrying pea pathogenicity (PEP) gene clusters in Nectria haematococca. Mol. Plant-Microbe Interact. 20: 1495–1504.

Garmaroodi H. S., and M. Taga, 2015 Meiotic inheritance of a fungal supernumerary chromosome and its effect on sexual fertility in Nectria haematococca. Fungal Biol. 119: 929–939.

Gasch A. P., P. T. Spellman, C. M. Kao, O. Carmel-Harel, M. B. Eisen, *et al.*, 2000 Genomic expression programs in the response of yeast cells to environmental changes. Mol. Biol. Cell 11: 4241–4257.

Gladyshev E., and N. Kleckner, 2017 Recombination-independent recognition of DNA homology for repeat-induced point mutation. Curr. Genet. 63: 389–400. https://doi.org/10.1007/s00294-016-0649-4

Goodwin S. B., S. Ben M'barek, B. Dhillon, A. H. J. Wittenberg, C. F. Crane, *et al.*, 2011 Finished genome of the fungal wheat pathogen Mycosphaerella graminicola reveals dispensome structure,

chromosome plasticity, and stealth pathogenesis. PLoS Genet. 7: e1002070. https://doi.org/10.1371/journal.pgen.1002070

Greciano P. G., and C. Goday, 2006 Methylation of histone H3 at Lys4 differs between paternal and maternal chromosomes in Sciara ocellaris germline development. J. Cell Sci. 119: 4667–4677. https://doi.org/10.1242/jcs.03279

Habig M., J. Quade, and E. H. Stukenbrock, 2017 Forward Genetics Approach Reveals Host Genotype-Dependent Importance of Accessory Chromosomes in the Fungal Wheat Pathogen Zymoseptoria tritici, (C. B. Kistler   Judith, Ed.). MBio 8: e01919-17. https://doi.org/10.1128/mBio.01919-17

Habig M., G. H. J. Kema, E. H. Stukenbrock, and E. Genomics, 2018 Meiotic drive of female-inherited supernumerary chromosomes in a pathogenic fungus. 1–20.

Holland A. J., and D. W. Cleveland, 2012 Losing balance: the origin and impact of aneuploidy in cancer: 'Exploring aneuploidy: the significance of chromosomal imbalance'review series. EMBO Rep. 13: 501–514.

Kema G. H. J., E. C. P. Verstappen, M. Todorova, and C. Waalwijk, 1996 Successful crosses and molecular tetrad and progeny analyses demonstrate heterothallism in Mycosphaerella graminicola. Curr. Genet. 30: 251–258. https://doi.org/10.1007/s002940050129

Kema G. H. J., A. Mirzadi Gohari, L. Aouini, H. A. Y. Gibriel, S. B. Ware, et al., 2018 Stress and sexual reproduction affect the dynamics of the wheat pathogen effector AvrStb6 and strobilurin resistance. Nat. Genet. 50: 375–380. https://doi.org/10.1038/s41588-018-0052-9

Komluski J., M. Habig, and E. H. Stukenbrock, 2022 Repeat-induced point mutation and gene conversion coinciding with heterochromatin shape the genome of a plant pathogenic fungus. bioRxiv 2022.11.30.518637. https://doi.org/10.1101/2022.11.30.518637

Langmead B., and S. L. Salzberg, 2012 Fast gapped-read alignment with Bowtie 2. Nat. Methods 9: 357–359. https://doi.org/10.1038/nmeth.1923

Levine M. S., and A. J. Holland, 2018 The impact of mitotic errors on cell proliferation and tumorigenesis. Genes Dev. 32: 620–638.

Li H., B. Handsaker, A. Wysoker, T. Fennell, J. Ruan, et al., 2009 The Sequence Alignment/Map format and SAMtools. Bioinformatics 25: 2078–2079. https://doi.org/10.1093/bioinformatics/btp352

Lynn A., R. Soucek, and G. V. Börner, 2007 ZMM proteins during meiosis: crossover artists at work. Chromosom. Res. an Int. J. Mol. Supramol. Evol. Asp. Chromosom. Biol. 15: 591–605. https://doi.org/10.1007/s10577-007-1150-1

Ma L.-J., H. C. van der Does, K. A. Borkovich, J. J. Coleman, M.-J. Daboussi, et al., 2010 Comparative genomics reveals mobile pathogenicity chromosomes in Fusarium. Nature 464: 367–373. https://doi.org/10.1038/nature08850

Macdonald W. A., 2012 Epigenetic mechanisms of genomic imprinting: common themes in the regulation of imprinted regions in mammals, plants, and insects. Genet. Res. Int. 2012: 585024. https://doi.org/10.1155/2012/585024

Miao V. P., S. F. Covert, and H. D. VanEtten, 1991 A fungal gene for antibiotic resistance on a dispensable ("B") chromosome. Science (80-.). 254: 1773 LP – 1776. https://doi.org/10.1126/science.1763326

Möller M., M. Habig, M. Freitag, and E. H. Stukenbrock, 2018 Extraordinary Genome Instability and Widespread Chromosome Rearrangements During Vegetative Growth. Genetics 210: 517–529. https://doi.org/10.1534/genetics.118.301050

Musacchio A., and E. D. Salmon, 2007 The spindle-assembly checkpoint in space and time. Nat. Rev. Mol. Cell Biol. 8: 379–393. https://doi.org/10.1038/nrm2163

Nasmyth K., and C. H. Haering, 2009 Cohesin: its roles and mechanisms. Annu. Rev. Genet. 43: 525–558. https://doi.org/10.1146/annurev-genet-102108-134233

Pedersen B. S., and A. R. Quinlan, 2018 Mosdepth: quick coverage calculation for genomes and exomes. Bioinformatics 34: 867–868. https://doi.org/10.1093/bioinformatics/btx699

Quinlan A. R., and I. M. Hall, 2010 BEDTools: a flexible suite of utilities for comparing genomic features. Bioinformatics 26: 841–842. https://doi.org/10.1093/bioinformatics/btq033

Reik W., and J. Walter, 2001 Genomic imprinting: parental influence on the genome. Nat. Rev. Genet. 2: 21–32. https://doi.org/10.1038/35047554

Russo A., F. Pacchierotti, D. Cimini, N. J. Ganem, A. Genescà, *et al.*, 2015 Genomic instability: Crossing pathways at the origin of structural and numerical chromosome changes. Environ. Mol. Mutagen. 56: 563–580. https://doi.org/https://doi.org/10.1002/em.21945

Santaguida S., A. Richardson, D. R. Iyer, O. M'Saad, L. Zasadil, *et al.*, 2017 Chromosome mis-segregation generates cell-cycle-arrested cells with complex karyotypes that are eliminated by the immune system. Dev. Cell 41: 638–651.

Schotanus K., J. L. Soyer, L. R. Connolly, J. Grandaubert, P. Happel, *et al.*, 2015 Histone modifications rather than the novel regional centromeres of Zymoseptoria tritici distinguish core and accessory chromosomes. Epigenetics Chromatin 8: 41. https://doi.org/10.1186/s13072-015-0033-5

Selker E. U., 2002 Repeat-induced gene silencing in fungi. Adv. Genet. 46: 439–450

Selmecki A., A. Forche, and J. Berman, 2006 Aneuploidy and isochromosome formation in drug-resistant Candida albicans. Science 313: 367–370. https://doi.org/10.1126/science.1128242

Sheltzer J. M., H. M. Blank, S. J. Pfau, Y. Tange, B. M. George, *et al.*, 2011 Aneuploidy drives genomic instability in yeast. Science (80-.). 333: 1026–1030.

Siegel J. J., and A. Amon, 2012 New insights into the troubles of aneuploidy. Annu. Rev. Cell Dev. Biol. 28: 189–214. https://doi.org/10.1146/annurev-cellbio-101011-155807

Sophie A., F. Diana, S. Charles, S. Shreyas, W. Peipei, *et al.*, 2017 Fluconazole-Induced Ploidy Change in Cryptococcus neoformans Results from the Uncoupling of Cell Growth and Nuclear Division. mSphere 2: e00205-17. https://doi.org/10.1128/mSphere.00205-17

Thompson S. L., S. F. Bakhoum, and D. A. Compton, 2010 Mechanisms of chromosomal instability. Curr. Biol. 20: R285-95. https://doi.org/10.1016/j.cub.2010.01.034

Torres E. M., T. Sokolsky, C. M. Tucker, L. Y. Chan, M. Boselli, *et al.*, 2007 Effects of aneuploidy on cellular physiology and cell division in haploid yeast. Science (80-.). 317: 916–924.

Waalwijk C., O. Mendes, E. C. P. Verstappen, M. A. de Waard, and G. H. J. Kema, 2002 Isolation and Characterization of the Mating-Type Idiomorphs from the Wheat Septoria Leaf Blotch Fungus Mycosphaerella graminicola. Fungal Genet. Biol. 35: 277–286. https://doi.org/https://doi.org/10.1006/fgbi.2001.1322

Wilhelm T., I. Magdalou, A. Barascu, H. Técher, M. Debatisse, *et al.*, 2014 Spontaneous slow replication fork progression elicits mitosis alterations in homologous recombination-deficient mammalian cells. Proc. Natl. Acad. Sci. U. S. A. 111: 763–768. https://doi.org/10.1073/pnas.1311520111

Wittenberg A. H. J., T. A. J. van der Lee, S. Ben M'Barek, S. B. Ware, S. B. Goodwin, *et al.*, 2009 Meiosis Drives Extraordinary Genome Plasticity in the Haploid Fungal Plant Pathogen Mycosphaerella graminicola. PLoS One 4: e5863.

Zhu J., H.-J. Tsai, M. R. Gordon, and R. Li, 2018 Cellular Stress Associated with Aneuploidy. Dev. Cell 44: 420–431. https://doi.org/10.1016/j.devcel.2018.02.002

Zickler D., and N. Kleckner, 2015 Recombination, Pairing, and Synapsis of Homologs during Meiosis. Cold Spring Harb. Perspect. Biol. 7. https://doi.org/10.1101/cshperspect.a016626
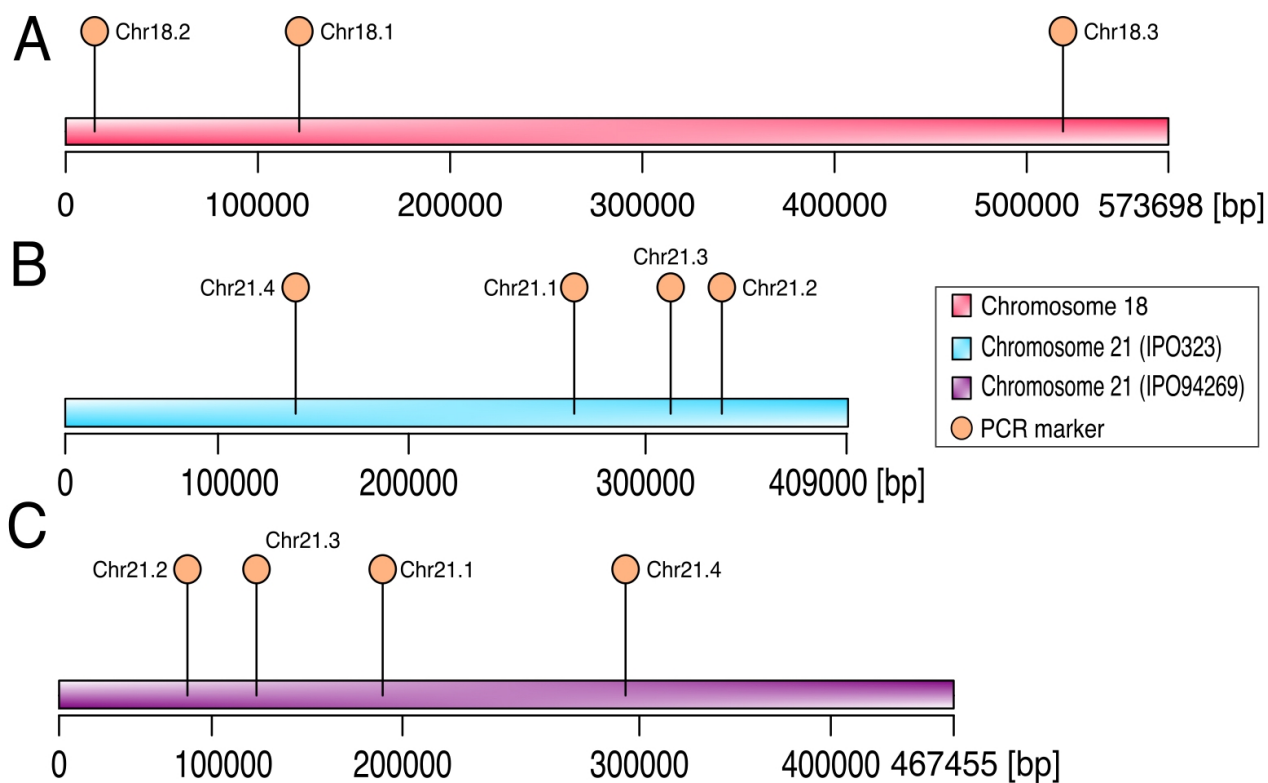
Supplementary Figures

Fig S1. Distribution of PCR karyotyping markers along chromosome are disomic in parental strain. **A** chromosome 18 derived from the IPO323 parent; **B** chromosome 21 derived from IPO323 parental strain; **C** chromosome 21 derived from IPO94269 parental strain.
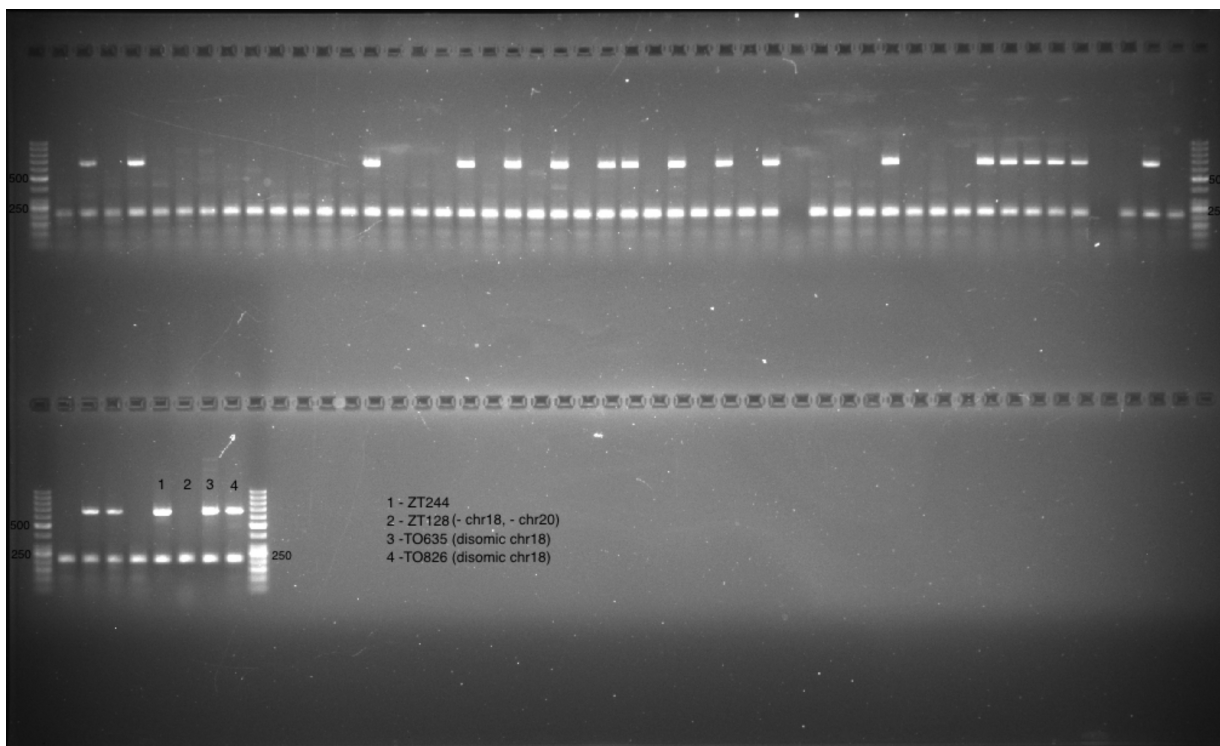
Fig S2. Gel electrophoresis of PCR products for Chr18.1 marker for ascospores isolated from disomic chromosome 18 crosses. Expected fragment size: Chr18.1-651 bp; GAPDH-207 bp. Controls: **1**-IPO323; **2**-Δchr18, Δchr20); **3,4**-disomic chr18 (T0635, T0826); (2% agarose, 120 V, 1h, 50 bp ladder)
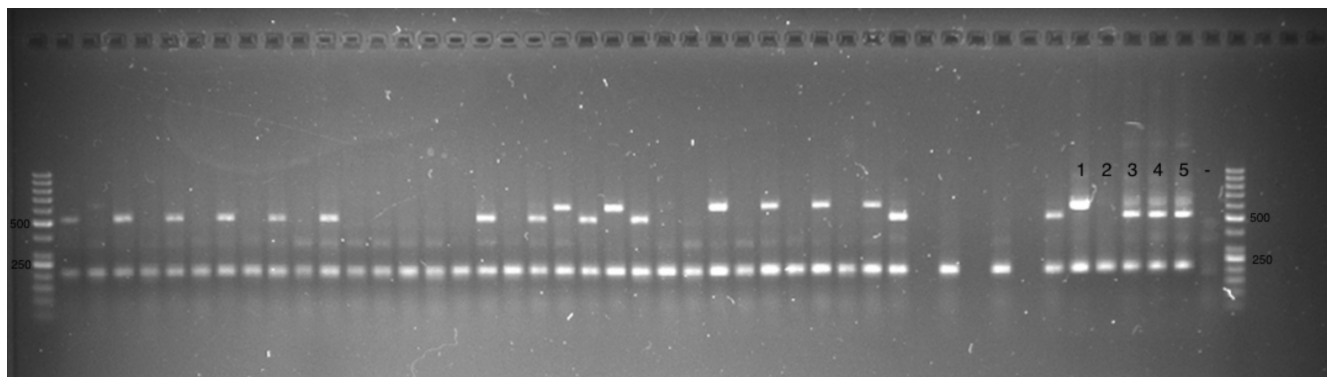

Fig S3. Gel electrophoresis of PCR products for Chr21.4 marker for ascospores isolated from disomic chromosome 21 crosses. Expected fragment size: Chr21.4: **IPO323**-600 bp; **IPO94269**-516 bp; GAPDH-207 bp. Controls: **1**-IPO323; **2**-Δchr21; **3,4,5**-disomic chr21; **-** negative control; (2% agarose, 120 V, 1 h, 50 bp ladder)
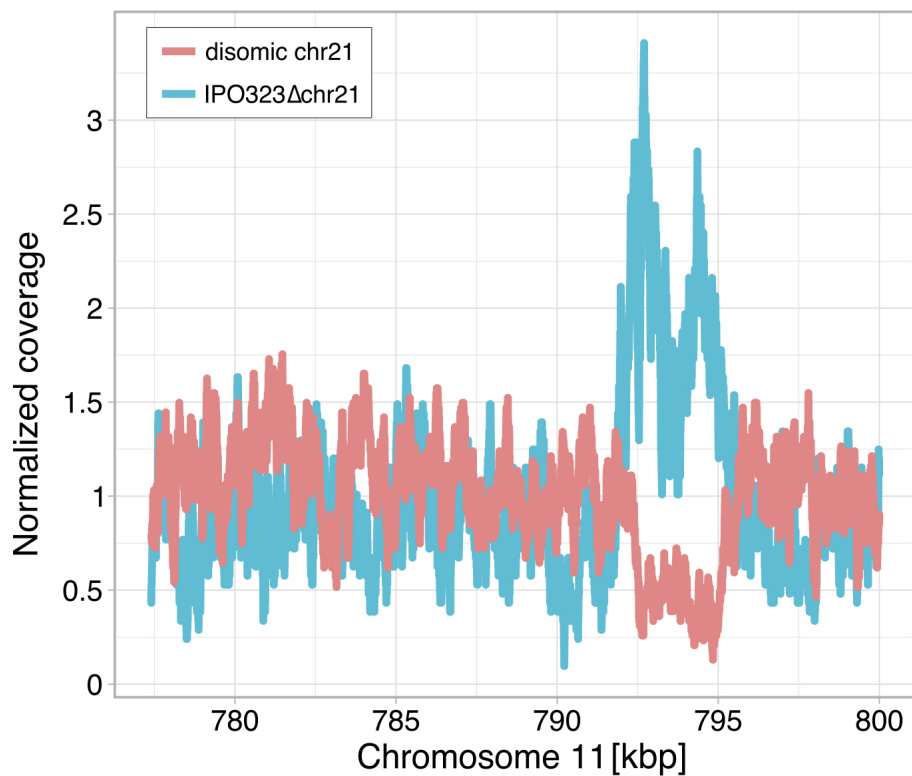
Fig S4. Comparison of normalized coverage of the parental strains in regions with the high frequency of CG:TA transitions on chromosome 11 in crosses with strains with disomic chromosome 21.
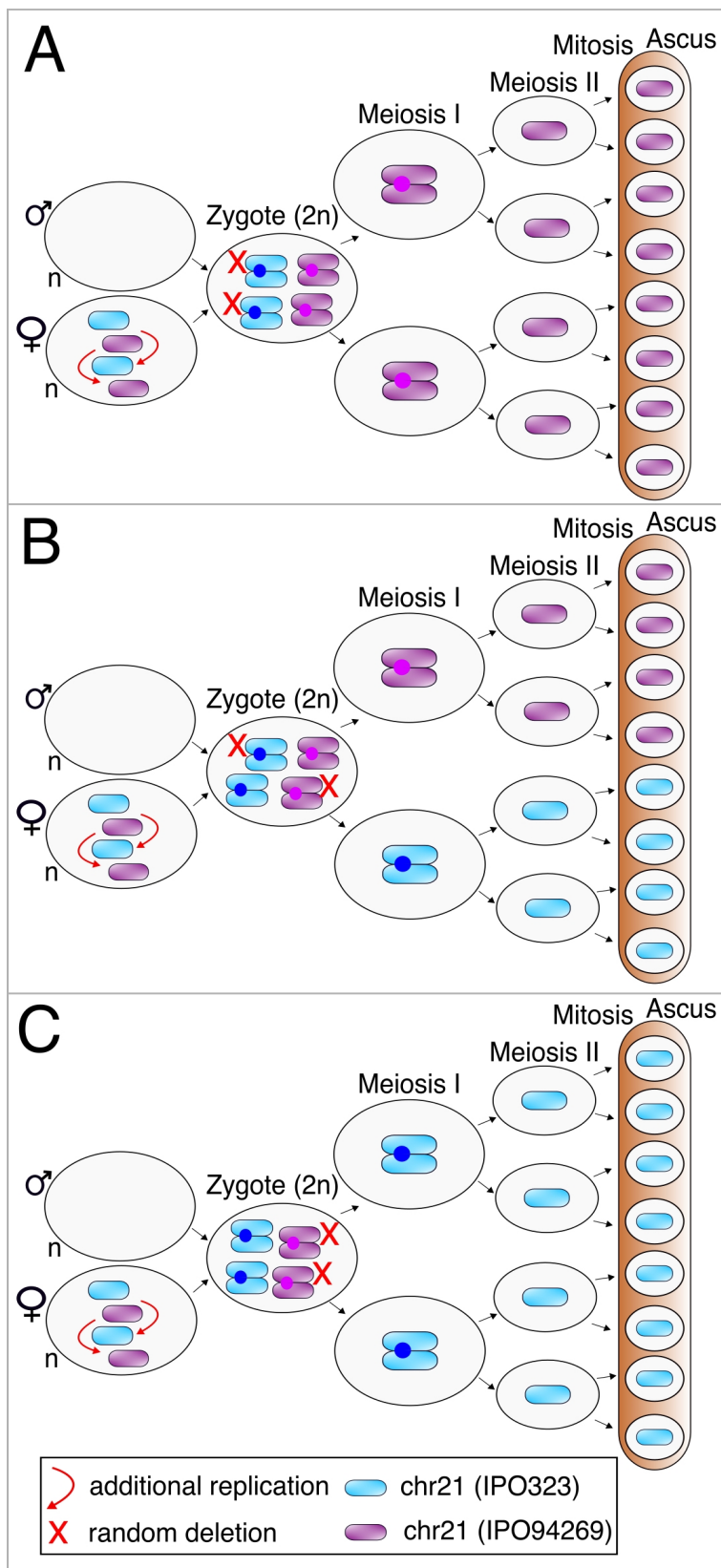
Fig S5. Potential outcomes of crosses with strains disomic for chromosome 21 if model 2 is accurate. Disomic accessory chromosome 21 (one chromosome 21 derived from IPO323 strain and one chromosome 21 derived from IPO94269 strain) is unpaired in our crosses and thus under the meiotic drive. According to model 2 of the meiotic drive, unpaired disomic accessory chromosome 21 is re-replicated before karyogamy, and extra copies are randomly deleted. Random deletion of additional copies of disomic chromosome 21 will result in **A** asci showing non-Mendelian segregation of accessory chromosome 21 derived from the IPO94269 strain (purple) or **B** asci showing Mendelian segregation of chromosome 21 derived from IPO94269 strain (purple) and chromosome 21 derived from IPO323 strain (light blue) or **C** asci showing non-Mendelian segregation of chromosome 21 derived from the IPO323 strain (light blue).
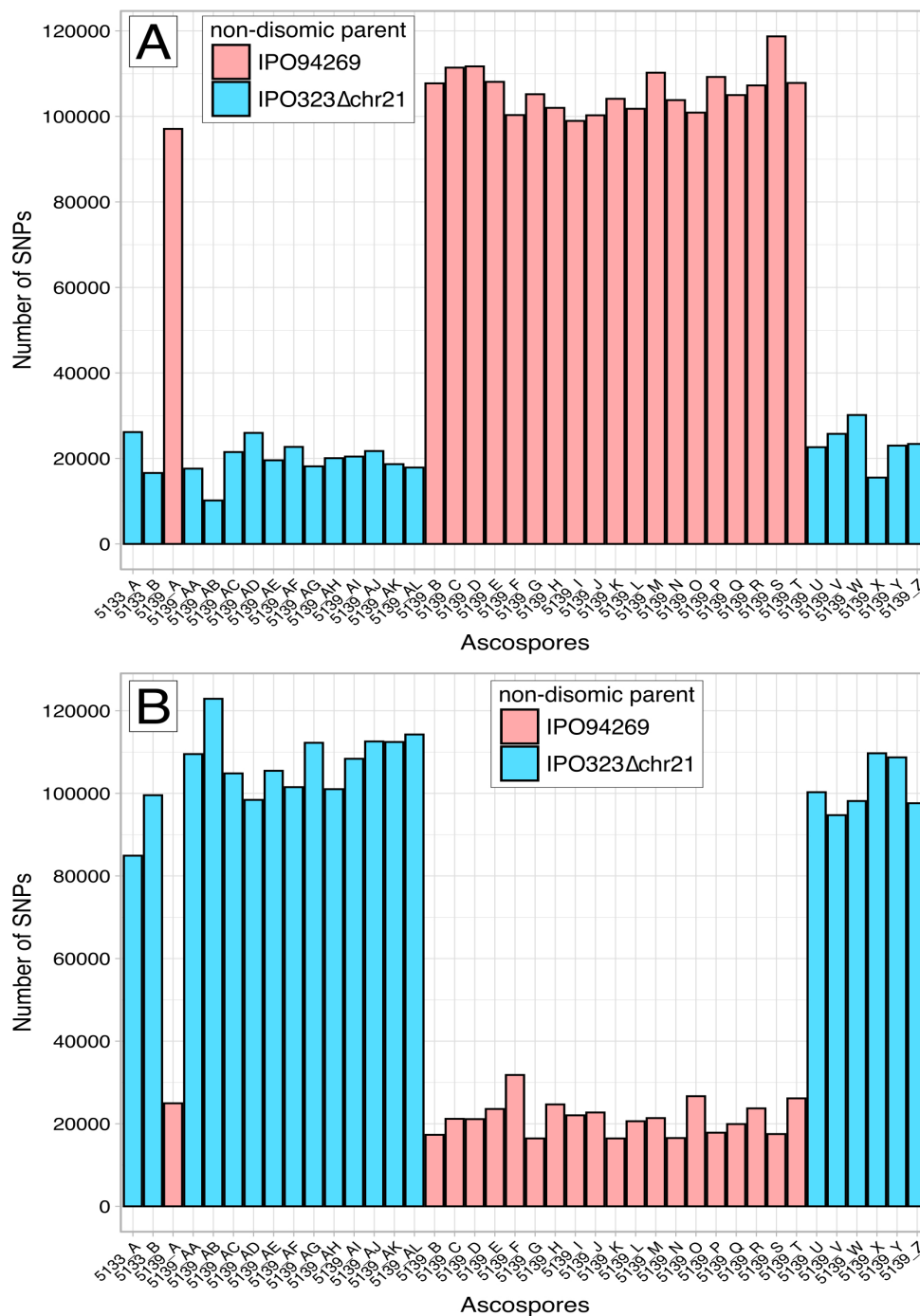
Fig S6. Number of SNPs per ascospore for sequencing reads mapped to **A** IPO323 reference genome and **B** to IPO94269 genome. Crosses with the strains with disomic accessory chromosome 21 are backcross for the IPO323 parent; thus SNP number will be low when reads of progeny from these crosses are mapped to the IPO323 genome. Crosses with the strains with disomic accessory chromosome 18 are backcross for the IPO94269 parent; therefore, the SNP number will be low when reads of progeny from these crosses are mapped to the IPO94269 genome. Ascospores colored in light red are progeny from crosses with disomic chromosome 18 strains and had IPO94269 strain as a

non-disomic parent. Ascospores colored in light blue are progeny from crosses with disomic chromosome 21 strains and had IPO323Δchr21 strain as a non-disomic parent.
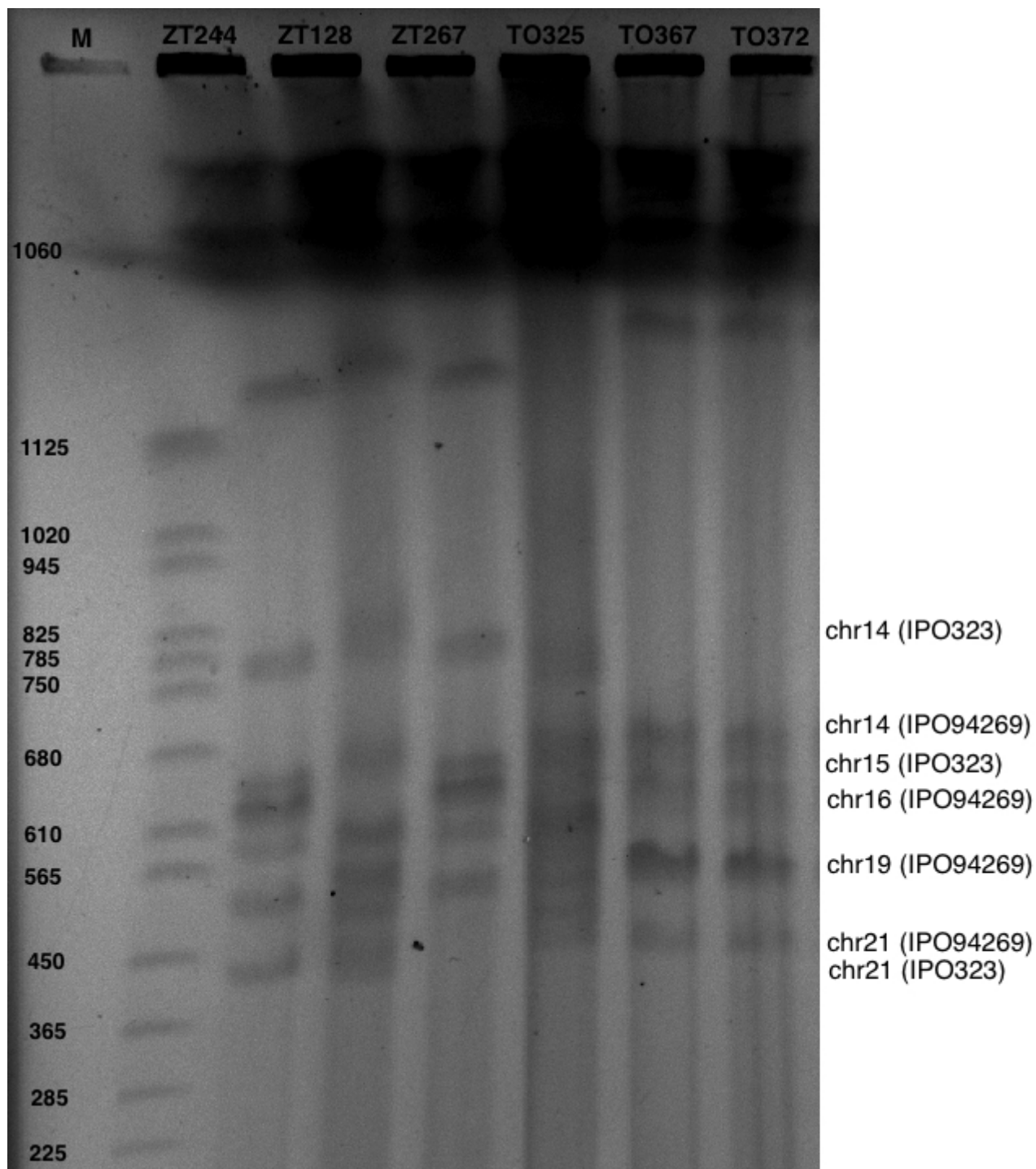

Fig S7. PFGE of strains disomic for the accessory chromosome 21. **M**–*S. cerevisiae* DNA (marker); **ZT244**–**IPO323** reference strain; **ZT128 (IPO94269)**–(Δchr18,Δchr20); **ZT267**-IPO323Δchr21; **T0325,**

T0367, T0372–disomic chromosome 21 (1x IPO323; 1x IPO94269). IPO323 chromosome 21 expected size is 409213 bp; IPO94269 chromosome 21 expected size is 467455 bp.

Supplementary

All supplementary tables are deposited on the supplementary USB card.

Supplementary Tables

Table S1A: PCR data for disomic chromosome 18 crosses.

Table S1B: PCR data for disomic chromosome 21 crosses.

Table S1C: Informative markers in parental strains.

Table S2: List of primers used for tetrad verification and segregation of disomic chromosomes.

Table S3: Coverage data for Fig 2D and Fig 3D.

Table S4: List of identified *de novo* mutations.

General Discussion and Perspectives

Meiosis is a highly conserved cellular process involving the pairing and segregation of homologous chromosomes (Da Ines *et al.* 2014; Zickler and Kleckner 2015). Segregation and pairing of homologous chromosomes during meiosis have been well studied; however, how pairing and segregation of chromosomes progress for unpaired chromosomes is less known. Some fungal species carry non-essential accessory chromosomes that often show presence/absence polymorphisms among individuals and are thus frequently unpaired during meiosis. Fungi are therefore intriguing models for studying the segregation of unpaired chromosomes during meiosis. Interestingly, in *Z. tritici* – a fungal wheat pathogen – unpaired accessory chromosomes show meiotic drive when inherited from the female parent. Here, I have used *Z. tritici* as a model to study the transmission of unpaired accessory chromosomes during meiosis. My thesis aimed to improve the understanding of the mechanism of the meiotic drive of accessory chromosomes in *Z. tritici*. In addition, we explored genetic changes during meiosis and their association with chromatin marks, as these processes can also affect the pairing and segregation of chromosomes during meiosis.

My main findings are the following:

- Accessory chromosomes have higher recombination and gene conversion rates than core chromosomes.
- Higher recombination and gene conversion rates are associated with regions enriched in heterochromatin modifications, especially H3K9me3.
- A repeat-induced point mutation (RIP) is active in *Z. tritici* and causes majority of *de novo* mutations during meiosis.
- Disomic accessory chromosomes that are male-inherited are eliminated during meiosis in *Z. tritici*.
- Additional replication of unpaired and female-inherited accessory chromosomes prior to karyogamy is the mechanism of meiotic drive of accessory chromosome in *Z. tritici*.

In Chapter II, I performed *in silico* tetrad analysis to explore genetic changes associated with meiosis. Meiosis is associated with genetic changes via recombination, gene conversion, and mutations, which

directly impact the genetic structure of the germline. Recombination and gene conversion rearrange genetic material and create a new combination of alleles, affecting sequence composition, nucleotide variation, and rates of adaptation (Stukenbrock and Dutheil 2018). Besides rearranging the genetic material, gene conversion also changes allele frequencies and could have an impact on, for instance, the evolution of pathogenicity traits (Korunes and Noor 2017). High genome-wide recombination and gene conversion rates we estimated in *Z. tritici* are potentially the response to the environment. *Z. tritici* is often present in agriculture systems, where various biotic and abiotic stressors constantly challenge the growth and survival of this fungal pathogen. Therefore, high recombination and gene conversion rates likely increase the number of favorable genotypes on which selection can act, thereby promoting the rapid adaptation and evolution of this pathogen.

Recombination and gene conversion rates are higher on accessory chromosomes in *Z. tritici*. Increased recombination and gene conversion rates on accessory chromosomes could potentially result from their smaller size, since smaller chromosomes have higher rates of genetic changes (Martin *et al.* 2019), and their enrichment in chromatin modifications. My study has shown that higher recombination and gene conversion rates are associated with the regions enriched in heterochromatin, especially H3K9me3, indicating the effect chromatin modifications could have on the repair of DSBs and heteroduplex DNA. The results from Chapter II, however, do not show causality between heterochromatin marks and recombination events during meiosis. Thus, it would be interesting to measure recombination and gene conversion rates in tetrads from crosses that include deletion mutants of *kmt1* and *kmt6*, two histone methyltransferases that mediate H3K9me3 and H3K27me3. Comparison of recombination and gene conversion rates between the following crosses: Δ*kmt1* x Δ*kmt1*, Δ*kmt6* x Δ*kmt6*, and Δ*kmt1* x Δ*kmt6* with recombination and gene conversion rates from wildtype crosses could further address potential causality between heterochromatin marks and rates of recombination and gene conversion in *Z. tritici*.

Besides recombination and gene conversion rates, I estimate the rate of mutations occurring during meiosis. The rate of mutations that occur during meiosis in *Z. tritici* is approx. three orders of magnitude higher than the rate of mutations during mitotic division. This increased mutation rate during sexual reproduction is caused by repeat-point induced mutations (RIP), a fungal defense mechanism against duplicated DNA sequences that occurs in the haploid nuclei before meiosis and that induces CG:TA transitions in duplications and transposable elements (Selker 1990). In Chapter II, I, for the first time, experimentally confirmed the presence of a RIP mechanism in *Z. tritici*. The

increase in the *de novo* mutation rate caused by RIP is limited because RIP is not highly efficient in detecting large duplicated sequences and whole chromosome duplications in *Z. tritici*. Indeed, highly efficient RIP could also negatively affect *Z. tritici* because effector genes and genes responsible for adaption are frequently co-localized with transposable elements in plant pathogenic fungi (Torres *et al.* 2020; Singh *et al.* 2021). Highly efficient RIP could also inactivate all duplications, which could have severe consequences on the genome evolution of this plant pathogen, similar to *N. crassa*, where most paralogs diverged before RIP emergence (Galagan and Selker 2004). Therefore, the lower efficiency of RIP in *Z. tritici* likely represents a trade-off between defense against duplicated sequences and using duplications as a source of variation in the genome.

In Chapter III, I conducted crosses including homozygous and heterozygous disomic strains to monitor the transmission of disomic accessory chromosomes during meiosis in *Z. tritici*. Interestingly, male-inherited disomic accessory chromosomes were eliminated during meiosis, resembling paternal genomic elimination reported in many insect species. In *Z. tritici*, two individuals with different mating types are necessary for successful sexual reproduction, but either of the two mating types (*mat1-1* or *mat1-2*) can act as a female parent (Kema *et al.* 2018). Hence, the differentiation between male and female-inherited chromosomes during meiosis is unexpected in this fungus. However, the data collected in this thesis and from the previous meiotic drive study (Habig *et al.* 2018) indicate that the difference between male-inherited and female-inherited accessory chromosomes during meiosis exists. Chromatin modifications are the distinctive feature between male and female chromosomes in some insect species that exhibit paternal genome elimination, for instance, in jewel wasp (*Nasonia vitripennis*) and mealybug (*Planococcus citri*) (Aldrich and Ferree 2017; Bain 2019). Interestingly, paternal chromatin in jewel wasps obtains abnormally high levels of several methylation marks after fertilization, including H3K9me3, H3K27, and H4K20, causing subsequent elimination of paternal chromosomes (Aldrich and Ferree 2017). Therefore, alterations in methylation levels between male and female-inherited accessory chromosomes during meiosis could be a distinctive feature affecting transmission of these chromosomes. Further experiments that involve ChIP-seq with markers for H3K9me3 and H3K27me3 could elucidate if the difference in methylation levels is the distinguishing feature between the male and female-inherited accessory chromosomes in *Z. tritici*.

Accessory chromosomes are maintained in populations of *Z. tritici* via a meiotic drive restricted to accessory chromosomes that are unpaired and female-inherited despite their negative fitness cost in this plant pathogen (Habig *et al.* 2017, 2018). The meiotic drive of accessory chromosomes in *Z.*

tritici is mechanistically different from previously known meiotic drives in plants and animals. Such drive mechanisms involve either i) preferential segregation of chromosomes during asymmetric pre-meiotic, meiotic, or post-meiotic cell divisions and ii) death of gametes that do not carry the drive element. If preferential segregation of chromosomes or death of gametes without the drive element were a drive mechanism in *Z. tritici*, isolation of complete tetrads would not be possible. Since complete tetrads can be isolated, neither of the two previously known drive mechanisms is active in *Z. tritici* (Habig *et al.* 2018). Therefore, it is highly likely that accessory chromosomes under the meiotic drive are additionally amplified either prior to karyogamy or in the zygote.

I show in Chapter III that accessory chromosomes amplified via meiotic drive are likely re-replicated before karyogamy. The exact mechanism of this re-replication is unknown, but it could involve regulating the replication licensing system. The replication licensing system is responsible for preventing DNA from re-replicating in a single cell cycle, and artificial misregulation of this system causes the re-replication of DNA (Blow and Hodgson 2002). Replication licensing is highly conserved across all eukaryotes (Tada and Blow 1998) and it starts with the binding of the origin recognition complex (ORC) to chromatin at multiple potential origins of replication and is followed by the assembly of two other proteins, Cdc6 (cell division cycle 6) and Cdt1 (chromatin licensing and DNA replication factor 1) (Bell and Dutta 2002). After being assembled, Cdc6 and Cdt1 interact with the MCM2–7 (minichromosomal maintenance) DNA helicase complex (Tanaka and Diffley 2002). A vital component of replication licensing system is the S phase-dependent degradation of Cdt1, an essential replication protein for licensing DNA replication origins (Zhang 2021). Degradation of Cdt1 or the inhibitory binding of geminin to Cdt1 inhibits the re-replication of DNA, thus if Cdt1 is not inhibited or degraded, DNA is re-replicated (Kim and Huberman 2001; Saxena and Dutta 2005). Heterochromatic regions are preferentially re-replicated when degradation of Cdt1 is abolished and replication licensing mechanisms are absent (Ding and MacAlpine 2010). Interestingly, the fourth chromosome of *Drosophila* that exhibits similar traits to accessory chromosomes of *Z. tritici* – small size, high density of transposable elements, and enrichment in heterochromatin marks – was re-replicated entirely in the study of Ding and MacAlpine in 2010. Furthermore, repressive chromatin in *Drosophila* is marked with H3K9me3 and H3K27me3, the same chromatin marks present on accessory chromosomes of *Z. tritici*. If a chromosome similar in traits to accessory chromosomes of *Z. tritici* is entirely re-replicated when expression of Cdt1 is misregulated in *Drosophila*, it is plausible to assume that the unpaired state of accessory chromosomes and their chromatin structure potentially affects the activity of Cdt1 in *Z. tritici*, thereby enabling the re-replication of these chromosomes.

119

Further analyses that involve synchronized cell cultures, flow cytometry, and ChIP-seq of mutant strains with fluorescently tagged Cdt1 could give more insights into the regulation of the replication licensing system on core and accessory chromosomes of *Z. tritici*. Cell cultures of *Z. tritici* can be synchronized by hydroxyurea (HU), a chemical agent that arrests cells in the late G1\early S phase of the cell cycle (Apraiz *et al.* 2017). Synchronized cell cultures with fluorescently labeled Cdt1 would overcome the bias of simultaneously having cells at the different life cycle stages. Simultaneous sampling of synchronized cell culture samples with fluorescently tagged Cdt1 at separate time points for flow cytometry and ChIP-seq would allow for spatiotemporal monitoring of DNA replication progress in *Z. tritici*. Furthermore, including cell cultures with fluorescently tagged MCM and ORC in this experiment could additionally improve understanding of the regulation of the replication licensing system on core and accessory chromosomes of *Z. tritici*.

Here, I have provided novel evidence of how genetic changes associated with meiosis shape genome evolution in *Z. tritici*. Via *in silico* tetrad analysis, I described some of the main aspects of meiosis: recombination rate, gene conversion rate, and their association with heterochromatin structure. Importantly, my work here represents the first estimation of the *de novo* mutation rate and the first experimental verification of RIP activity in *Z. tritici.* Furthermore, I show that RIP causes approx. three orders of magnitude higher meiotic mutation rate in contrast to mitotic mutation rates and thus has a significant influence in the shaping of the *Z. tritici* genome. I confirmed that the re-replication of female-inherited and unpaired accessory chromosomes before karyogamy is the mechanism of the meiotic drive of these chromosomes in *Z. tritici*. Future comparisons of the replication licensing system between core and accessory chromosomes will allow further identification of factors causing the re-replication of unpaired and female-inherited accessory chromosomes. In conclusion, my work demonstrates that genetic changes during meiosis are a major source of variability in *Z. tritici* and therefore have a major impact on the genome structure of an important plant pathogen.

References Introduction and General Discussion and Perspectives

Ågren J. A., and A. G. Clark, 2018 Selfish genetic elements. PLOS Genet. 14: e1007700.

Akera T., L. Chmátal, E. Trimm, K. Yang, C. Aonbangkhen, *et al.*, 2017 Spindle asymmetry drives non-Mendelian chromosome segregation. Science (80-.). 358: 668–672.

Aldrich J. C., and P. M. Ferree, 2017 Genome Silencing and Elimination: Insights from a "Selfish" B Chromosome. Front. Genet. 8. https://doi.org/10.3389/fgene.2017.00050

Alleva B., and S. Smolikove, 2017 Moving and stopping: Regulation of chromosome movement to promote meiotic chromosome pairing and synapsis. Nucleus 8: 613–624. https://doi.org/10.1080/19491034.2017.1358329

Apraiz A., J. Mitxelena, and A. Zubiaga, 2017 Studying Cell Cycle-regulated Gene Expression by Two Complementary Cell Synchronization Protocols. J. Vis. Exp. https://doi.org/10.3791/55745

Bain S. A., 2019 Epigenetic mechanisms underlying paternal genome elimination

Bell S. P., and A. Dutta, 2002 DNA replication in eukaryotic cells. Annu. Rev. Biochem. 71: 333–374.

Blow J. J., and B. Hodgson, 2002 Replication licensing--defining the proliferative state? Trends Cell Biol. 12: 72–78. https://doi.org/10.1016/s0962-8924(01)02203-6

Croll D., M. Zala, and B. A. McDonald, 2013 Breakage-fusion-bridge Cycles and Large Insertions Contribute to the Rapid Evolution of Accessory Chromosomes in a Fungal Pathogen. PLOS Genet. 9: e1003567.

Croll D., M. H. Lendenmann, E. Stewart, and B. A. McDonald, 2015 The Impact of Recombination Hotspots on Genome Evolution of a Fungal Plant Pathogen. Genetics 201: 1213–1228. https://doi.org/10.1534/genetics.115.180968

Crous P. W., 1998 Mycosphaerella spp. and their anamorphs associated with leaf spot diseases of Eucalyptus . 21: 1-170 BT-Mycologia Memoir.

Ding Q., and D. M. MacAlpine, 2010 Preferential Re-Replication of Drosophila Heterochromatin in the Absence of Geminin. PLOS Genet. 6: 1–12. https://doi.org/10.1371/journal.pgen.1001112

Galagan J. E., and E. U. Selker, 2004 RIP: the evolutionary cost of genome defense. TRENDS Genet. 20: 417–423.

Gerton J. L., and R. S. Hawley, 2005 Homologous chromosome interactions in meiosis: diversity amidst conservation. Nat. Rev. Genet. 6: 477–487. https://doi.org/10.1038/nrg1614

Gladyshev E., and N. Kleckner, 2016 Recombination-Independent Recognition of DNA Homology for Repeat-Induced Point Mutation (RIP) Is Modulated by the Underlying Nucleotide Sequence. PLoS Genet. 12: e1006015. https://doi.org/10.1371/journal.pgen.1006015

Gladyshev E., 2017 Repeat-Induced Point Mutation and Other Genome Defense Mechanisms in Fungi. Microbiol. Spectr. 5. https://doi.org/10.1128/microbiolspec.FUNK-0042-2017

Goodwin S. B., S. Ben M'barek, B. Dhillon, A. H. J. Wittenberg, C. F. Crane, *et al.*, 2011 Finished genome of the fungal wheat pathogen Mycosphaerella graminicola reveals dispensome structure, chromosome plasticity, and stealth pathogenesis. PLoS Genet. 7: e1002070. https://doi.org/10.1371/journal.pgen.1002070

Grandaubert J., A. Bhattacharyya, and E. H. Stukenbrock, 2015 RNA-seq-Based Gene Annotation and Comparative Genomics of Four Fungal Grass Pathogens in the Genus Zymoseptoria Identify Novel Orphan Genes and Species-Speci fi c Invasions of Transposable Elements. 5: 1323–1333. https://doi.org/10.1534/g3.115.017731

Habig M., J. Quade, and E. H. Stukenbrock, 2017 Forward Genetics Approach Reveals Host Genotype-Dependent Importance of Accessory Chromosomes in the Fungal Wheat Pathogen Zymoseptoria tritici, (C. B. Kistler Judith, Ed.). MBio 8: e01919-17. https://doi.org/10.1128/mBio.01919-17

Habig M., G. H. J. Kema, and E. Holtgrewe Stukenbrock, 2018 Meiotic drive of female-inherited supernumerary chromosomes in a pathogenic fungus, (A. Rokas, and D. Weigel, Eds.). Elife 7: e40251. https://doi.org/10.7554/eLife.40251

Hammond T. M., D. G. Rehard, H. Xiao, and P. K. T. Shiu, 2012 Molecular dissection of Neurospora Spore killer meiotic drive elements. Proc. Natl. Acad. Sci. 109: 12093 LP – 12098. https://doi.org/10.1073/pnas.1203267109

Hassine M., A. Siah, P. Hellin, T. Cadalen, P. Halama, *et al.*, 2019 Sexual reproduction of Zymoseptoria tritici on durum wheat in Tunisia revealed by presence of airborne inoculum, fruiting bodies and high levels of genetic diversity. Fungal Biol. 123: 763–772. https://doi.org/https://doi.org/10.1016/j.funbio.2019.06.006

Henikoff S., K. Ahmad, and H. S. Malik, 2001 The centromere paradox: stable inheritance with rapidly evolving DNA. Science (80-.). 293: 1098–1102.

Hesse S., M. Zelkowski, E. I. Mikhailova, C. J. Keijzer, A. Houben, *et al.*, 2019 Ultrastructure and Dynamics of Synaptonemal Complex Components During Meiotic Pairing and Synapsis of Standard (A) and Accessory (B) Rye Chromosomes. Front. Plant Sci. 10. https://doi.org/10.3389/fpls.2019.00773

Houben A., A. M. Banaei-Moghaddam, S. Klemme, and J. N. Timmis, 2014 Evolution and biology of supernumerary B chromosomes. Cell. Mol. Life Sci. 71: 467–478. https://doi.org/10.1007/s00018-013-1437-7

Houben A., 2017 B Chromosomes - A Matter of Chromosome Drive. Front. Plant Sci. 8: 210. https://doi.org/10.3389/fpls.2017.00210

Ines O. Da, M. E. Gallego, and C. I. White, 2014 Recombination-Independent Mechanisms and Pairing of Homologous Chromosomes during Meiosis in Plants. Mol. Plant 7: 492–501. https://doi.org/https://doi.org/10.1093/mp/sst172

Kema G. H. J., E. C. P. Verstappen, M. Todorova, and C. Waalwijk, 1996 Successful crosses and molecular tetrad and progeny analyses demonstrate heterothallism in Mycosphaerella graminicola. Curr. Genet. 30: 251–258. https://doi.org/10.1007/s002940050129

Kema G. H. J., A. Mirzadi Gohari, L. Aouini, H. A. Y. Gibriel, S. B. Ware, *et al.*, 2018 Stress and sexual reproduction affect the dynamics of the wheat pathogen effector AvrStb6 and strobilurin resistance. Nat. Genet. 50: 375–380. https://doi.org/10.1038/s41588-018-0052-9

Kim S. M., and J. A. Huberman, 2001 Regulation of replication timing in fission yeast. EMBO J. 20: 6115–6126. https://doi.org/10.1093/emboj/20.21.6115

Korunes K. L., and M. A. F. Noor, 2017 Gene conversion and linkage: effects on genome evolution and speciation. Mol. Ecol. 26: 351–364. https://doi.org/10.1111/mec.13736

Kruger A. N., and J. L. Mueller, 2021 Mechanisms of meiotic drive in symmetric and asymmetric meiosis. Cell. Mol. Life Sci. 78: 3205–3218. https://doi.org/10.1007/s00018-020-03735-0

Li R., E. Bitoun, N. Altemose, R. W. Davies, B. Davies, *et al.*, 2019 A high-resolution map of non-crossover events reveals impacts of genetic diversity on mammalian meiotic recombination. Nat. Commun. 10: 3900. https://doi.org/10.1038/s41467-019-11675-y

Ma L.-J., H. C. van der Does, K. A. Borkovich, J. J. Coleman, M.-J. Daboussi, *et al.*, 2010 Comparative genomics reveals mobile pathogenicity chromosomes in Fusarium. Nature 464: 367–373. https://doi.org/10.1038/nature08850

Malik H. S., 2009 The centromere-drive hypothesis: a simple basis for centromere complexity. Centromere 33–52.

Martin S. H., J. W. Davey, C. Salazar, and C. D. Jiggins, 2019 Recombination rate variation shapes barriers to introgression across butterfly genomes. PLOS Biol. 17: e2006288.

Martis M. M., S. Klemme, A. M. Banaei-Moghaddam, F. R. Blattner, J. Macas, *et al.*, 2012 Selfish supernumerary chromosome reveals its origin as a mosaic of host genome and organellar sequences. Proc. Natl. Acad. Sci. U. S. A. 109: 13343–13346. https://doi.org/10.1073/pnas.1204237109

McClintock B., 1941 The Stability of Broken Ends of Chromosomes in Zea Mays. Genetics 26: 234–282.

Möller M., M. Habig, M. Freitag, and E. H. Stukenbrock, 2018 Extraordinary Genome Instability and Widespread Chromosome Rearrangements During Vegetative Growth. Genetics 210: 517–529. https://doi.org/10.1534/genetics.118.301050

Ni M., M. Feretzaki, S. Sun, X. Wang, and J. Heitman, 2011 Sex in Fungi. Annu. Rev. Genet. 45: 405–430. https://doi.org/10.1146/annurev-genet-110410-132536

Rattray A., G. Santoyo, B. Shafer, and J. N. Strathern, 2015 Elevated mutation rate during meiosis in Saccharomyces cerevisiae. PLoS Genet. 11: e1004910. https://doi.org/10.1371/journal.pgen.1004910

Saxena S., and A. Dutta, 2005 Geminin–Cdt1 balance is critical for genetic stability. Mutat. Res. Mol. Mech. Mutagen. 569: 111–121.

Schotanus K., J. L. Soyer, L. R. Connolly, J. Grandaubert, P. Happel, *et al.*, 2015 Histone modifications rather than the novel regional centromeres of Zymoseptoria tritici distinguish core and accessory chromosomes. Epigenetics Chromatin 8: 41. https://doi.org/10.1186/s13072-015-0033-5

Selker E. U., 1990 Premeiotic instability of repeated sequences in Neurospora crassa. Annu. Rev. Genet. 24: 579–613.

Selker E. U., 2002 Repeat-induced gene silencing in fungi. Adv. Genet. 46: 439–450.

Singh N. K., T. Badet, L. Abraham, and D. Croll, 2021 Rapid sequence evolution driven by transposable elements at a virulence locus in a fungal wheat pathogen. BMC Genomics 22: 393. https://doi.org/10.1186/s12864-021-07691-2

Stukenbrock E. H., and J. Y. Dutheil, 2018 Fine-Scale Recombination Maps of Fungal Plant Pathogens Reveal Dynamic Recombination Landscapes and Intragenic Hotspots. Genetics 208: 1209–1229. https://doi.org/10.1534/genetics.117.300502

Svedberg J., A. A. Vogan, N. A. Rhoades, D. Sarmarajeewa, D. J. Jacobson, *et al.*, 2021 An introgressed gene causes meiotic drive in Neurospora sitophila Proc. Natl. Acad. Sci. 118: e2026605118. https://doi.org/10.1073/pnas.2026605118

Tada S., and J. J. Blow, 1998 The replication licensing system. Biol. Chem. 379: 941–949.

Tanaka S., and J. F. X. Diffley, 2002 Interdependent nuclear accumulation of budding yeast Cdt1 and Mcm2–7 during G1 phase. Nat. Cell Biol. 4: 198–207.

Torres D. E., U. Oggenfuss, D. Croll, and M. F. Seidl, 2020 Genome evolution in fungal plant pathogens: looking beyond the two-speed genome model. Fungal Biol. Rev. 34: 136–143. https://doi.org/https://doi.org/10.1016/j.fbr.2020.07.001

Wang L., Y. Sun, X. Sun, L. Yu, L. Xue, *et al.*, 2020 Repeat-induced point mutation in Neurospora crassa causes the highest known mutation rate and mutational burden of any cellular life. Genome Biol. 21: 142. https://doi.org/10.1186/s13059-020-02060-w

Wittenberg A. H. J., T. A. J. van der Lee, S. Ben M'Barek, S. B. Ware, S. B. Goodwin, *et al.*, 2009 Meiosis Drives Extraordinary Genome Plasticity in the Haploid Fungal Plant Pathogen Mycosphaerella graminicola. PLoS One 4: e5863.

Zhang H., 2021 Regulation of DNA Replication Licensing and Re-Replication by Cdt1. Int. J. Mol. Sci. 22. https://doi.org/10.3390/ijms22105195

Zickler D., and N. Kleckner, 1999 Meiotic Chromosomes: Integrating Structure and Function. Annu. Rev. Genet. 33: 603–754. https://doi.org/10.1146/annurev.genet.33.1.603

Zickler D., and N. Kleckner, 2015 Recombination, Pairing, and Synapsis of Homologs during Meiosis. Cold Spring Harb. Perspect. Biol. 7. https://doi.org/10.1101/cshperspect.a016626

Acknowledgements

Firstly, I would like to thank to my Prof. Eva Stukenbrock for giving me the opportunity to do a PhD thesis in her group. I am very happy that I had a chance to be your student. Thank you for being the best professor one could ask for.

I would like to thank Michael Habig for his supervision. Your discipline and dedication are something I admired from the beginning of working with you. During these last four years, I have seen a significant improvement in my work and you had a significant contribution to it. Thank you!

I would like to thank to Tal Dagan, Linda Odental-Hesse, Frank Kempken and Mathias Leippe for being my TAC and defense committee members. Thank you for being the part of the process.

Next, I thank to Janine Haueisen for the super nice working atmosphere in the office and mostly for great life advices that help me to finish my PhD. I am thankful that I had opportunity to work with such a nice person like you.

I also thank to Eli and Idalia, for their great energy and for all chocolates that they have given me when they thought I need them. I enjoyed sharing the office with you guys.

I also thank to Kim Hufnagel and Janine Muller for their help in the lab and greenhouse work.

I would also like to thank to all of past and present members of EnvGen group in the last four years. All of you were very helpful and nice to me and I am truly thankful that I had a chance to work with people like you.

Big thanks goes to my friends Avneesh, Sarah, Chirlon, Andjela and Toza. I hope our friendships always stay so nice like they have been over the years.

I thank to my girlfriend Elsa for all of the nice moments that we share together.

Most importantly, I would like say thank you to my family for their love and support over the years: to my sister Maša, for always being my best friend; to my mother Ljiljana, for teaching me from an early age that giving your best effort in everything that you do is something nobody can take away from you; and lastly to my father Slobodan, for helping me to overcome the speech deficiency that I had as a child and allowing me to experience the new dimension of life.

Thank you.

Affidavit

I, **Jovan Komluski**, hereby declare that this dissertation:

- concerning content and design is the product of my own work under guidance of my supervisor. I used no other tools or sources but the cited ones. Contributions of other authors are listed in detail in the 'Author's contribution' section of this thesis.

- has not been submitted elsewhere partially or wholly as part of a doctoral degree to another examining body, and no other materials are published or submitted for publication than indicated in the thesis.

- has been conducted and prepared following the Rules of Good Scientific Practice of the German Research Foundation (DFG).

- no academic degree has been withdrawn.

Signature:

Kiel, 09.03.2023